IMPEDANCE AND POWER TRANSFORMATIONS BY THE ISOMETRIC CIRCLE METHOD AND NON-EUCLIDEAN HYPERBOLIC GEOMETRY

E. FOLKE BOLINDER

TECHNICAL REPORT 312

JUNE 14, 1957

MASSACHUSETTS INSTITUTE OF TECHNOLOGY
RESEARCH LABORATORY OF ELECTRONICS
CAMBRIDGE, MASSACHUSETTS

The Research Laboratory of Electronics is an interdepartmental laboratory of the Department of Electrical Engineering and the Department of Physics.

The research reported in this document was made possible in part by support extended the Massachusetts Institute of Technology, Research Laboratory of Electronics, jointly by the U. S. Army (Signal Corps), the U. S. Navy (Office of Naval Research), and the U. S. Air Force (Office of Scientific Research, Air Research and Development Command), under Signal Corps Contract DA36-039-sc-64637, Department of the Army Task 3-99-06-108 and Project 3-99-00-100.

MASSACHUSETTS INSTITUTE OF TECHNOLOGY

RESEARCH LABORATORY OF ELECTRONICS

Technical Report 312 June 14, 1957

IMPEDANCE AND POWER TRANSFORMATIONS BY THE ISOMETRIC CIRCLE METHOD AND NON-EUCLIDEAN HYPERBOLIC GEOMETRY

E. Folke Bolinder

Abstract

An introductory investigation on the means by which modern (higher) geometry can be used for solving microwave problems is presented. It is based on the use of an elementary inversion method for the linear fractional transformation, called the "isometric circle method," and on the use of models of non-Euclidean hyperbolic geometry.

After a description of the isometric circle method, the method is applied to numerous examples of impedance and reflection-coefficient transformations through bilateral two-port networks. The method is then transferred to, and generalized in, the Cayley-Klein model of two-dimensional hyperbolic space, the "Cayley-Klein diagram," for impedance transformations through lossless two-port networks. A similar transfer and generalization is performed in the Cayley-Klein model of three-dimensional hyperbolic space for impedance transformations through lossy two-port networks.

In the Cayley-Klein models a bilateral two-port network is geometrically represented by a configuration consisting of an "inner axis" and two non-Euclidean perpendiculars to the inner axis. The position of the configuration in the models depends upon the fixed points and the multiplier of the linear fractional transformation. By using this geometric representation, an impedance transformation through a bilateral two-port network is performed by consecutive non-Euclidean reflections in the two perpendiculars.

The Cayley-Klein model of three-dimensional hyperbolic space is used: (a) for creating a general method of analyzing bilateral two-port networks from three arbitrary impedance or reflection-coefficient measurements; (b) for creating a general method of cascading bilateral two-port networks by "the Schilling figure"; (c) for determining the efficiency of bilateral two-port networks; (d) for classifying two-port networks; (e) for splitting a two-port network into resistive and reactive parts; and (f) for comparing the iterative impedance method and the image impedance method.

Table of Contents

Table of Contents (continued)

I. INTRODUCTION

1.1 SCOPE OF THE RESEARCH WORK

The purpose of the work that is presented in this report has been to perform an introductory investigation on the means by which modern (higher) geometry can be used for solving microwave problems and simplifying solutions that are already being applied to these problems.

At the beginning of this investigation at the Research Laboratory of Electronics, Massachusetts Institute of Technology, in September 1955, the writer decided to try to follow a certain plan for performing the research work. Two rules were prescribed: first, to start with simple problems and gradually extend the ideas and methods to more complex problems, and, second, to divide the treatment of the problems into three parts: a geometric part yielding a graphic picture of the problem, an analytic part constituting an analytic interpretation of the geometric part, and a part consisting of simple constructive examples to clarify the geometric and analytic treatments.

These rules have been strictly followed. This fact, and the fact that numerous papers in mathematics, engineering, and physics, published in six languages (German, English, French, Italian, Dutch, and Swedish), were studied led, naturally, to rather slow progress in the research work. But the thoroughness of the study has resulted in the construction of a firm foundation on which future research can be built.

Before a brief outline of the research work is given, two geometric works, which provide the mathematical foundation of the present work, are discussed.

1.2 TWO BASIC GEOMETRIC WORKS

The branches of mathematics that are useful in dealing with impedance and power transformation problems in electrical engineering are analysis, algebra, and geometry. Of these, the first two have found extensive application. Although both engineers and physicists favor graphic representation of the problems they are trying to solve, geometry seems to have been applied to a limited extent. The reason seems to be that by the nature of his training, a person who is able to use both analysis and modern algebra, often considers elementary geometrical treatment difficult to understand. It is important to stress that modern (higher) geometry has advanced beyond the graphical constructions that can be performed with ruler and compass. This will be understood by a quick glance at the geometric portions of the collected works of Gauss, Riemann, Cayley, Klein, Lie, Clifford, and Poincaré. Two papers stand out as having been of fundamental importance in the development of modern geometry. These are Riemann's "Über die Hypothesen, welche der Geometrie zu Grunde liegen," which was completed in 1854 and published in 1868 (80-82), and Klein's "Vergleichende Betrachtungen über neuere geometrische Forschungen," published in 1872 (62).

In the first paper, which initiated the development of Differential Geometry, Riemann discusses, among other things, manifolds of n dimensions of constant

curvature. If this curvature is negative, and if n = 3, we have the non-Euclidean geometry of Gauss, Bolyai, and Lobachevsky, to which Klein gave the name "hyperbolic geometry" (63). If the curvature is zero, we have Euclidean geometry, which he called "parabolic geometry." Finally, for a positive curvature, Riemann created another non-Euclidean geometry, which Klein called "elliptic geometry." (We cannot be sure, however, whether Riemann thought of his geometry as spherical or elliptical.) In elliptic geometry space is unbounded but finite.

In the second paper, Klein proposed a program, the well-known "Erlangen Program," for the unification of the principal geometries. He classified geometric properties and assigned them to different geometries according to the invariant properties of corresponding transformation groups. The program was partially initiated by Lie's theory of transformation groups. For almost fifty years it remained unmodified, until the enunciation of the theory of general relativity.

1.3 BRIEF OUTLINE OF THE RESEARCH WORK

The complex impedance (admittance) plane has been one of the most important tools for analyzing and synthesizing networks under stationary conditions, ever since Steinmetz, in the early days of network theory (1893), pointed out that the vectors which Bedell and Crehore had introduced into electrical engineering (1892) could be interpreted as points in a complex plane. For example, Feldtkeller (54) studied symmetric networks by using this tool and, likewise, Schulz (97) studied unsymmetric networks. With the advent of television, radar, and pulse-communication systems, the complex-frequency plane, in which transient conditions can be studied by means of the theory of the Laplace transform, took over the rôle of main tool. The complex impedance plane did not lose its entire significance; in fact, it had a revival of importance at higher frequencies, in the microwave region. A consistent microwave theory in the form of a circular geometric theory was created by Weissfloch (110) in 1942-43.

In the complex impedance plane and the complex reflection-coefficient plane transformations are usually performed by the linear fractional transformation. The fact that it transforms configurations conformally suggests the use of graphical methods. The "isometric circle method" (55, 5) is a method of this kind. The method, an elementary inversion method, is thoroughly described and applied to some simple problems in Section II. Its name is derived from its utilization of two circles called the "isometric circles."

One of the operations prescribed by the isometric circle method consists of an inversion in one of the isometric circles. But it is not practical to use this method with circles of large radii. In order to compress the complex impedance plane, the writer began the study of models of non-Euclidean hyperbolic geometry. Some of the two- and three-dimensional models are briefly described in Appendix 1, their interconnections are discussed in Appendix 2, and a short historical note on the evolution of non-Euclidean geometry is given in Appendix 3. A survey of the use of non-Euclidean

geometry in electrical engineering is presented in Appendix 4.

The Cayley-Klein model of two-dimensional hyperbolic space turned out be be very suitable for transfer of the isometric circle method in cases of impedance transformations through bilateral lossless two-port networks (9). The procedure is outlined in Section III. Similarly, the three-dimensional Cayley-Klein model was found to be equally suited to impedance transformations through bilateral lossy two-port networks (11). The extension of the isometric circle method to the three-dimensional hyperbolic space is presented in Section IV.

From a geometrical point of view, a lossless impedance transformation can be performed by using real angles and distances, whereas a lossy transformation actually requires "complex angles" (or "complex distances"). Since it has been shown by Schilling (88, 89) that a geometric representation of a complex angle (distance) requires three dimensions, we may therefore state that the Cayley-Klein model of three-dimensional hyperbolic space is the natural tool for treating impedance transformations through lossy two-port networks.

Contrary to de Buhr, who in a recent work (38) has discussed the three-dimensional representation of impedance transformations through lossy two-port networks by the three-dimensional Cayley-Klein model, although he insists on performing the transformations geometrically in two dimensions, the writer has used the three-dimensional Cayley-Klein model itself, performing the transformations geometrically and analytically in three dimensions. Thus, the model has been used in a simple study of the exponentially tapered transmission line (7), outlined in Section II. It has also been used in creating a general method of analyzing two-port networks from three arbitrary impedance or reflection-coefficient measurements (15), and in creating a general method of cascading two-port networks by "the Schilling figure" (11). These methods are presented in Sections V and VI. The Schilling figure consists of six straight lines all of which cut the surface of the Riemann unit sphere and all of which are consecutively non-Euclidean perpendicular (88, 89, 96, 67). Furthermore, the three-dimensional Cayley-Klein model has been used in determining the efficiency of two-port networks (10), as outlined in Section VII, and for classifying such networks. The latter application is presented in Section VIII, which also contains a discussion on the splitting of a two-port network into resistive and reactive parts, and a comparison of the iterative impedance method and the image impedance method.

During the course of the research work some of the results were published as contributions to the Quarterly Progress Report, Research Laboratory of Electronics, Massachusetts Institute of Technology (see references 16-27).

II. IMPEDANCE TRANSFORMATIONS BY THE ISOMETRIC CIRCLE METHOD

2.1 INTRODUCTION

In the solution of transmission problems in electrical engineering, impedance transformations are usually carried out either in the complex impedance (admittance) plane or in the complex reflection-coefficient plane (the Smith chart). If notations

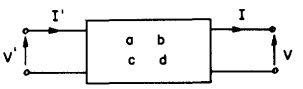

Fig. 1. Two-port network notations.

are introduced in accordance with Fig. 1, the input voltage V' and the input current I' are expressed in the output voltage V and the output current I by the transformation equations:

$$\left.\begin{aligned} V' &= aV + bI \\ I' &= cV + dI \end{aligned}\right\} \tag{1}$$

or in matrix notation by

$$\begin{pmatrix} V' \\ I' \end{pmatrix} = \begin{pmatrix} a & b \\ c & d \end{pmatrix} \begin{pmatrix} V \\ I \end{pmatrix} \tag{2}$$

The complex constants a, b, c, and d characterize completely, for a fixed frequency, a two-port network. If the network is bilateral, the determinant of the transformation matrix is identically equal to unity (57), so that we obtain the following reciprocity condition:

$$ad - bc = 1 \tag{3}$$

If we let:

$$\left.\begin{aligned} \frac{V'}{I'} &= Z' \\ \frac{V}{I} &= Z \end{aligned}\right\} \tag{4}$$

Eq. 1 yields

$$Z' = \frac{aZ + b}{cZ + d} \tag{5}$$

This is a linear fractional transformation (also called a homographic, a bilinear, or a Mŏbius transformation) that transforms the complex impedance Z = R + jX into the impedance Z' = R' + jX', with the R's denoting resistances and the X's denoting reactances.

2.2 THE LINEAR FRACTIONAL TRANSFORMATION

The mathematical properties of Eq. 5 are well known (see, for example, references 70 and 55). The properties that characterize transformations and lead to their classification are usually the invariant properties. Equation 5, which is the most general transformaiion that transforms the whole complex plane conformally into itself, is characterized by the invariance of a cross ratio, by the fixed points, and by the isometric circles.

If we denote four points in the Z-plane by Z_1, Z_2, Z_3, and Z_4, and their image points in the Z'-plane by Z'_1, Z'_2, Z'_3, and Z'_4, a simple calculation yields (55)

$$\frac{(Z'_1 - Z'_2)(Z'_3 - Z'_4)}{(Z'_1 - Z'_3)(Z'_2 - Z'_4)} = \frac{(Z_1 - Z_2)(Z_3 - Z_4)}{(Z_1 - Z_3)(Z_2 - Z_4)} \tag{6}$$

Thus the linear fractional transformation leaves the cross ratio of four points invariant.

In performing Eq. 5, two points, which may coalesce, remain invariant and therefore they are called "fixed points." These points are found by setting Z' = Z in Eq. 5. Thus we obtain

$$\left.\begin{matrix} Z_{f1} \\ Z_{f2} \end{matrix}\right\} = \frac{a - d \pm \sqrt{(a+d)^2 - 4}}{2c}; \quad ad - bc = 1 \tag{7}$$

By using the fixed points, Eq. 5 can be expressed in the following normal (canonic) form (70, 55):

$$\frac{Z' - Z_{f1}}{Z' - Z_{f2}} = q \frac{Z - Z_{f1}}{Z - Z_{f2}} \tag{8}$$

where q, called the multiplier (multiplicator) of the transformation, can be expressed as

$$q = e^{2\lambda} = e^{2(\lambda' + j\lambda'')} = \left[\frac{a + d \mp \sqrt{(a+d)^2 - 4}}{2}\right]^2 \tag{9}$$

or

$$q = \frac{a + d}{2}\left[a + d \mp \sqrt{(a+d)^2 - 4}\right] - 1 \tag{10}$$

or

$$q = \frac{a - c\, Z_{f1}}{a - c\, Z_{f2}} \tag{11}$$

Here, the expressions

$$\left.\begin{matrix}\nu_1\\ \nu_2\end{matrix}\right\} = \frac{a + d \mp \sqrt{(a+d)^2 - 4}}{2}; \quad ad - bc = 1 \tag{12}$$

are the eigenvalues of the matrix in Eq. 2: They are reciprocal, i.e., $\nu_1\nu_2 = 1$. In Eqs. 9 and 10 the minus sign is used in transforming impedances from the output of the network to the input, $Z \rightarrow Z'$. The inverse transformation of Eq. 5, $Z' \rightarrow Z$,

$$Z = \frac{dZ' - b}{-cZ' + a}; \quad ad - bc = 1 \tag{13}$$

which has the same fixed points as the direct transformation (Eq. 5) is used with the plus sign in Eqs. 9 and 10.

It is important to distinguish between an inverse transformation and a reverse transformation in connection with impedance transformations through two-port networks. At this last transformation the signs of the input and output currents are reversed (30).

2.3 THE ISOMETRIC CIRCLES

The isometric circle is defined as the circle that is the complete locus of points in the neighborhood of which lengths are unaltered in magnitude by the linear fractional transformation (55). From Eq. 5, we obtain

$$\frac{dZ'}{dZ} = \frac{1}{(cZ + d)^2}; \quad ad - bc = 1 \tag{14}$$

so that the isometric circle is

$$|cZ + d| = 1; \quad c \neq 0 \tag{15}$$

Similarly, the inverse transformation (Eq. 13) has the isometric circle

$$|cZ' - a| = 1; \quad c \neq 0 \tag{16}$$

Thus the isometric circle of the direct transformation, C_d, has its center at $O_d = -d/c$ and the radius $R_c = 1/|c|$; the isometric circle of the inverse transformation, C_i, has its center at $O_i = a/c$ and the same radius.

Equation 5 transforms the circle C_d into a circle C with the same radius. An inverse transformation transforms C back to C_d again. Hence, C coincides with C_i, so that a linear fractional transformation transforms the isometric circle of the direct transformation into the isometric circle of the inverse transformation (55).

2.4 THE ISOMETRIC CIRCLE METHOD

In the theory of a complex variable Eq. 5 is usually divided in the following way:

$$Z' = \frac{a}{c} - \frac{\frac{1}{c^2}}{Z + \frac{d}{c}}; \quad ad - bc = 1 \tag{17}$$

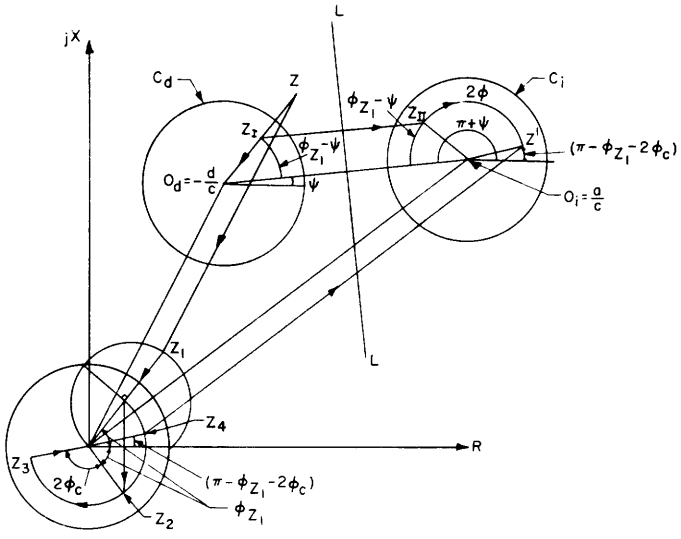

Fig. 2. Graphical interpretation of the linear fractional transformation.

The following operations, suggested by Eq. 17, are then usually performed in the complex Z-plane (see Fig. 2):

1. a translation, $Z_1 = Z + (d/c)$;
2. a complex inversion, $Z_1 Z_2 = 1/|c|^2$;
3. a rotation around the origin through the angle $-2\phi_c$, which yields Z_3 ($c = |c| \exp j\phi_c$);
4. a projection through the origin (a rotation around the origin through the angle π), which yields Z_4; and
5. a translation, $Z' = (a/c) + Z_4$.

If we now draw the two isometric circles C_d and C_i that have the same radius $R_c = 1/|c|$ and their centers at $O_d = -d/c$ and $O_i = a/c$ (see Fig. 2), the graphical method can be simplified by the performance of the following operations: An inversion in C_d, yielding Z_I; a reflection in the symmetry line L of the two isometric circles, yielding Z_{II}; and a rotation around the center O_i through an angle -2ϕ.

With the notations of Fig. 2, we obtain

$$\phi = \psi + \phi_c \tag{18}$$

But $\psi = \arg[(a+d)/c]$, and $\phi_c = \arg c$. Therefore,

$$\phi = \arg(a+d) \tag{19}$$

Thus the following constructions, performed in the complex Z-plane, yield a graphical method, which we shall call the "isometric circle method" (see Fig. 3):

1. an inversion in the isometric circle of the direct transformation, C_d, $Z \rightarrow Z_1$;
2. a reflection in the symmetry line L of the two circles, $Z_1 \rightarrow Z_2$; and
3. a rotation around the center O_i of the isometric circle of the inverse

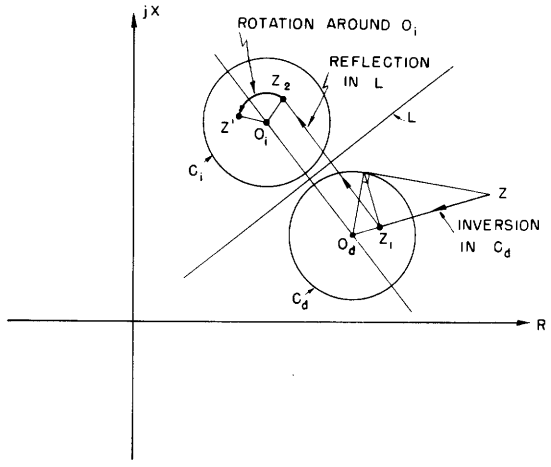

Fig. 3. The isometric circle method.

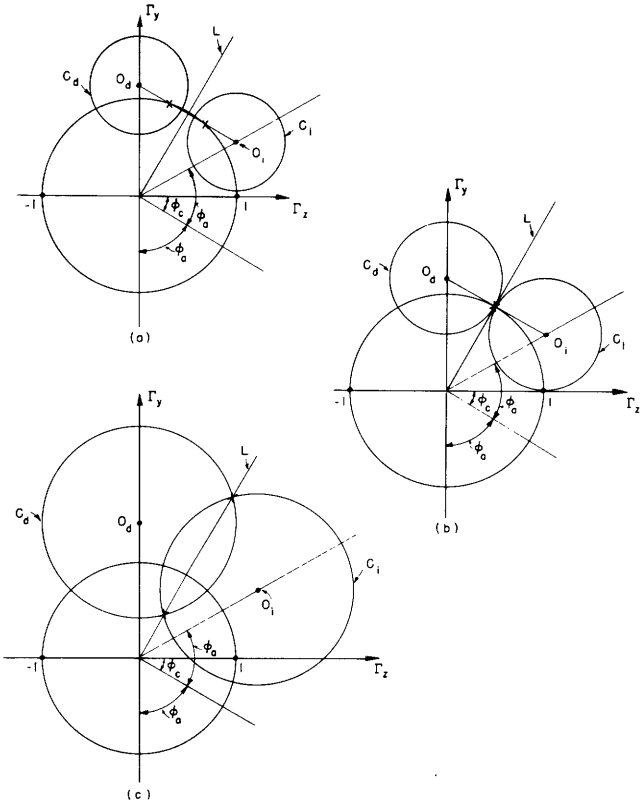

Fig. 4. Examples of nonloxodromic transformations.
(a) Hyperbolic transformation. ($\phi_a = 60°$, $\phi_c = 30°$, $\psi = \cosh^{-1}\sqrt{5}$);
(b) Parabolic transformation. ($\phi_a = 60°$, $\phi_c = 30°$, $\psi = \cosh^{-1} 2$);
(c) Elliptic transformation. ($\phi_a = 60°$, $\phi_c = 30°$, $\psi = \cosh^{-1}\sqrt{2}$).

transformation through an angle -2 arg(a+d), $Z_2 \rightarrow Z'$. The isometric circle method was used by Ford (55) in a study of automorphic functions.

2.5 CLASSIFICATION OF IMPEDANCE TRANSFORMATIONS THROUGH BILATERAL TWO-PORT NETWORKS

Mathematically, Eq. 5 is divided into two classes of transformation: the loxodromic transformation, characterized by a + d = complex; and the nonloxodromic transformation, characterized by a + d = real. The second transformation is further divided into hyperbolic, parabolic, and elliptic transformations, specified by $|a+d| \gtreqless 2$.

If a loxodromic transformation (Greek: loxo-, oblique + -dromos, a running course), centered, for simplicity, around the origin and infinity in the complex plane, is stereographically mapped on a sphere, a curve is obtained (by varying a parameter of the network or the frequency) that, in this case, cuts the meridians under a constant angle. The curve, that uniformly turns around both poles an infinite number of times, is called a "loxodrome."

If we set the multiplier in Eq. 9,

$$q = e^{2\lambda} = e^{2(\lambda'+j\lambda'')} = A\, e^{j\phi} \tag{20}$$

the impedance transformations through all bilateral two-port networks can be classified (68, 70, 55) as follows:

1. If $q = A$, $A \neq 1$, transformation 8 is hyperbolic; a pure (non-Euclidean) stretching is obtained from one fixed point to the other.

2. If $q = e^{j\phi}$, $\phi \neq n\pi$, with $n = 0, 1, 2, \ldots$, transformation 8 is elliptic; a pure (non-Euclidean) rotation is obtained around the fixed points.

3. If $q = A\, e^{j\phi}$, $A \neq 1$, $\phi \neq n\pi$, with $n = 0, 1, 2, \ldots$, transformation 8 is loxodromic; it can be considered as a hyperbolic transformation followed by an elliptic transformation, or vice versa.

4. In the special case of $Z_{f1} = Z_{f2} = Z_f$, $q = 1$, transformation 8 can be written

$$\frac{1}{Z' - Z_f} = \frac{1}{Z - Z_f} \pm c \tag{21}$$

in which, from Eq. 7,

$$Z_f = \frac{a - d}{2c} \tag{22}$$

A transformation with a single fixed point (two coalescing fixed points), $a + d = \pm 2$, is parabolic. In Eq. 21 we use +c, if $a + d = +2$, and -c, if $a + d = -2$.

The aforementioned classifications have been used in network theory by Le Corbeiller and Lange (42), Feldtkeller (54), König (71), Guillemin (57), Schulz (97), Weissfloch (109, 110), Van Slooten (98, 99), Rybner (84, 85), and others.

In accordance with the results of Section 2.4, the distance between the centers of the two isometric circles is $|(a+d)/c|$, while the sum of the two radii is $2/|c|$.

Therefore, if we follow the classification given above, we have the hyperbolic case, if the two circles are external; the parabolic case, if they are tangent; and the elliptic case, if they intersect. See Fig. 4. In the loxodromic case each circle may have any position with relation to the other. The positions of the fixed points in relation to the isometric circles can now be obtained easily from Eq. 7. The fixed points are marked as crosses in Fig. 4.

2.6 IMPEDANCE TRANSFORMATIONS THROUGH LOSSLESS TWO-PORT NETWORKS

In order to study the linear fractional transformation, Eq. 5, when it corresponds to impedance transformations through lossless two-port networks (8), we shall first transform it into the complex reflection-coefficient plane (Smith chart). Using the well-known formula,

$$\Gamma = \frac{\frac{Z}{\sqrt{2}} - \frac{1}{\sqrt{2}}}{\frac{Z}{\sqrt{2}} + \frac{1}{\sqrt{2}}} \tag{23}$$

where Γ is the complex reflection coefficient, and Z is the (normalized) complex impedance, we obtain, from Eq. 5

$$\Gamma' = \frac{\Gamma(a-b-c+d)/2 + (a+b-c-d)/2}{\Gamma(a-b+c-d)/2 + (a+b+c+d)/2} \tag{24}$$

In the lossless case the imaginary axis in the impedance plane, which corresponds to the unit circle in the reflection-coefficient plane, is transformed into itself, i.e., a reactance is transformed into a reactance. The most general linear fractional transformation that transforms the unit circle into itself, so that the interior of the unit circle is transformed into the interior of the new unit circle, can be written

$$\Gamma' = \frac{A\Gamma + C^*}{C\Gamma + A^*}; \qquad |A|^2 - |C|^2 = 1 \tag{25}$$

A star indicates a complex conjugate quantity. If the coefficients a, b, c, and d are split into their real and imaginary parts,

$$\left.\begin{aligned} a &= a' + ja'' \\ b &= b' + jb'' \\ c &= c' + jc'' \\ d &= d' + jd'' \end{aligned}\right\} \tag{26}$$

then Eqs. 24 and 25 yield

$$a'' = b' = c' = d'' = 0 \tag{27}$$

Thus Eqs. 5 and 24 can be written

$$Z' = \frac{a'Z + jb''}{jc''Z + d'}; \quad a'd' + b''c'' = 1 \tag{28}$$

and

$$\Gamma' = \frac{\Gamma[(a' + d')/2 - j(b'' + c'')/2] + [(a' - d')/2 + j(b'' - c'')/2]}{\Gamma[(a' - d')/2 - j(b'' - c'')/2] + [(a' + d')/2 + j(b'' + c'')/2]} \tag{29}$$

In Eq. 28, $a + d = a' + d' =$ real, so that impedance transformations through lossless two-port networks correspond to nonloxodromic transformations. These form a group, the transformations of which have a common fixed circle (fixed straight line), each transformation carrying the interior of the fixed circle into itself. It can easily be shown that the isometric circles of the transformations of such a group are orthogonal to the fixed circle (55).

We can write Eq. 25 in the form

$$\Gamma' = \frac{\Gamma \cosh \psi\, e^{j\phi_a} + \sinh \psi\, e^{-j\phi_c}}{\Gamma \sinh \psi\, e^{j\phi_c} + \cosh \psi\, e^{-j\phi_a}} \tag{30}$$

where ψ, ϕ_a, and ϕ_c can be expressed in a', b", c", and d' by a comparison of Eqs. 29 and 30. The isometric circles of Eq. 30 are given by

$$\left.\begin{aligned} O_d &= -\coth \psi\, e^{-j(\phi_a + \phi_c)} \\ O_i &= \coth \psi\, e^{j(\phi_a - \phi_c)} \\ R_c &= \frac{1}{|\sinh \psi|} \end{aligned}\right\} \tag{31}$$

The hyperbolic, parabolic, and elliptic cases are obtained from the condition

$$\cosh \psi \cos \phi_a \gtreqless 1 \tag{32}$$

See Fig. 4.

For nonloxodromic transformations, the fixed points play a fundamental rôle. Setting $\Gamma' = \Gamma$ in Eq. 30, we obtain

$$\left.\begin{matrix} \Gamma_{f1} \\ \Gamma_{f2} \end{matrix}\right\} = e^{-j\phi_c}\left(j \coth \psi \sin \phi_a \pm \sqrt{1 - \coth^2 \psi \sin^2 \phi_a}\right) \tag{33}$$

Some of the equations given above were derived by Lueg (73), who extended some work of Weissfloch (109, 110), but in a slightly different form. For example, Lueg

(in our notation) uses:

$$Z' = \frac{ja''Z + b'}{c'Z + jd''} \tag{34}$$

instead of Eq. 28, and

$$\Gamma' = \frac{\Gamma e^{j\phi_1} - \Gamma_o e^{j\phi_2}}{\Gamma\Gamma_o e^{-j\phi_2} - e^{-j\phi_1}} \tag{35}$$

instead of Eq. 30. Equation 35 in normalized form is

$$\Gamma' = \frac{\Gamma \dfrac{e^{j\phi_1}}{j\sqrt{1-\Gamma_o^2}} - \dfrac{\Gamma_o e^{j\phi_2}}{j\sqrt{1-\Gamma_o^2}}}{\Gamma \dfrac{\Gamma_o e^{-j\phi_2}}{j\sqrt{1-\Gamma_o^2}} - \dfrac{e^{-j\phi_1}}{j\sqrt{1-\Gamma_o^2}}} \tag{36}$$

Here $\Gamma_o = |\Gamma'|$ for $\Gamma = 0$, $0 \leq \Gamma_o \leq 1$. We obtain

$$\left.\begin{aligned} \phi_1 &= \phi_a + \tfrac{\pi}{2} \\ \phi_2 &= -\phi_c - \tfrac{\pi}{2} \\ \Gamma_o &= \tanh \psi \end{aligned}\right\} \tag{37}$$

2.7 THE ISOMETRIC CIRCLE METHOD IN ANALYTIC FORM

The three operations of the isometric circle method can be written in the following form:

$$Z_1^* = -\frac{\dfrac{d^*}{c^*} Z + \dfrac{dd^* - 1}{cc^*}}{Z + \dfrac{d}{c}} \equiv \text{inversion in } C_d \tag{38a}$$

$$Z_2 = \frac{-\dfrac{a+d}{c} Z_1^* + \dfrac{aa^* - dd^*}{cc^*}}{\dfrac{a^* + d^*}{c^*}} \equiv \text{reflection in } L \tag{38b}$$

$$Z' - \frac{a}{c} = \left(Z_2 - \frac{a}{c}\right) e^{-j\,2\arg(a+d)} \equiv \text{rotation around } C_i \tag{38c}$$

If the network is lossless, Eqs. 38 simplify to

$$Z_1^* = \frac{d'Z - j\frac{d'^2 - 1}{c''}}{jc''Z + d'} \equiv \text{inversion in } C_d \tag{39a}$$

$$Z' = Z_2 = Z_1^* - j\frac{a' - d'}{c''} \equiv \text{reflection in L} \tag{39b}$$

In the lossless case, the corresponding transformations in the complex reflection-coefficient plane are

$$\Gamma_1 = \frac{-\frac{A^*}{C}\Gamma^* - 1}{\Gamma^* + \frac{A}{C^*}} \equiv \text{inversion in } C_d \tag{40a}$$

$$\Gamma' = -\frac{C^*}{C}\Gamma_1^* \equiv \text{reflection in L} \tag{40b}$$

Equations 38a, 38b, 39a, 39b, 40a, and 40b are all of the form:

$$Z' = \frac{aZ^* + b}{cZ^* + d}, \qquad \Gamma' = \frac{A\Gamma^* + B}{C\Gamma^* + D} \tag{41}$$

Following Cartan (39), we call Eq. 5 a homography and Eq. 41 an antihomography. The antihomographies are of two kinds: the anti-involutions of the first kind, which are characterized by having at least one fixed point (Examples: $Z' = 1/Z^*$, $Z' = Z^*$), and the anti-involutions of the second kind, which have no fixed point (Example: $Z' = -1/Z^*$). In the complex plane every anti-involution of the first kind is represented by an inversion with positive power or by a symmetry in relation to a straight line. The following theorems are valid (39):

1. Every homography can be considered as a product of two involutions.
2. Every involution is the product of two exchangeable anti-involutions of the first kind.

Thus, every homography can be considered as a product of four anti-involutions of the first kind. An involution is a loxodromic transformation with a multiplier q = -1. Since a rotation may be considered as a product of two reflections, the isometric circle method is basically composed of four anti-involutions of the first kind. In the non-loxodromic case when the third operation, the rotation, is eliminated, the number is reduced to two.

2.8 COMPARISON OF THE "TRIANGULAR METHOD" AND THE ISOMETRIC CIRCLE METHOD

In an unpublished paper, Mason (75) describes a simple graphical method for the linear fractional transformation. Because he bases this method on the similitude of two

triangles, the method may be called "the triangular method" (13).

Mason presupposes that one pair of corresponding quantities $Z_a \rightarrow Z'_a$ is known for the linear fractional transformation, Eq. 5, together with $Z' = O_i = a/c$ for $Z = \infty$, and $Z' = \infty$ for $Z = O_d = -d/c$. For an arbitrary Z, he then constructs the image point Z' by drawing the similar triangles $O_d Z_a Z$ and $O_i Z' Z'_a$ (see Fig. 5). The connection between the triangular method and the isometric circle method is immediately obtained from Fig. 5. The transformation shown in the figure is loxodromic and the angle $-2 \arg(a+d)$ is denoted by θ. The different operations of the isometric circle method (marked by arrows in Fig. 5) are indicated by the points Z, Z_1, Z_2, and Z'.

2.9 SOME APPLICATIONS OF THE ISOMETRIC CIRCLE METHOD TO IMPEDANCE TRANSFORMATIONS THROUGH BILATERAL TWO-PORT NETWORKS

a. Example of a Loxodromic Transformation

An example of the use of the isometric circle method for a loxodromic transformation is shown in Fig. 6. This is the same example that was used by Storer, Sheingold, and Stein (101). The transformation formula for the reflection coefficient is expressed in the components of the scattering matrix:

$$\Gamma' = \frac{\frac{s_{12}^2 - s_{11}s_{22}}{s_{12}}\Gamma + \frac{s_{11}}{s_{12}}}{-\frac{s_{22}}{s_{12}}\Gamma + \frac{1}{s_{12}}} \tag{42}$$

where

$$s_{11} = 0.331\, e^{j\,135.0^\circ}$$

$$s_{12} = 0.808\, e^{j\,70.6^\circ}$$

$$s_{22} = 0.328\, e^{j\,132.8^\circ}$$

Hence

$$O_d = 1/s_{22} = 3.05\, e^{-j\,132.8^\circ}$$

$$O_i = -\left(s_{12}^2 - s_{11}s_{22}\right)/s_{22} = 2.20\, e^{-j\,178.5^\circ}$$

$$R_c = |s_{12}/s_{22}| = 2.47$$

$$-2 \arg(a+d) = 49.0^\circ$$

In their example Storer, Sheingold, and Stein use $\Gamma' = 0.70 \exp(j\,60^\circ)$. Following the procedure of the isometric circle method in reverse order, we rotate Γ' around O_i through the angle -49.0°, reflect in L, and invert in C_d. The value obtained

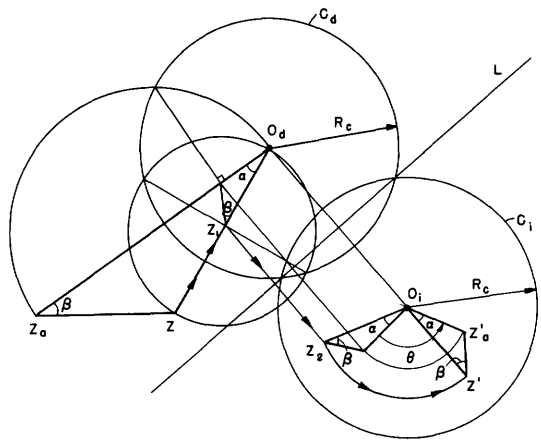

Fig. 5. Connection between the triangular method and the isometric circle method.

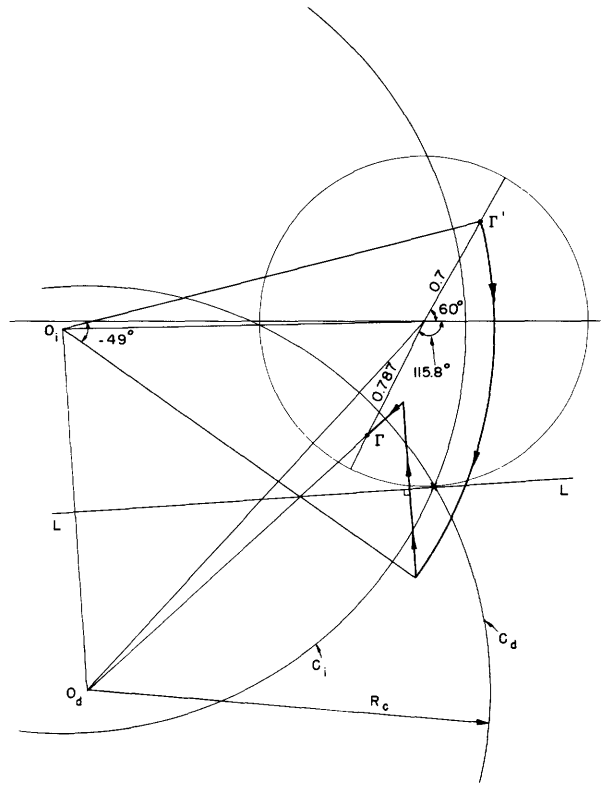

Fig. 6. Example of a loxodromic transformation.

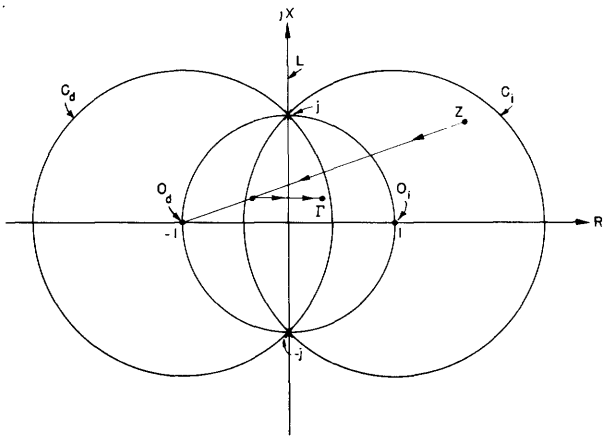

Fig. 7. Transformation of the right half-plane of the Z-plane into the unit circle (Smith chart).

approximates nicely the value $\Gamma = 0.787 \exp(-j\,115.8°)$ obtained by Storer et al.

b. Transformation of the Right Half-Plane of the Z-Plane into the Unit Circle (Smith Chart)

The well-known transformation formula expressing the complex reflection coefficient Γ in the complex impedance Z was given in section 2.6. It is

$$\Gamma = \frac{\frac{Z}{\sqrt{2}} - \frac{1}{\sqrt{2}}}{\frac{Z}{\sqrt{2}} + \frac{1}{\sqrt{2}}} \tag{23}$$

Thus, referring to Fig. 7, we find that

$$O_d = -d/c = -1$$

$$O_i = a/c = 1$$

$$R_c = 1/|c| = \sqrt{2}$$

$$a + d = \sqrt{2} = \text{real}$$

The transformation is clearly nonloxodromic and elliptic, since a + d is real and the isometric circles intersect. The fixed points are $\pm j$. Thus Γ is simply obtained from an arbitrary Z by inverting in C_d and reflecting in L, the imaginary axis. The imaginary axis is mapped on the unit circle; the right half-plane of the Z-plane falls inside the circle. The constant-R and constant-X lines are transformed into two sets of orthogonal circles through the point +1. The diagram inside the unit circle is the familiar Smith chart. An inverse transformation $\Gamma \rightarrow Z$ is simply obtained by inverting in C_i and reflecting in L.

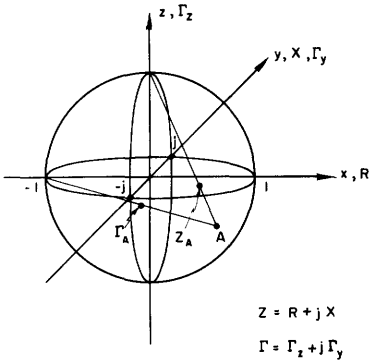

Fig. 8. The Riemann unit sphere.

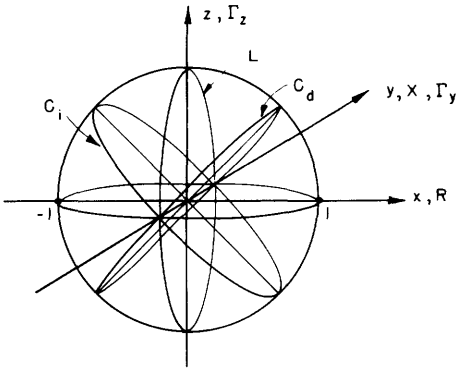

Fig. 9. Stereographic mapping of Fig. 7 on the unit sphere.

The transformation between the Z-plane and the Γ-plane was recently treated by de Buhr (32). He used the C_i circle as the inversion circle, but he did not realize that this circle is one of the isometric circles; nor did he recognize that his graphical construction is a special case of a more general method.

A graphic picture of the $Z \rightarrow \Gamma$ transformation is obtained by a stereographic mapping of Fig. 7 on the Riemann unit sphere. In Fig. 8 the impedance Z_A is projected on the unit sphere with the top of the sphere as the projection center. The point A on the surface of the sphere is obtained. Now, the $Z \rightarrow \Gamma$ transformation corresponds to a 90° rotation of the sphere around an axis through the fixed points $\pm j$. Another stereographic projection from the top of the sphere, after the rotation, yields the Γ-plane as the xy-plane. However, instead of rotating the sphere and having a fixed projection center, we can just as well keep the sphere fixed and turn the projection center from the point (0, 0, 1) by a 90° rotation to (-1, 0, 0) (100, 104, 99, 46). The Γ-plane is now obtained as the yz-plane, so that $\Gamma = \Gamma_z + j\Gamma_y$. In Fig. 8 the point Γ_A is obtained.

Figure 9 shows the isometric circles of Fig. 7 mapped on the unit sphere. C_d and C_i transform into great circles tilted 45° and 135°, and the symmetry line L transforms into a great circle in the yz-plane. It is interesting to observe that it is possible to extend the operations of the isometric circle method directly to the surface of the sphere. They consist of two reflections in the planes through C_d and L. Thus, for example, the top of the sphere, (0, 0, 1), is transformed into (1, 0, 0) by a reflection in the plane through C_d, and into (-1, 0, 0) by a second reflection in the plane through L.

At this point, it is important to stress that the isometric circles of Eq. 5 in the Z-plane do, of course, not transform into the isometric circles of the transformed linear fractional transformation, Eq. 24, in the Γ-plane. However, for the sake of simplicity, the writer will sometimes use the same notations in the Z-plane and on the surface of the sphere.

c. Uniform Lossless Transmission Line

The impedance transformation through a piece of uniform lossless transmission line can be written

$$\frac{Z'}{Z_o} = \frac{\frac{Z}{Z_o}\cos\phi + j\sin\phi}{\frac{Z}{Z_o} j\sin\phi + \cos\phi} \tag{43}$$

where Z_o is the characteristic impedance; $\phi = 2\pi\ell/\lambda$, with ℓ the length of the line, and λ the wavelength. Here

$$O_d = -d/c = j\cot\phi$$

$$O_i = a/c = -j\cot\phi$$

$$R_c = 1/|\sin\phi|$$

The fixed points are ± 1. The transformation is elliptic, since $a + d = 2\cos\phi < 2$. Figure 10 shows a simple example, in which $Z/Z_o = 2$ is transformed graphically by

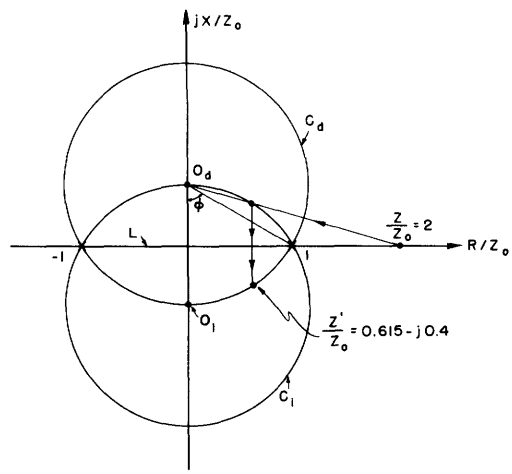

Fig. 10. Uniform lossless transmission line example.

the isometric circle method into $Z'/Z_o = 0.615 - j\,0.4$ by using a transmission line with $\phi = 60°$. The two operations, inversion in C_d and reflection in L, are marked by arrows in Fig. 10.

In the Γ-plane, using Eq. 29, we obtain

$$\Gamma' = \frac{\Gamma e^{-j\phi}}{e^{j\phi}} = \Gamma e^{-j2\phi} \tag{44}$$

Thus, in Eq. 30, $\phi_a = -\phi$, $\phi_c = 0$, and $\psi = 0$. The quantities O_d, O_i, and R_c of Eq. 44

are all infinite (c=0), so that the isometric circles are indefinite. Figure 11 shows Fig. 10 stereographically mapped on the unit sphere. The image circles of C_d, C_i, and L are all great circles through the fixed points ±1. Therefore, they appear as straight lines through the origin in the Γ-plane (see Fig. 12). Using the same example as in Fig. 10, $|\Gamma'| = |\Gamma| = 1/3$, $\phi = 60°$, we find that the resultant transformation is a rotation around the origin of the Γ-plane through an angle $2\phi = 2.60° = 120°$ in the negative direction, which checks with Eq. 44.

d. Lossless Transformers

A lossless transformer, composed of the inductances L_1 and L_2 with the mutual inductance M, can be represented by the transformation

$$Z' = \frac{\frac{n}{k} Z - j\omega M\left(1 - \frac{1}{k^2}\right)}{\frac{Z}{j\omega M} + \frac{1}{kn}} \tag{45}$$

where the transformation ratio is $n = \sqrt{L_1/L_2}$, and the coupling factor is $k = M/\sqrt{L_1 L_2} \leq 1$. See, for example, reference 99.

Transforming Eq. 45 into the Γ-plane, with the use of Eq. 29, we obtain

$$\Gamma' = \frac{\Gamma\left\{\frac{1}{2k}\left(n + \frac{1}{n}\right) + j\left[\frac{1}{2\omega M} - \frac{\omega M}{2}\left(\frac{1}{k^2} - 1\right)\right]\right\} + \left\{\frac{1}{2k}\left(n - \frac{1}{n}\right) + j\left[\frac{1}{2\omega M} + \frac{\omega M}{2}\left(\frac{1}{k^2} - 1\right)\right]\right\}}{\Gamma\left\{\frac{1}{2k}\left(n - \frac{1}{n}\right) - j\left[\frac{1}{2\omega M} + \frac{\omega M}{2}\left(\frac{1}{k^2} - 1\right)\right]\right\} + \left\{\frac{1}{2k}\left(n + \frac{1}{n}\right) - j\left[\frac{1}{2\omega M} - \frac{\omega M}{2}\left(\frac{1}{k^2} - 1\right)\right]\right\}} \tag{46}$$

Thus, from Eq. 30, we have

$$\left.\begin{aligned} \phi_a &= \tan^{-1} \frac{\frac{1}{2\omega M} - \frac{\omega M}{2}\left(\frac{1}{k^2} - 1\right)}{\frac{1}{2k}\left(n + \frac{1}{n}\right)} \\ \phi_c &= -\tan^{-1} \frac{\frac{1}{2\omega M} + \frac{\omega M}{2}\left(\frac{1}{k^2} - 1\right)}{\frac{1}{2k}\left(n - \frac{1}{n}\right)} \\ \sinh \psi &= \sqrt{\frac{1}{4k^2}\left(n - \frac{1}{n}\right)^2 + \left[\frac{1}{2\omega M} + \frac{\omega M}{2}\left(\frac{1}{k^2} - 1\right)\right]^2} \end{aligned}\right\} \tag{47}$$

Obviously, the transformation is hyperbolic, since

$$a + d = \frac{1}{k}\left(n + \frac{1}{n}\right) > 2, \qquad k < 1$$

In Fig. 13 the isometric circles of Eq. 46 are shown, with k = 1/2, $\omega M = 1$, and n = 2.

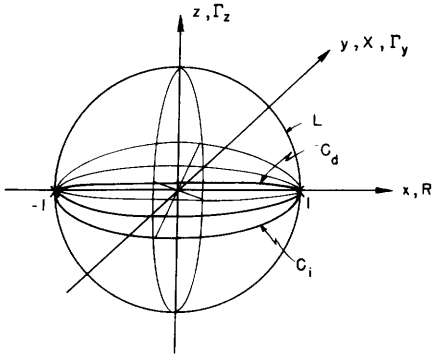

Fig. 11. The isometric circles of Fig. 10 mapped on the unit sphere.

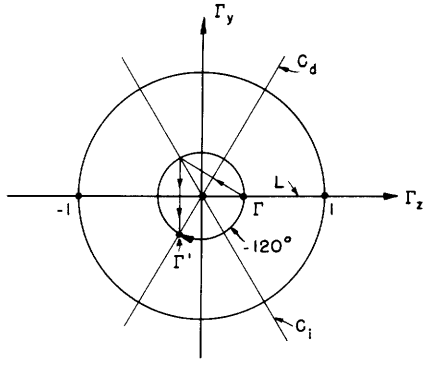

Fig. 12. Uniform lossless transmission line example in the Γ-plane.

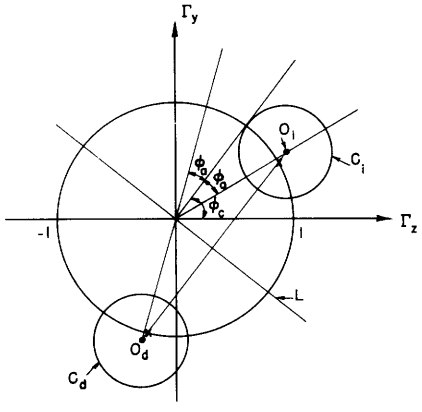

Fig. 13. Lossless transformer example. ($k = 0.5$, $\omega M = 1$, $n = 2$; $\phi_a = 21.8°$, $\phi_c = -53.1°$, $\psi = 1.647$).

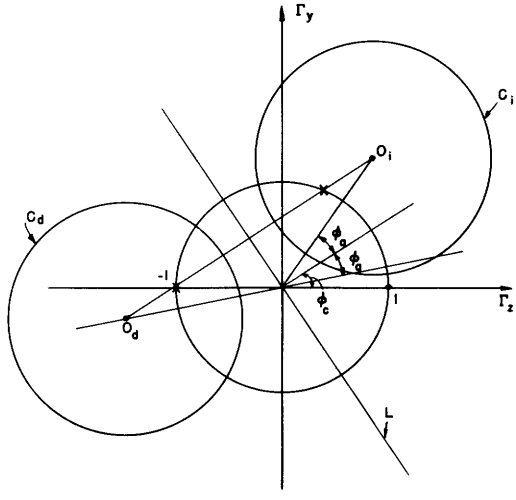

Fig. 14. Lossless transformer example. ($k = 1$, $\omega M = 1$, $n = 2$; $\phi_a = 21.8°$, $\phi_c = -33.7°$, $\psi = 0.808$).

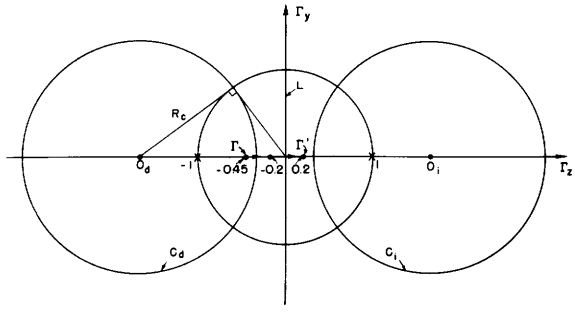

Fig. 15. Lossless transformer example. ($k = 1$, $\omega M = \infty$, $n = 2$; $\phi_a = 0$, $\phi_c = 0$, $\psi = 0.693$).

If we make k = 1 in Eq. 46, we obtain

$$\Gamma' = \frac{\Gamma\left[\frac{1}{2}\left(n+\frac{1}{n}\right)+\frac{j}{2\omega M}\right]+\left[\frac{1}{2}\left(n-\frac{1}{n}\right)+\frac{j}{2\omega M}\right]}{\Gamma\left[\frac{1}{2}\left(n-\frac{1}{n}\right)-\frac{j}{2\omega M}\right]+\left[\frac{1}{2}\left(n+\frac{1}{n}\right)-\frac{j}{2\omega M}\right]} \tag{48}$$

and

$$\left.\begin{aligned} \phi_a &= \tan^{-1}\frac{\frac{1}{2\omega M}}{\frac{1}{2}\left(n+\frac{1}{n}\right)} \\ \phi_c &= -\tan^{-1}\frac{\frac{1}{2\omega M}}{\frac{1}{2}\left(n-\frac{1}{n}\right)} \\ \sinh\psi &= \sqrt{\frac{1}{4}\left(n-\frac{1}{n}\right)^2+\frac{1}{4\omega^2M^2}} \end{aligned}\right\} \tag{49}$$

With the use of Eq. 7 we obtain the fixed points

$$\left.\begin{aligned} \Gamma_1 &= -1 \\ \Gamma_2 &= \frac{\frac{1}{2}\left(n-\frac{1}{n}\right)+\frac{j}{2\omega M}}{\frac{1}{2}\left(n-\frac{1}{n}\right)-\frac{j}{2\omega M}} \end{aligned}\right\} \tag{50}$$

Thus one fixed point is always at (-1, 0) in the Γ-plane (36). Figure 14 shows the isometric circles of Eq. 48, with $\omega M = 1$ and $n = 2$.

If we make $k \to 1$, $\omega M = \infty$ in Eq. 46, we have

$$\Gamma' = \frac{\Gamma\,\frac{1}{2}\left(n+\frac{1}{n}\right)+\frac{1}{2}\left(n-\frac{1}{n}\right)}{\Gamma\,\frac{1}{2}\left(n-\frac{1}{n}\right)+\frac{1}{2}\left(n+\frac{1}{n}\right)} \tag{51}$$

which is the transformation performed by an ideal transformer. In the Z-plane Eq. 51 corresponds to

$$Z' = \frac{nZ}{\frac{1}{n}} = n^2 Z \tag{52}$$

Equation 51 yields

$$\left.\begin{aligned} \phi_a &= 0 \\ \phi_c &= 0 \\ \sinh \psi &= \frac{1}{2}\left(n - \frac{1}{n}\right) \end{aligned}\right\} \tag{53}$$

In Fig. 15 the isometric circles of Eq. 51 are shown, with n = 2. Here we have

$$\left.\begin{aligned} O_d &= -\frac{n^2+1}{n^2-1} = -\coth \psi \\ O_i &= \frac{n^2+1}{n^2-1} = \coth \psi \\ R_c &= \left|\frac{2n}{n^2-1}\right| = 1/|\sinh \psi| \end{aligned}\right\} \tag{54}$$

For $n > 1$, the isometric circle of the direct transformation, C_d, falls in the left half-plane. When n approaches unity, the radii of the isometric circles increase until, at

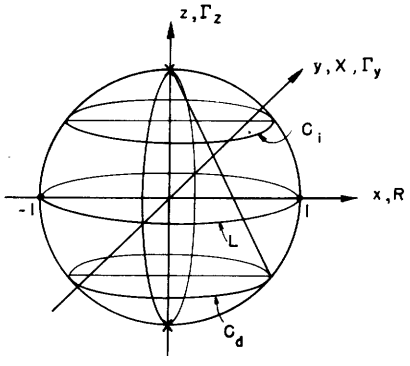

Fig. 16. The isometric circles of Fig. 15 mapped on the unit sphere.

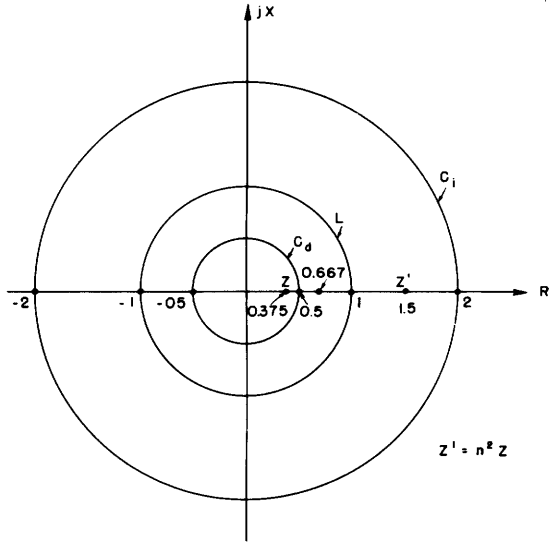

Fig. 17. The isometric circles of Fig. 15 in the Z-plane.

n = 1, they coincide with the symmetry line L. The identity $\Gamma' = \Gamma$ is obtained. For $n < 1$, C_d appears in the right half-plane.

In Fig. 16 the isometric circles in Fig. 15 are mapped on the unit sphere. Another mapping yields in the Z-plane the image circles shown in Fig. 17. As is shown in Fig. 17, in this case, the symmetry line L transforms into the unit circle of the Z-plane. Z' is obtained from Z by two inversions in C_d and L

(or L and C_i). A simple example, n = 2, Z = 0.375, is indicated by arrows in Figs. 15 and 17.

e. A New Proof of the Weissfloch Transformer Theorem for Lossless Two-Port Networks

Weissfloch's transformer theorem states that for a given frequency any bilateral lossless two-port network can be converted into an ideal transformer by coupling certain lengths of uniform lossless transmission line to each side of the network. The theorem was originally proved by Weissfloch (107) by means of the complex impedance plane. A proof in which the complex reflection-coefficient plane was utilized was given later by Weissfloch (109), and by Lueg (73, 74). An elegant graphical method for proving the theorem was given by Van Slooten (99). He used non-Euclidean geometry constructions. Such constructions, which have also been used by Deschamps (49), will be discussed in Section III.

A new simple proof of Weissfloch's transformer theorem will now be given by means of the isometric circle method. We know, from section 2.6, that for a lossless two-port network the isometric circles are orthogonal to the imaginary axis in the Z-plane and to the unit circle in the Γ-plane. Let us assume that an arbitrary lossless two-port network is represented by the isometric circles C_d and C_i in Fig. 18. The network that is chosen is elliptic, since the isometric circles intersect. The fixed points are marked as crosses. If the circles are separated, the fixed points will coalesce in the tangential case and then continue along the unit circle. These are the parabolic and the hyperbolic cases. Since the ideal transformer has its fixed points at ±1 in the Γ-plane, we shall

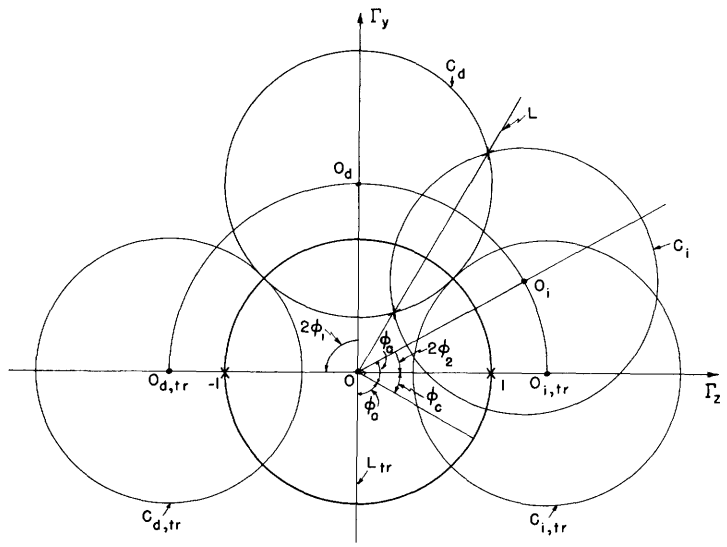

Fig. 18. The isometric circles of an arbitrary lossless two-port network.

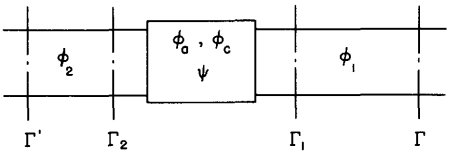

Fig. 19. An arbitrary lossless two-port network between uniform lossless transmission lines.

try to move the fixed points in Fig. 18 to these positions by connecting uniform lossless transmission lines to the input and output. With the notations of Fig. 19 we obtain (see Eqs. 44 and 30):

$$\left.\begin{aligned} \Gamma_1 &= \Gamma\, e^{-j2\phi_1}, \qquad \phi_1 = \frac{2\pi\ell_1}{\lambda_1} \\ \Gamma_2 &= \frac{\Gamma_1 \cosh\psi\, e^{j\phi_a} + \sinh\psi\, e^{-j\phi_c}}{\Gamma_1 \sinh\psi\, e^{j\phi_c} + \cosh\psi\, e^{-j\phi_a}} \\ \Gamma' &= \Gamma_2\, e^{-j2\phi_2}, \qquad \phi_2 = \frac{2\pi\ell_2}{\lambda_2} \end{aligned}\right\} \tag{55}$$

These equations yield

$$\Gamma' = \frac{\Gamma \cosh\psi\, e^{j(\phi_a-\phi_1-\phi_2)} + \sinh\psi\, e^{-j(\phi_c-\phi_1+\phi_2)}}{\Gamma \sinh\psi\, e^{j(\phi_c-\phi_1+\phi_2)} + \cosh\psi\, e^{-j(\phi_a-\phi_1-\phi_2)}} \tag{56}$$

The equation for an ideal transformer is, however, according to Eqs. 51 and 53,

$$\Gamma' = \frac{\Gamma \cosh\psi + \sinh\psi}{\Gamma \sinh\psi + \cosh\psi} \tag{57}$$

Therefore, by comparing Eqs. 56 and 57, we obtain

$$\left.\begin{aligned} \phi_1 &= \tfrac{1}{2}(\phi_a + \phi_c) \\ \phi_2 &= \tfrac{1}{2}(\phi_a - \phi_c) \end{aligned}\right\} \tag{58}$$

Thus, by choosing the lengths of the uniform transmission lines in accordance with Eq. 58, the isometric circle of the direct transformation, C_d, in Fig. 18 is rotated counterclockwise through an angle $2\phi_1$, and the isometric circle of the inverse transformation, C_i, is rotated clockwise through an angle $2\phi_2$. An ideal transformer, with the isometric circles $C_{d,tr}$ and $C_{i,tr}$, fixed points at ± 1, and a transformation ratio n^2 given by

$$Z' = n^2 Z = e^{2\psi} Z \tag{59}$$

is obtained. This proves the Weissfloch transformer theorem. It can easily be shown that the connection between the radius R_c of the isometric circles and the transformation ratio n^2 is

$$R_c = \frac{2}{\left|n - \frac{1}{n}\right|} \tag{60}$$

To illustrate this proof geometrically, a transformation of an arbitrary reflection coefficient Γ on the unit circle in the Γ-plane through an ideal transformer is shown in Fig. 20. It is seen that the transformations performed by the uniform lossless transmission line of length $\lambda\phi_1/4\pi$, the arbitrary lossless two-port network, and the uniform transmission line of length $\lambda\phi_2/4\pi$ give the same reflection coefficient Γ' as that obtained directly by a transformation through the ideal transformer.

f. Cascading of a Set of Equal Lossless Two-Port Networks

In Fig. 21 an arbitrary lossless two-port network is represented by the isometric circles C_d and C_i in the Γ-plane. An arbitrary reactance corresponding to the point Γ on the unit circle is transformed into Γ_1 by inverting in C_d and reflecting in L. If another network that is exactly equal to the first one is coupled in series, the reflection coefficient Γ_2 at its input is obtained by the same operations that have just been performed. For a set of equal networks, the reflection coefficients Γ_1, Γ_2, Γ_3, ... are obtained. It is seen in Fig. 21 that because the transformation is elliptic, a (non-Euclidean) rotation is obtained around the inner fixed point. Similar constructions can easily be performed in the parabolic and the hyperbolic cases.

g. Lossless Exponentially Tapered Transmission Lines

The fact that the exponentially tapered transmission line is one of the few examples of nonuniform transmission lines that can be calculated exactly has led to a thorough study of lines of that kind. In this section, lossless exponentially tapered transmission lines will be studied by means of the isometric circle method (7).

By expressing the ratio of the input impedance Z^i and the input characteristic impedance Z_o^i in the ratio of the output impedance Z^o and the output characteristic impedance Z_o^o, Ruhrmann (86, 87) obtains the following linear fractional transformation for the impedance transformation through a lossless exponential line:

$$\frac{\frac{Z^i}{Z_o^i}}{} = \frac{\frac{Z^o}{Z_o^o}\cos(\beta'\ell + \phi) + j \sin \beta'\ell}{\frac{Z^o}{Z_o^o} j \sin \beta'\ell + \cos(\beta'\ell - \phi)} \tag{61}$$

where

$$\sin \phi = -\frac{\mu}{2\beta} \tag{62}$$

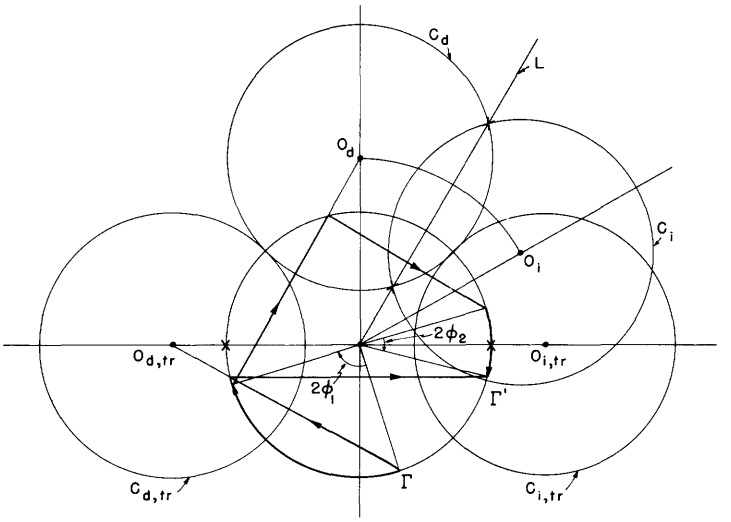

Fig. 20. A circular geometric proof of the Weissfloch transformer theorem.

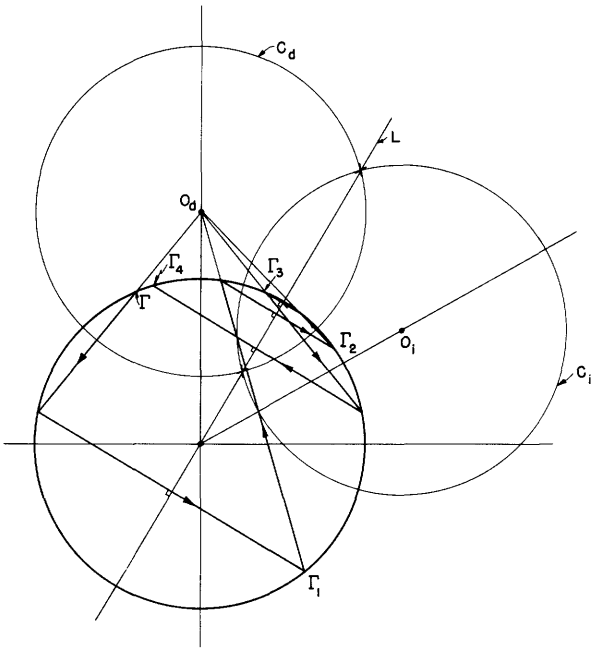

Fig. 21. Reflection-coefficient transformation through a set of equal lossless two-port networks.

Here μ is the (logarithmic) taper constant; $\beta'\ell = \beta\ell\sqrt{1 - q^2}$; $q = \sin\phi = \lambda/\lambda_c$; λ is the wavelength; λ_c is the cutoff wavelength; $\beta = 2\pi\ell/\lambda$; and ℓ is the length of the exponential line.

The characteristic impedance varies along the tapered line in accordance with the expression

$$Z_o^o = Z_o^i \, e^{\mu\ell} \tag{63}$$

If $\mu = 0$, then $\phi = 0$, and Eq. 61 reduces to the well-known expression for a lossless uniform transmission line.

In order to study Eq. 61 by the isometric circle method, we begin by "normalizing" the expression, so that the reciprocity condition, Eq. 3, is valid. We obtain

$$\frac{Z^i}{Z_o^i} = \frac{\dfrac{Z^o}{Z_o^o}\dfrac{\cos(\beta'\ell + \phi)}{\cos\phi} + j\dfrac{\sin\beta'\ell}{\cos\phi}}{\dfrac{Z^o}{Z_o^o} j\dfrac{\sin\beta'\ell}{\cos\phi} + \dfrac{\cos(\beta'\ell - \phi)}{\cos\phi}} \tag{64}$$

which is a nonloxodromic transformation, since $a + d = 2\cos\beta'\ell$ is real.

From Eq. 64 we obtain

$$\left.\begin{aligned} O_d &= j\frac{\cos(\beta'\ell - \phi)}{\sin\beta'\ell} \\ O_i &= -j\frac{\cos(\beta'\ell + \phi)}{\sin\beta'\ell} \\ R_c &= \left|\frac{\cos\phi}{\sin\beta'\ell}\right| \end{aligned}\right\} \tag{65}$$

The fixed points of Eq. 64, with the use of Eq. 7, are

$$\left.\begin{matrix} Z_{f1} \\ Z_{f2} \end{matrix}\right\} = \left\{\begin{matrix} e^{j\phi} \\ e^{j(\pi-\phi)} \end{matrix}\right. \tag{66}$$

An example of the use of the isometric circle method in the Z/Z_o-plane is shown in Fig. 22. The chosen values correspond to one of a series of examples calculated by Ruhrmann (86). The values are: $\mu = 1.074$, $\ell = 1.5$, $\lambda = 8$, $\beta = 0.785$, $\sin\phi = -0.685$, $\phi = -43.25°$, $\beta' = 0.571$, and $\beta'\ell = 49.1°$. The isometric circles are given by

$$O_d = -j\,0.0543$$

$$O_i = -j\,1.316$$

$$R_c = 0.963$$

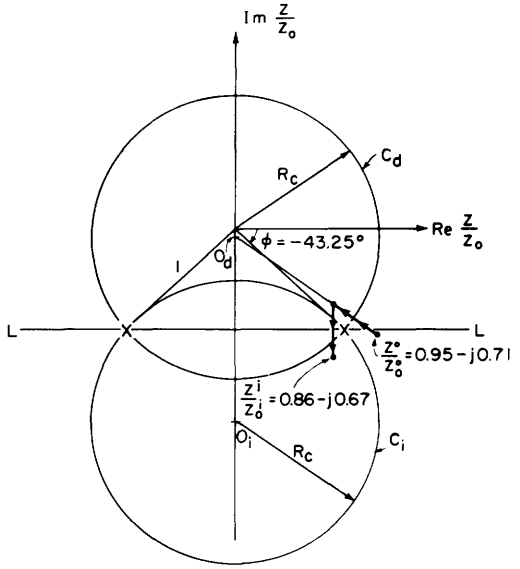

Fig. 22. Example of impedance transformation through a lossless exponential line by the isometric circle method.

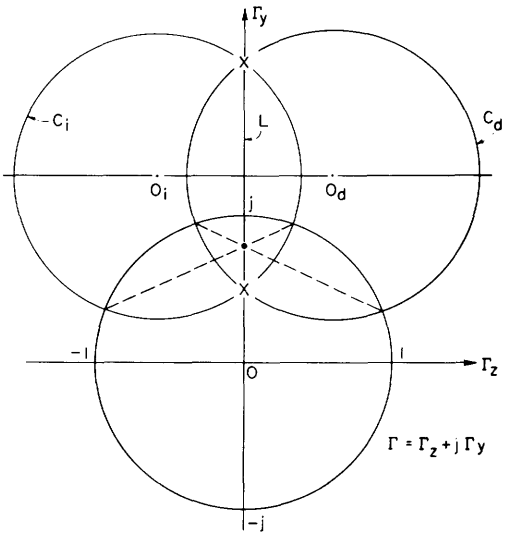

Fig. 23. Elliptic transformation in the Γ-plane.

Figure 22 shows that, by an inversion in C_d and a reflection in L, the impedance ratio $Z^o/Z_o^o = 0.95 - j\,0.71$ is transformed into $Z^i/Z_o^i = 0.67 - j\,0.86$, which checks with the values obtained by Ruhrmann.

It is interesting to compare this simple graphical method with the method described by Ruhrmann (86). Ruhrmann sets

$$\left.\begin{aligned} \frac{Z^o}{Z_o^o} &= s + jt \\ \frac{Z^i}{Z_o^i} &= u + jv \\ t &= t' + \sin\phi \end{aligned}\right\} \qquad (67)$$

After substituting Eq. 67 in Eq. 61, the equation that is obtained is split into its real and imaginary constituents u and v. Ruhrmann then lets $t' = 0$ and eliminates $\beta'\ell$ between the constituents. After some calculations, he achieves a set of circles for different s-values around the fixed points in the uv-plane. Similarly, by eliminating s between the u- and v-expressions, he obtains a set of circles for different $\beta'\ell$-values, with all circles passing through the fixed points. With an arbitrary output impedance he is able to read off the input impedance by means of the two calibrated sets of circles, provided that the coordinate system for the output impedance has been properly adjusted. By using Eq. 24, Eq. 64 transforms into

$$\Gamma' = \frac{\Gamma\left(\cos\beta'\ell - \frac{j}{\sqrt{1-q^2}}\sin\beta'\ell\right) - \frac{q}{\sqrt{1-q^2}}\sin\beta'\ell}{-\Gamma\frac{q}{\sqrt{1-q^2}}\sin\beta'\ell + \left(\cos\beta'\ell + \frac{j}{\sqrt{1-q^2}}\sin\beta'\ell\right)} \tag{68}$$

Equation 68 has the fixed points

$$\left.\begin{matrix}\Gamma_{f1}\\ \Gamma_{f2}\end{matrix}\right\} = j\left(\frac{1}{q} \mp \sqrt{\frac{1}{q^2} - 1}\right) \tag{69}$$

If $q < 1$, we have the above-cutoff, or elliptic, case (see Fig. 23).

If $q = 1$, we have the cutoff, or parabolic, case. By a limiting process Eq. 64 can be written (87)

$$\frac{Z^i}{Z^i_o} = \frac{\frac{Z^o}{Z^o_o}(1 - \beta\ell) + j\beta\ell}{\frac{Z^o}{Z^o_o}j\beta\ell + (1 + \beta\ell)} \tag{70}$$

so that

$$\Gamma' = \frac{\Gamma(1 - j\beta\ell) - \beta\ell}{-\Gamma\beta\ell + (1 + j\beta\ell)} \tag{71}$$

See Fig. 24.

If $q > 1$, we have the below-cutoff, or hyperbolic, case. If we let $\beta' = j\alpha_1$, then Eq. 64 transforms into

$$\frac{Z^i}{Z^i_o} = \frac{\frac{Z^o}{Z^o_o}\left(\cosh\alpha_1\ell - \frac{q}{\sqrt{q^2-1}}\sinh\alpha_1\ell\right) + \frac{j}{\sqrt{q^2-1}}\sinh\alpha_1\ell}{\frac{Z^o}{Z^o_o}\frac{j}{\sqrt{q^2-1}}\sinh\alpha_1\ell + \left(\cosh\alpha_1\ell + \frac{q}{\sqrt{q^2-1}}\sinh\alpha_1\ell\right)} \tag{72}$$

which, by Eq. 24, transforms into

$$\Gamma' = \frac{\Gamma\left(\cosh\alpha_1\ell - \frac{j}{\sqrt{q^2-1}}\sinh\alpha_1\ell\right) - \frac{q}{\sqrt{q^2-1}}\sinh\alpha_1\ell}{-\Gamma\frac{q}{\sqrt{q^2-1}}\sinh\alpha_1\ell + \left(\cosh\alpha_1\ell + \frac{j}{\sqrt{q^2-1}}\sinh\alpha_1\ell\right)} \tag{73}$$

The fixed points of Eq. 73 are

$$\left.\begin{matrix}\Gamma_{f1}\\ \Gamma_{f2}\end{matrix}\right\} = \frac{j}{q} \mp \sqrt{1 - \frac{1}{q^2}} \tag{74}$$

See Fig. 25.

It is interesting to study the elliptic-parabolic-hyperbolic transformation transition by projecting the Γ-plane stereographically on the Riemann unit sphere. See Fig. 26. In the elliptic case the fixed points are situated on the unit circle in the xy-plane. In Fig. 26 a straight line L_{1e} is drawn through the fixed points. The line L_{1e} has a polar L_{2e} external to the sphere. If we increase the value of q, the two lines L_{1e} and L_{2e} approach each other until, at q = 1, they cut each other perpendicularly at the point

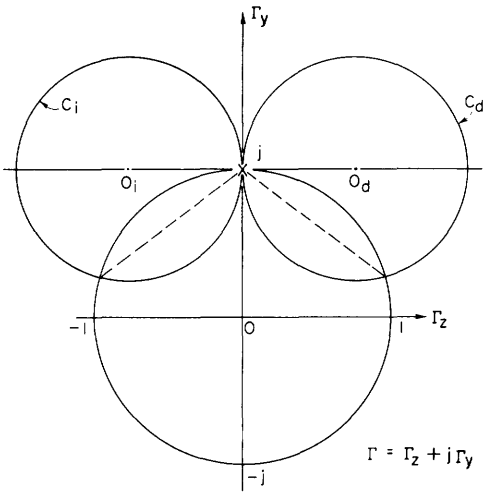

Fig. 24. Parabolic transformation in the Γ-plane.

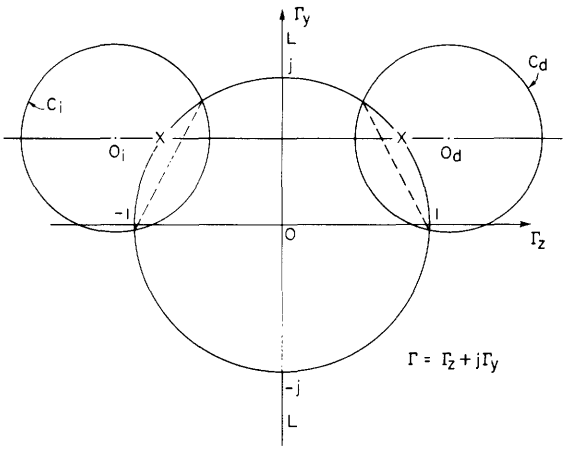

Fig. 25. Hyperbolic transformation in the Γ-plane.

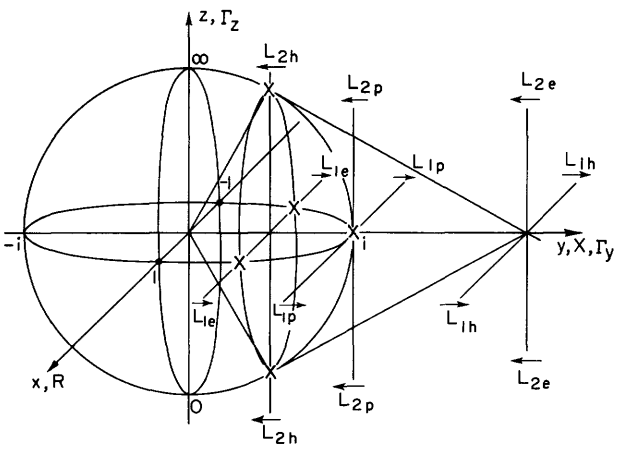

Fig. 26. Positions of the fixed points for an exponential line on the Riemann unit sphere.

$(x, y, z) = (0, 1, 0)$: this is the parabolic case, and the lines are denoted L_{1p} and L_{2p} in Fig. 26. If q is increased more, L_{1p} and L_{2p}, now called L_{1h} and L_{2h}, separate, and L_{2h} cuts the sphere in the fixed points of the hyperbolic case, while L_{1p} is external. Theoretically, if q is varied between the limits $0 \leq q \leq \infty$, we obtain uniform transmission line → exponential line → ideal transformer, in the limits.

h. Lossless Waveguides

Impedance transformations through pieces of lossless waveguide can be treated by the isometric circle method in the same way as the exponential line (8) in section 2.8g. Both a lossless waveguide and a lossless exponentially tapered transmission line act as highpass filters. However, in the parabolic case, the exponential line has its fixed point at $(\Gamma_z, \Gamma_y) = (0, 1)$; the TE mode in a rectangular waveguide has its fixed point at (1, 0); and the TM mode has its fixed point at (-1, 0).

III. IMPEDANCE TRANSFORMATIONS BY THE CAYLEY-KLEIN MODEL OF TWO-DIMENSIONAL HYPERBOLIC SPACE

3.1 INTRODUCTION

Besides the disadvantage of not transforming the isometric circles in the impedance plane into the isometric circles in the reflection-coefficient plane, the isometric circle method often requires a considerable amount of space when the radii of the isometric circles are large. In order to compress the complex plane, the writer began a study of non-Euclidean hyperbolic geometry. Of the two applicable existing models of two-dimensional hyperbolic space, the Poincaré model and the Cayley-Klein model (see Appendix 1), the latter proved to be quite useful for impedance transformations through bilateral lossless two-port networks.

3.2 THE CAYLEY-KLEIN DIAGRAM

The Cayley-Klein model of two-dimensional hyperbolic space has been used in engineering since 1946 (see Appendix 4). The model is called "the hyperbolic plane" by Klein (66), "the Cayley diagram" (C-diagram) by Van Slooten (99), and "the projective chart" by Deschamps (48). In honor of the two mathematicians, A. Cayley and F. Klein, whose papers,"A Sixth Memoir upon Quantics" (41) and "Über die Sogenannte Nicht-Euklidische Geometrie" (63), form the basis for the creation of the diagram, the writer has chosen to call the model "the Cayley-Klein diagram" (CK-diagram).

The Cayley-Klein model of two-dimensional hyperbolic space, or the Cayley-Klein diagram, is obtained by stereographically mapping a complex plane on the Riemann unit sphere and then projecting the sphere orthographically on an arbitrary plane (see Appendix 2). Thus the whole complex plane is mapped into a circle, every point inside the circle corresponding to two points of the complex plane. In network theory the Cayley-Klein diagram is usually situated in the reflection-coefficient plane. The transformation of the Smith chart into the Cayley-Klein diagram, and vice versa, can easily be performed by means of the transformation $\mathscr{B}$ ($\mathscr{B}^{-1}$) introduced by Deschamps (48).

In the Cayley-Klein diagram the geometry of Gauss, Bolyai, and Lobachevsky is valid (66). This geometry was called "hyperbolic" by Klein. In the diagram, distance is defined as one-half of the natural logarithm of the cross ratio between the given points and the two points on the unit circle which are cut out by a line through the given points. The distance, called "hyperbolic," can be measured directly by means of the ingenious hyperbolic protractor invented by Deschamps (49). A hyperbolic distance is invariant for projective transformations that transform the fundamental or absolute curve (in this case, the unit circle) into

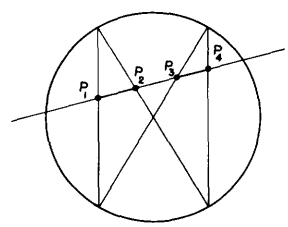

Fig. 27. Equal hyperbolic distances.

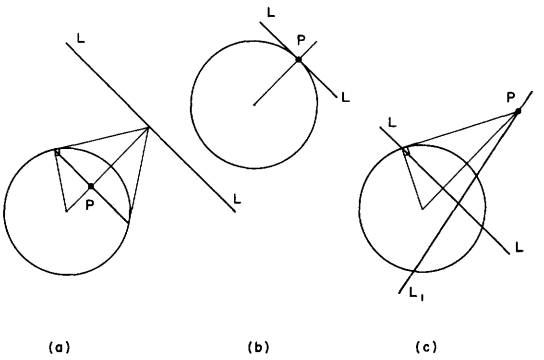

Fig. 28. Definition of pole and polar.

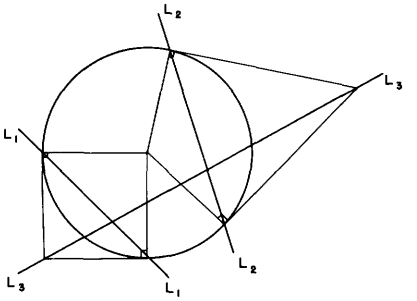

Fig. 29. Construction of a line L_3, non-Euclidean perpendicular to two lines, L_1 and L_2.

itself. A definition similar to the one for distance is valid for the angle in the Cayley-Klein diagram.

In Fig. 27, the distances $\overline{P_1P_2}$ and $\overline{P_3P_4}$ on the same straight line are equal hyperbolic distances. If we slide the "vector" $\overline{P_1P_2}$ along the line (99), it grows smaller and smaller from the Euclidean point of view, as we approach the unit circle. Thus the circle corresponds to infinity, which is the reason why it is called the "fundamental" or "absolute" curve of the two-dimensional hyperbolic space.

In Fig. 28a, b, and c the point P is called the "pole" of the line L, and L is the "polar" of the point P. A line L_1, through the pole P of a line L, cuts L perpendicularly inside the unit circle from the point of view of non-Euclidean hyperbolic geometry (see Fig. 28c). Figure 29 shows the constructions for finding the common perpendicular L_3 to two given lines L_1 and L_2 which do not intersect within or on the absolute curve. At the center of the sphere, the non-Euclidean (elliptic) angle and the ordinary Euclidean angle are equal. Therefore, if we want to find the value of a non-Euclidean angle between two straight lines, both of which cut the unit circle, then the simplest procedure is to perform projective transformations so that the crossover point of the two lines is moved to the center of the unit circle. Such a transformation was introduced by Deschamps (48, 49). Deschamps' construction is shown in Fig. 30. The elliptic angle

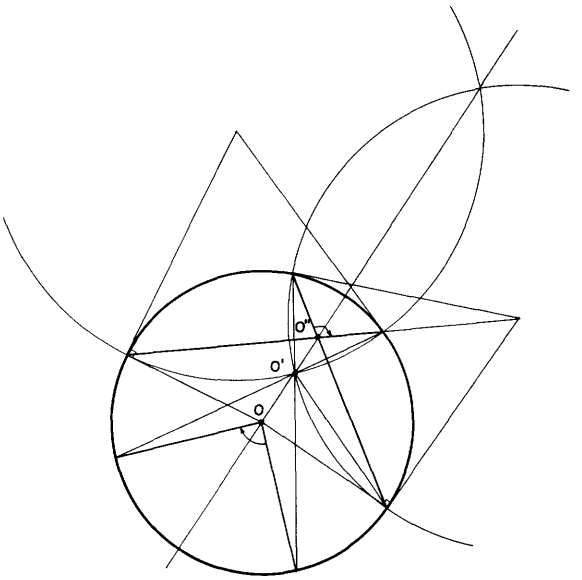

Fig. 30. Deschamps' construction for measuring an elliptic angle.

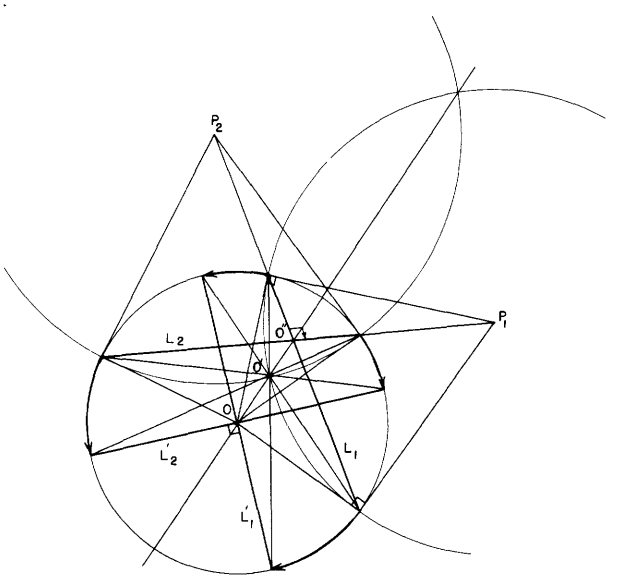

Fig. 31. Elliptic angle evaluation.

at O" is, by a projection through the "iconocenter" O', moved to the center O of the circle. Figure 31 shows the construction in more detail. The straight lines L_1 and L_2 are transformed by a stretching along the line through O" and O to the positions L'_1 and L'_2 (the stretching is indicated by arrows). Figure 31 is also helpful in convincing us that a line through an arbitrary point P_1 cuts its polar L_1 perpendicularly, from a non-Euclidean point of view.

3.3 VAN SLOOTEN'S METHOD

Van Slooten uses the Cayley-Klein diagram for the purpose of transforming reactances through lossless two-port networks. Since the unit circle of the diagram corresponds to the imaginary axis of the complex impedance plane, the three measurements that are needed to characterize the network yield six points on the circle. If two points, for instance A and B, are connected crosswise with their image points A' and B', and this operation is repeated for B, C, B', and C', and for A, C, A', and C', three crossover points, P_1, P_2, and P_3, are obtained. These points are, according to the Pascal theorem (56), situated on a straight line, the "Pascal line" (see Fig. 32). The Pascal theorem states: If a hexalateral, a configuration with six sides, is inscribed in a nondegenerate conic, the points of intersection of the pairs of opposite sides are collinear. In Fig. 32, the conic is a circle and the hexalateral is AB'CA'BC'A. Depending upon whether or not the Pascal line cuts the circle in two real, two coalescing, or two imaginary points, which are the fixed points of the transformation, the hyperbolic, parabolic, or elliptic case is obtained.

In the hyperbolic case, Fig. 33, all points are stretched from one fixed point to the other. Points on the Pascal line remain on this line. The amount of stretching is obtained graphically by Van Slooten by the performance of two perspectivities, the centers of which are situated on the line. These perspectivities transform an arbitrary point on the unit circle into its image point that is also on the unit circle. In Fig. 33, the points C and C' furnish an example. Any two points on the Pascal line with the same hyperbolic distance can be selected. A sliding vector is obtained along the line by Van Slooten. In Fig. 34 all marked lengths on the Pascal line have the same non-Euclidean distance.

Outside the circle hyperbolic geometry is not valid. Here the geometry is "elliptic," which means that a straight line has to be considered closed, and to have the finite length $j\pi$. Also, the length of a distance, the end points of which are absolute conjugate poles (i.e., one end point is situated on the polar of the other) is $j\pi/2$ (cf. references 91 and 94). The centers of perspectivity can, however, be constructed in exactly the same way as before, as shown in Fig. 34. The only difference is that the sliding vector outside the circle is directed in the opposite direction to the one inside the circle.

In performing one of the perspectivities, for instance, C to C_1 in Fig. 33, we actually rotate C 180° around the center of perspectivity P_1. The same operation can be thought of when the center of perspectivity is outside the circle. The distance $\overline{C'P_2}$ in Fig. 35 is equal to the distance $\overline{P_2C'}$ which is determined along the line $C'P_2$ that passes through the point corresponding to infinity in Euclidean space. This property can easily be proved by constructing the polar of the point P_2 (see Fig. 35), and taking into consideration the second property of elliptic space which was mentioned above. From Fig. 35, we obtain

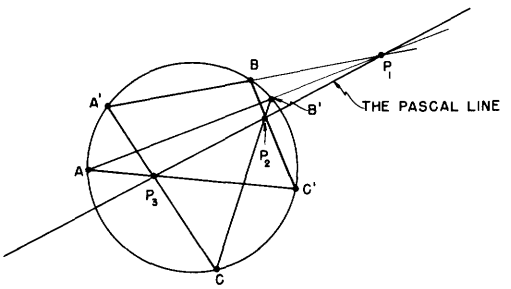

Fig. 32. Pascal's theorem.

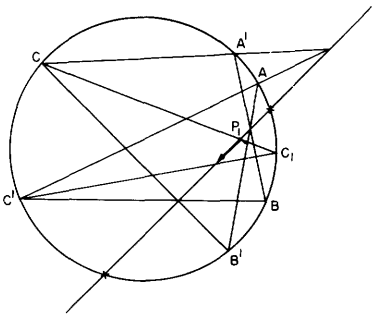

Fig. 33. Example of a hyperbolic transformation in the Cayley-Klein diagram.

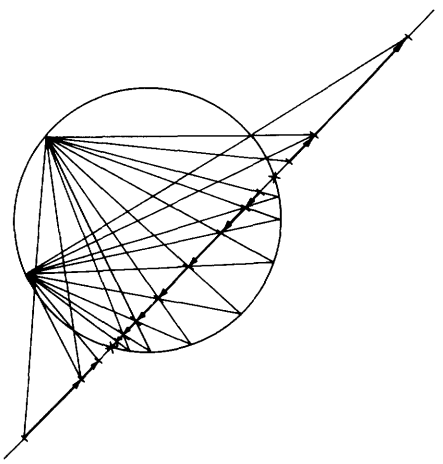

Fig. 34. Construction of equal non-Euclidean distances along the Pascal line.

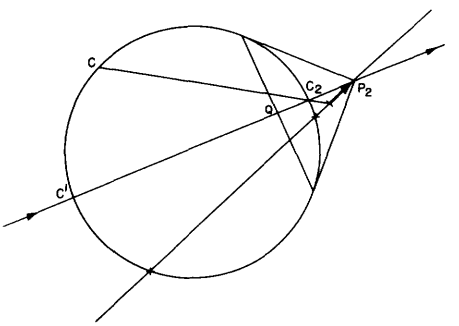

Fig. 35. A perspectivity with its center outside the circle.

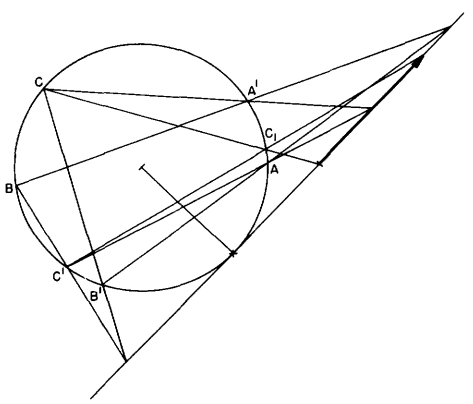

Fig. 36. Example of a parabolic transformation in the Cayley-Klein diagram.

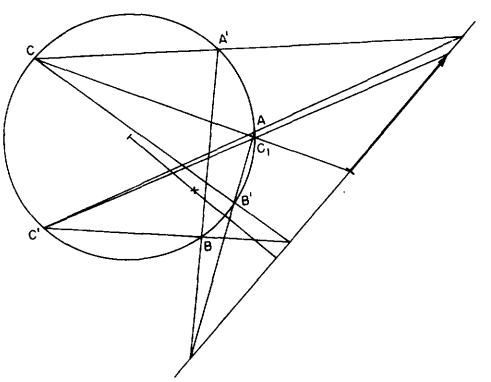

Fig. 37. Example of an elliptic transformation in the Cayley-Klein diagram.

$$C'Q = QC_2$$

$$QC_2 + C_2P_2 = P_2C' + C'Q = j\pi/2$$

$$C'P_2 = C'Q + QC_2 + C_2P_2 = C'Q + P_2C' + C'Q$$

$$= QC_2 + P_2C' + C'Q = P_2C' + C'Q + QC_2 = P_2C_2$$

Q. E. D.

In the parabolic case, the Pascal line is tangent to the unit circle of the Cayley-Klein diagram (see Fig. 36). All graphical constructions are the same as in the previous case.

In the elliptic case, the Pascal line is completely outside the circle. The constructions are the same as in the former cases (see Fig. 37).

3.4 EXTENSION OF VAN SLOOTEN'S METHOD

The principle of transforming arbitrary impedances through lossless two-port networks is very simple. Instead of a point on the circle, we now have a point inside the circle to transform by two 180° rotations around the two centers of perspectivity. The method is thus a direct extension of Van Slooten's method of transforming reactances through lossless two-port networks.

In the hyperbolic case, we use the construction in Fig. 34 to obtain equal hyperbolic distances. In Fig. 38, the point P_1 represents the given impedance value. We select an arbitrary point A on the circle, draw the butterfly-shaped figure shown in Fig. 27, and thus obtain the image point P_2 to the given point P_1. The operation is then repeated at the other center of perspectivity so that we obtain the final image point P_3 which represents the transformed impedance value. All points: P_1, P_2, P_3, and the two fixed points are situated on a non-Euclidean circle that has its center M outside the circle. The Pascal line is the polar to the point M. A circle like this is called an ideal circle or a hypocycle.

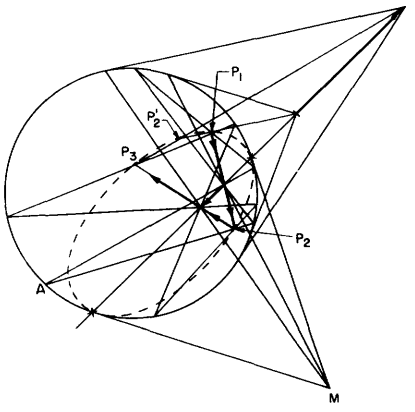

Fig. 38. Transformation of an arbitrary impedance through a hyperbolic network.

If, instead of the two centers of perspectivity inside the circle, we select two points outside the circle; for instance, the poles of the two lines (non-Euclidean) perpendicular to the Pascal line and through the two points inside the circle, the impedance transformation will be composed of two non-Euclidean reflections, P_1 to P_2', and

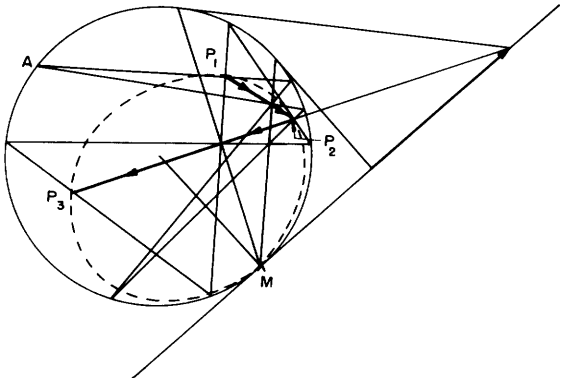

Fig. 39. Transformation of an arbitrary impedance through a parabolic network.

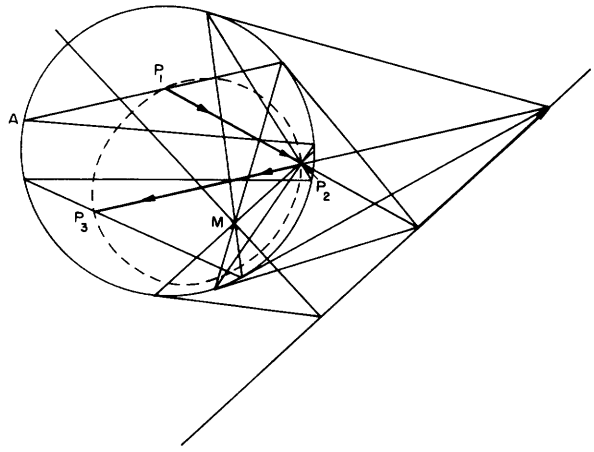

Fig. 40. Transformation of an arbitrary impedance through an elliptic network.

P_2' to P_3, in the two lines (see Fig. 38).

In the parabolic and elliptic cases, Figs. 39 and 40, the second method of graphical construction that was mentioned for the hyperbolic case is performed, since, in these cases, we do not have any centers of perspectivity inside the circle. In the parabolic case, the points P_1, P_2, P_3, and the fixed point (coalescing fixed points) are situated on a non-Euclidean circle with its center M in the fixed point. This circle is called a limit curve or a horicycle. In the elliptic case, the points P_1, P_2, and P_3 are situated on a "proper" non-Euclidean circle with the fixed point M as center.

The method of using the butterfly-shaped figure for the transformation of arbitrary impedances through lossless two-port networks was found independently by de Buhr (37) and by the author. If a hyperbolic protractor is available it may, of course, be used directly.

3.5 TRANSFER OF THE ISOMETRIC CIRCLE METHOD TO THE CAYLEY-KLEIN DIAGRAM

We have seen in previous sections that the isometric circles of a lossless two-port network are orthogonal to the unit circle of the complex reflection-coefficient plane. Examples of the three different nonloxodromic transformations are shown in Figs. 23-25. If these examples are transformed into the Cayley-Klein diagram, the isometric circles are transformed into straight lines indicated by dashed lines in Figs. 23-25. Thus, the operations prescribed by the isometric circle method, in which an inversion is made in the isometric circle for the direct transformation, followed by a reflection in the symmetry line L of the two isometric circles, correspond to the two non-Euclidean reflections performed in the two polars, as has been described. Therefore, the isometric

circle method, transferred to the Cayley-Klein diagram, is seen to be a special case of the extended Van Slooten method. In the transferred isometric circle method, one of the centers of perspectivity is situated at the point that corresponds to infinity in Euclidean space.

IV. IMPEDANCE TRANSFORMATIONS BY THE CAYLEY-KLEIN MODEL OF THREE-DIMENSIONAL HYPERBOLIC SPACE

4.1 INTRODUCTION

It was shown in Section III how the isometric circle method can be transferred to the Cayley-Klein model of two-dimensional hyperbolic space, called the Cayley-Klein diagram. In a generalized form, the method proved to be useful for impedance transformations through bilateral lossless two-port networks. In this section we shall show that a transfer of the isometric circle method to the Cayley-Klein model of three-dimensional hyperbolic space is, after a similar generalization, of equal value for impedance transformations through bilateral lossy two-port networks.

4.2 STEREOGRAPHIC MAPPING OF THE Z-PLANE ON THE RIEMANN UNIT SPHERE

A point $Z = R + jX$ in the complex impedance plane is transformed into a point (x, y, z) on the surface of the Riemann unit sphere by the following stereographic mapping with the top of the sphere $(0, 0, 1)$ as the projection center (see Fig. 8):

$$\left.\begin{aligned} x &= \frac{2R}{R^2 + X^2 + 1} \\ y &= \frac{2X}{R^2 + X^2 + 1} \\ z &= \frac{R^2 + X^2 - 1}{R^2 + X^2 + 1} \end{aligned}\right\} \tag{75}$$

The inverse transformation is

$$\left.\begin{aligned} R &= \frac{x}{1 - z} \\ X &= \frac{y}{1 - z} \end{aligned}\right\} \tag{76}$$

or

$$Z = \frac{x + jy}{1 - z} = \frac{1 + z}{x - jy} \tag{77}$$

4.3 IMPEDANCE AND POWER TRANSFORMATIONS IN THREE- AND FOUR-DIMENSIONAL SPACES

If we write

$$\left.\begin{aligned} R &= \frac{Z + Z^*}{2} \\ X &= \frac{Z - Z^*}{2j} \end{aligned}\right\} \tag{78}$$

then Eqs. 75 transform into

$$\left.\begin{aligned} x &= \frac{Z + Z^*}{ZZ^* + 1} \\ y &= -j\,\frac{Z - Z^*}{ZZ^* + 1} \\ z &= \frac{ZZ^* - 1}{ZZ^* + 1} \end{aligned}\right\} \tag{79}$$

An additional substitution,

$$Z = \frac{V}{I} \tag{4}$$

yields

$$\left.\begin{aligned} x &= \frac{VI^* + V^*I}{VV^* + II^*} \\ y &= -j\,\frac{VI^* - V^*I}{VV^* + II^*} \\ z &= \frac{VV^* - II^*}{VV^* + II^*} \end{aligned}\right\} \tag{80}$$

If we set

$$\left.\begin{aligned} P_1 &= \tfrac{1}{2}(VI^* + V^*I) = \mathrm{Re}(VI^*) &&= \tfrac{1}{2}(Q_2 + Q_3) \\ P_2 &= -\tfrac{j}{2}(VI^* - V^*I) = \mathrm{Im}(VI^*) &&= -\tfrac{j}{2}(Q_2 - Q_3) \\ P_3 &= \tfrac{1}{2}(VV^* - II^*) = \tfrac{1}{2}(|V|^2 - |I|^2) &&= \tfrac{1}{2}(Q_1 - Q_4) \\ P_4 &= \tfrac{1}{2}(VV^* + II^*) = \tfrac{1}{2}(|V|^2 + |I|^2) &&= \tfrac{1}{2}(Q_1 + Q_4) \end{aligned}\right\} \tag{81}$$

we obtain

$$\left.\begin{aligned} x &= \frac{P_1}{P_4} \\ y &= \frac{P_2}{P_4} \\ z &= \frac{P_3}{P_4} \end{aligned}\right\} \tag{82}$$

Thus, in homogeneous coordinates the equation for the unit sphere is

$$P_1^2 + P_2^2 + P_3^2 - P_4^2 = 0 \tag{83}$$

If we insert Eq. 1 in Eq. 81, we obtain a linear equation system expressing the power quantities P_i', i = 1, 2, 3, and 4, at the input of the two-port network into the power quantities P_i, i = 1, 2, 3, and 4, at the output:

$$\left.\begin{aligned} P_1' &= a_1P_1 + a_2P_2 + a_3P_3 + a_4P_4 \\ P_2' &= b_1P_1 + b_2P_2 + b_3P_3 + b_4P_4 \\ P_3' &= c_1P_1 + c_2P_2 + c_3P_3 + c_4P_4 \\ P_4' &= d_1P_1 + d_2P_2 + d_3P_3 + d_4P_4 \end{aligned}\right\} \tag{84}$$

in which, by using Eq. 26, we have

$$\left.\begin{aligned} a_1 &= a'd' + a''d'' + b'c' + b''c'' \\ a_2 &= a'd'' - a''d' + b''c' - b'c'' \\ a_3 &= a'c' + a''c'' - b'd' - b''d'' \\ a_4 &= a'c' + a''c'' + b'd' + b''d'' \\ b_1 &= a''d' - a'd'' + b''c' - b'c'' \\ b_2 &= a'd' + a''d'' - b'c' - b''c'' \\ b_3 &= a''c' - a'c'' - b''d' + b'd'' \\ b_4 &= a''c' - a'c'' + b''d' - b'd'' \\ c_1 &= a'b' + a''b'' - c'd' - c''d'' \\ c_2 &= a'b'' - a''b' - c'd'' + c''d' \\ c_3 &= \tfrac{1}{2}(a'^2 + a''^2 - b'^2 - b''^2 - c'^2 - c''^2 + d'^2 + d''^2) \\ c_4 &= \tfrac{1}{2}(a'^2 + a''^2 + b'^2 + b''^2 - c'^2 - c''^2 - d'^2 - d''^2) \\ d_1 &= a'b' + a''b'' + c'd' + c''d'' \\ d_2 &= a'b'' - a''b' + c'd'' - c''d' \\ d_3 &= \tfrac{1}{2}(a'^2 + a''^2 - b'^2 - b''^2 + c'^2 + c''^2 - d'^2 - d''^2) \\ d_4 &= \tfrac{1}{2}(a'^2 + a''^2 + b'^2 + b''^2 + c'^2 + c''^2 + d'^2 + d''^2) \end{aligned}\right\} \tag{85}$$

We write Eq. 84 in matrix form as

$$P' = MP \tag{86}$$

where M is a real 4×4 matrix. The fact that Eq. 83 is invariant under the transformation makes the matrix M belong to the G_+ subgroup of the proper Lorentz group (78). This implies the following conditions:

$$\left.\begin{aligned} a_i^2 + b_i^2 + c_i^2 - d_i^2 &= 1, \qquad i = 1,2,3 \\ -a_4^2 - b_4^2 - c_4^2 + d_4^2 &= 1 \\ a_1a_2 + b_1b_2 + c_1c_2 - d_1d_2 &= a_1a_3 + b_1b_3 + c_1c_3 - d_1d_3 \\ = a_1a_4 + b_1b_4 + c_1c_4 - d_1d_4 &= a_2a_3 + b_2b_3 + c_2c_3 - d_2d_3 \\ = a_2a_4 + b_2b_4 + c_2c_4 - d_2d_4 &= a_3a_4 + b_3b_4 + c_3c_4 - d_3d_4 = 0 \end{aligned}\right\} \tag{87}$$

Thus we have $16 - 10 = 6$ independent conditions that are valid for the coefficients in the matrix M, which checks with Eqs. 1, 3, and 26. Equation 86 can be considered as a transformation in a four-dimensional pseudo-Euclidean space with Lorentz metric. It can also be considered to represent ∞^6 different collineations that transform the surface of the unit sphere, expressed in homogeneous coordinates in Eq. 82, into itself. This surface can be considered the absolute surface of a Cayley-Klein model of three-dimensional hyperbolic space. In homogeneous coordinates, Eq. 86 is, then, a projective transformation and it is geometrically represented by a non-Euclidean movement in the Cayley-Klein model.

There are two possible series of correspondences in connection with the Riemann sphere. The first is the point-to-point relation between the complex plane, the surface of the Riemann sphere, and the complex projective line. The second series is the point-to-point relation between the interior of the Riemann sphere and the Gauss-Bolyai-Lobachevsky non-Euclidean hyperbolic geometry. The important rôle of the Riemann sphere, that of being the link between the two series of correspondences, is evident. In the study of different geometries and their invariant properties, we are irresistibly drawn back to the famous Erlangen program imparted by Klein in 1872, in which he unified the principal geometries (62). See section 1.2.

A simple calculation yields an interesting transformation for the quantities Q_1, Q_2, Q_3, and Q_4 in Eq. 81. If we form the quantities into a four-vector, we obtain

$$\begin{pmatrix} Q_1' \\ Q_2' \\ Q_3' \\ Q_4' \end{pmatrix} = \begin{pmatrix} V'V'^* \\ V'I'^* \\ V'^*I' \\ I'I'^* \end{pmatrix} = \begin{pmatrix} aa^* & ab^* & ba^* & bb^* \\ ac^* & ad^* & bc^* & bd^* \\ ca^* & cb^* & da^* & db^* \\ cc^* & cd^* & dc^* & dd^* \end{pmatrix} \begin{pmatrix} Q_1 \\ Q_2 \\ Q_3 \\ Q_4 \end{pmatrix} = LQ \tag{88}$$

The 4×4 matrix L in Eq. 88 is composed of the elements of the 2×2 matrix in Eq. 2 in a regular and simple manner. The matrix is called a Kronecker product (78).

4.4 TRANSFER OF THE ISOMETRIC CIRCLE METHOD TO THE CAYLEY-KLEIN MODEL OF THREE-DIMENSIONAL HYPERBOLIC SPACE

In order to study how the isometric circle method can be transferred to the three-dimensional Cayley-Klein model, let us select a simple example of a loxodromic transformation. The impedance transformation through a lossy uniform transmission line can be written

$$Z' = \frac{Z \cosh \psi + \sinh \psi}{Z \sinh \psi + \cosh \psi} \tag{89}$$

where the load impedance Z and the input impedance Z' are both normalized to the characteristic impedance, and $\psi = \psi' + j\psi'' = \gamma \ell$, where γ is the complex propagation constant, and ℓ is the length of the line. In Eq. 89 it is assumed that the losses are small; the characteristic impedance is considered real. This assumption simply corresponds to a rotation of the complex impedance plane and the Riemann sphere through an angle equal to the phase angle of the complex characteristic impedance, so that the fixed points move to the points $(\pm 1, 0, 0)$.

The loxodromic transformation, Eq. 89, can be split into a hyperbolic transformation that represents a pure stretching of the surface of the sphere along the x-axis and an elliptic transformation that represents a pure rotation of the sphere around the x-axis. Thus

$$\left.\begin{aligned} Z_1 &= \frac{Z \cosh \psi' + \sinh \psi'}{Z \sinh \psi' + \cosh \psi'} \\ Z' &= \frac{Z_1 \cos \psi'' + j \sin \psi''}{Z_1 j \sin \psi'' + \cos \psi''} \end{aligned}\right\} \tag{90}$$

If we select, for example, the values $\psi' = 0.7125$ and $\psi'' = 0.686$, then the isometric circles of the three different transformations are given by

$$O_{d,\,lox} = -\frac{\cosh \psi}{\sinh \psi} = 1.095\, e^{j\,153.4^\circ} = -O_{i,\,lox}$$

$$R_{c,\,lox} = 1$$

$$O_{d,\,hyp} = -\frac{\cosh \psi'}{\sinh \psi'} = -1.634 = -O_{i,\,hyp}$$

$$R_{c,\,hyp} = 1.291$$

$$O_{d,ell} = -\frac{\cos \psi''}{j \sin \psi''} = j\ 1.222 = -O_{i,ell}$$

$$R_{c,ell} = 1.577$$

In Fig. 41 the isometric circles are shown, together with their symmetry lines L_{lox}, L_{hyp}, and L_{ell}. According to the isometric circle method Z' is obtained graphically from Z in the complex plane by: (a) an inversion in the isometric circle of direct transformation, C_d; (b) a reflection in the symmetry line L; and (c) a rotation around the center O_i of the circle of the inverse transformation through an angle -2 arg (a+d). These transformations, $(1, 0) \rightarrow P_1 \rightarrow P_2 \rightarrow (1, 0)$, are indicated by arrows in Fig. 41, in which it is shown that the fixed point (1, 0) transforms into itself. The rotation angle is -2 arg (a+d) = -53.2°.

If we split the loxodromic transformation, 2 × 2 = 4 graphical constructions are obtained in Fig. 41, both sets transforming the fixed point (1, 0) into itself,

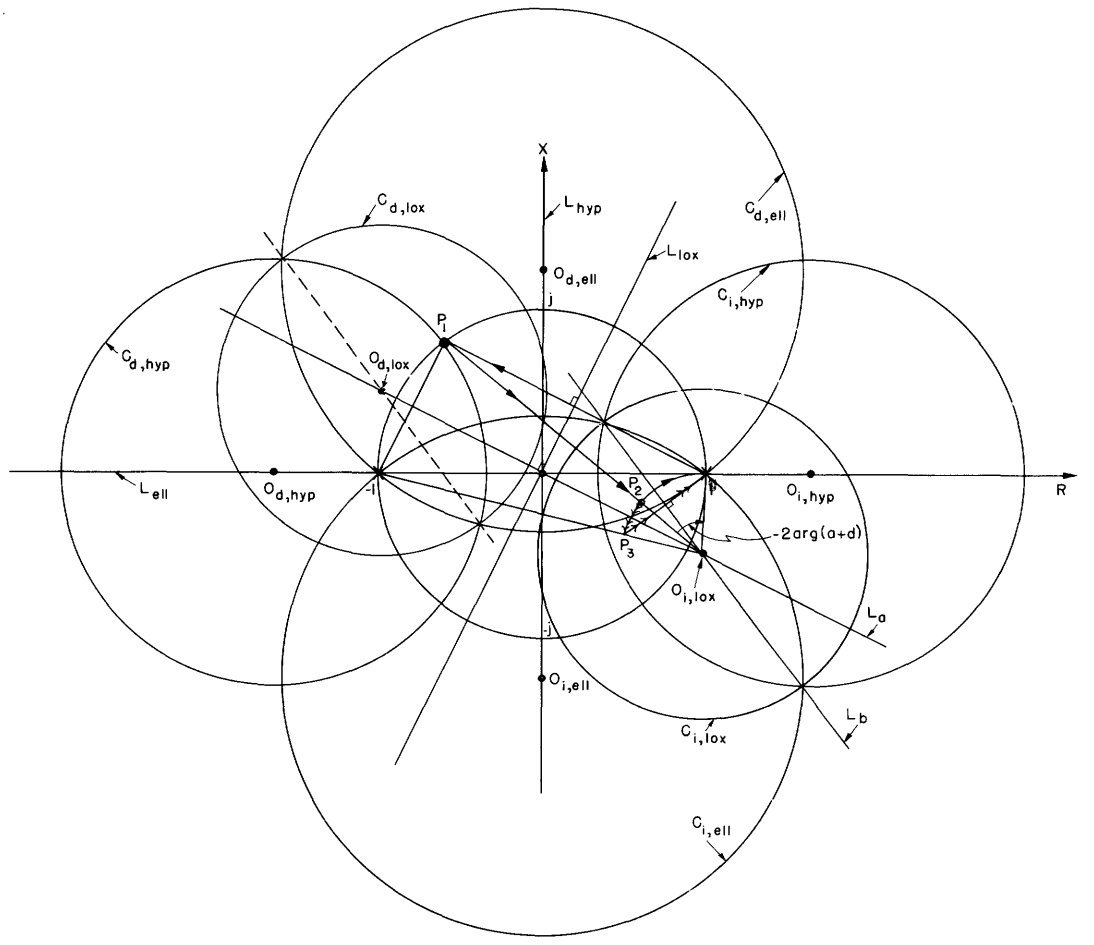

Fig. 41. Impedance transformation through a lossy transmission line.

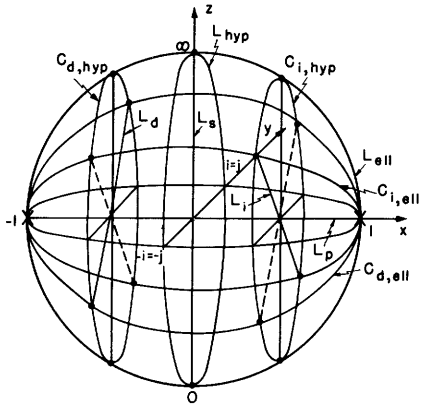

Fig. 42. The isometric circles and symmetry lines of the hyperbolic and elliptic constituents of a loxodromic transformation mapped on the unit sphere.

$(1, 0) \rightarrow (-1, 0) \rightarrow (1, 0)$ and $(1, 0) \rightarrow (1, 0) \rightarrow (1, 0)$. We now project Fig. 41 stereographically on the Riemann sphere. Both the isometric circles and the symmetry lines transform into circles on the sphere, which are great circles through the top of the sphere. On the sphere, the inversions and reflections in the complex plane correspond to non-Euclidean reflections in planes through the image circles on the sphere (66, 89). Figure 42 shows the isometric circles and symmetry lines belonging to the hyperbolic and elliptic transformations mapped on the sphere. It is evident that the four consecutive reflections in planes through $C_{d,hyp}$, L_{hyp}, $C_{d,ell}$, and L_{ell} can be exchanged for two reflections in the straight lines L_d and L_s, which are the cut lines between the planes through $C_{d,hyp}$ and $C_{d,ell}$, and L_{hyp} and L_{ell}, respectively. The loxodromic transformation can, of course, also be performed by two non-Euclidean reflections in the straight lines L_s and L_i, where L_s is the same as before, and L_i is the cut line between planes through $C_{i,hyp}$ and $C_{i,ell}$.

The two non-Euclidean reflections in L_s and L_i correspond to the three operations prescribed by the isometric circle method. This can be shown by splitting the third operation of this method, the rotation, into two reflections in two straight lines L_a and L_b, as indicated by double-headed arrows in Fig. 41. The loxodromic transformation can now be performed by two reflections in the straight lines L_{lox} and L_a, an inversion in $C_{i,lox}$, and a reflection in L_b ($(1, 0) \rightarrow P_1 \rightarrow (-1, 0) \rightarrow P_3 \rightarrow (1, 0)$ in Fig. 41). If we map L_{lox}, L_a, $C_{i,lox}$, and L_b on the sphere, we find that planes through L_{lox} and L_a cut perpendicularly through the straight line L_s, and that planes through $C_{i,lox}$ and L_b cut non-Euclidean perpendicularly through the line L_i. (The plane through L_b passes through the top of the sphere.) These properties are evident from the facts that the stereographic mapping is conformal and that planes through two orthogonal circles on the surface of the sphere are non-Euclidean perpendicular (66).

Thus we have found that for a loxodromic transformation, the three operations of the isometric circle method correspond to two non-Euclidean reflections in the straight lines L_d and L_s, or L_s and L_i in the three-dimensional Cayley-Klein model. The straight lines obtained by the isometric circle method constitute, however, only a special case, analogously to the two-dimensional case treated in section 3.3. Therefore, any two non-Euclidean lines perpendicular to the line through the fixed points, which

have the right non-Euclidean distance and angle, will do the job.

We can write the canonic form of the linear fractional transformation in the following form:

$$q = \frac{Z' - Z_{f1}}{Z' - Z_{f2}} \cdot \frac{Z - Z_{f2}}{Z - Z_{f1}} \tag{91}$$

Therefore, from Eq. 9, we obtain

$$\lambda' + j\lambda'' = \frac{1}{2} \ln \frac{Z' - Z_{f1}}{Z' - Z_{f2}} \cdot \frac{Z - Z_{f2}}{Z - Z_{f1}} \tag{92}$$

By using Schilling's geometrical representation (88, 89) of a "complex angle" (or "complex distance"), we find that λ' constitutes the non-Euclidean distance between L_d and L_s along L_{p1}, the straight line connecting the fixed points on the unit sphere, and that λ'' constitutes the non-Euclidean angle between planes through L_d and L_{p1}, and L_s and L_{p1}. In the loxodromic case, corresponding to impedance transformations through lossy two-port networks, the multiplier q is complex and we obtain a spiral movement around the line L_{p1} that transforms into itself. The line L_{p1} and its polar L_{p2} that is situated outside the sphere are the only lines that are transformed into themselves under the transformation. We therefore denote L_{p1} "the inner axis," and L_{p2} "the outer axis" of the transformation. A spiral movement around L_{p1} carries with it a spiral movement around L_{p2}.

The nonloxodromic transformations, which correspond to impedance transformations through lossless two-port networks, and which were treated in Section III, are special cases of the loxodromic transformation. If $\lambda'' = 0$, the hyperbolic case, corresponding to a stretching along the inner axis, is obtained. If $\lambda' = 0$, the elliptic case, corresponding to a non-Euclidean rotation around the inner axis, is obtained. In the limiting parabolic case the inner and outer axes are perpendicular and both tangent to the sphere.

The three-dimensional geometric representation of a bilateral two-port network that is obtained, i.e., the configuration consisting of the inner axis and its two non-Euclidean perpendiculars, provides us with a tool to study, not only simple examples (such as those presented in section 2.9) in which the inner axis of the transformation passed through the center of the sphere, but also examples in which the inner axis has an arbitrary position. Some applications of the geometric configuration will be studied in Sections V-VIII.

V. GENERAL METHOD OF ANALYZING BILATERAL TWO-PORT NETWORKS FROM THREE ARBITRARY IMPEDANCE OR REFLECTION-COEFFICIENT MEASUREMENTS

5.1 INTRODUCTION

In dealing with microwave transmission systems we often run into the problem of representing, at a fixed frequency, a linear two-port by an equivalent graph in the form, for example, of a T- or a π-network. A common procedure for finding the equivalent network is to connect known impedances at the output of the two-port and then to measure the input impedance (admittance) or reflection coefficient. In the linear fractional transformation (Eq. 5) we have 4 - 1 = 3 complex constants to determine, which means that three different measurements are sufficient. Therefore the problem is: Find the equivalent network (T or π) for a bilateral two-port from three arbitrary impedance or reflection-coefficient measurements.

If the series impedances of an equivalent T-network are denoted Z_1 and Z_3, and the shunt admittance by Y_2, Eq. 5 can be written (54) as

$$Z' = \frac{(1 + Z_1Y_2)\,Z + (Z_1 + Z_1Y_2Z_3 + Z_3)}{Y_2Z + (1 + Y_2Z_3)} \tag{93}$$

From Eq. 8 we obtain

$$Z' = \frac{Z\,\dfrac{Z_{f1}\dfrac{1}{\sqrt{q}} - Z_{f2}\sqrt{q}}{Z_{f1} - Z_{f2}} + \dfrac{Z_{f1}Z_{f2}}{Z_{f1} - Z_{f2}}\left(\sqrt{q} - \dfrac{1}{\sqrt{q}}\right)}{Z\,\dfrac{1}{Z_{f1} - Z_{f2}}\left(\dfrac{1}{\sqrt{q}} - \sqrt{q}\right) + \dfrac{Z_{f1}\sqrt{q} - Z_{f2}\dfrac{1}{\sqrt{q}}}{Z_{f1} - Z_{f2}}} \tag{94}$$

Comparing Eqs. 5, 93, and 94, and using $q = e^{2\lambda}$, we obtain

$$\left.\begin{aligned} Z_1 &= \frac{Z_{f2}(e^{\lambda} - 1) - Z_{f1}(e^{-\lambda} - 1)}{e^{\lambda} - e^{-\lambda}} = \frac{a - 1}{c} \\ Y_2 &= \frac{e^{\lambda} - e^{-\lambda}}{Z_{f2} - Z_{f1}} = c \\ Z_3 &= \frac{Z_{f2}(e^{-\lambda} - 1) - Z_{f1}(e^{\lambda} - 1)}{e^{\lambda} - e^{-\lambda}} = \frac{d - 1}{c} \end{aligned}\right\} \tag{95}$$

Similarly, if we denote the shunt impedances of an equivalent π-network by Y_4 and Y_6, and the series impedance by Z_5, Eq. 5 can be written as

$$Z' = \frac{(1 + Z_5 Y_6)\, Z + Z_5}{(Y_4 + Y_4 Z_5 Y_6)\, Z + (1 + Y_4 Z_5)} \tag{96}$$

A comparison of Eqs. 5, 92, and 94 yields

$$\left.\begin{aligned} Y_4 &= \frac{Z_{f1}(e^{\lambda} - 1) - Z_{f2}(e^{-\lambda} - 1)}{Z_{f1} Z_{f2}(e^{\lambda} - e^{-\lambda})} = \frac{d-1}{b} \\ Z_5 &= \frac{Z_{f1} Z_{f2}(e^{\lambda} - e^{-\lambda})}{Z_{f1} - Z_{f2}} = b \\ Y_6 &= \frac{Z_{f1}(e^{-\lambda} - 1) - Z_{f2}(e^{\lambda} - 1)}{Z_{f1} Z_{f2}(e^{\lambda} - e^{-\lambda})} = \frac{a-1}{b} \end{aligned}\right\} \tag{97}$$

It is clear that, if the six given and measured quantities are all impedances, the equivalent network can be directly determined analytically by inserting these values in Eq. 5 and by solving the resultant equation system. The values obtained for the complex constants a, b, c, and d immediately yield the equivalent network from Eqs. 95 and 97.

However, we shall present a more powerful method based on modern (higher) geometry. The presentation is divided into three parts. The first part (section 5.2) is purely geometric; the second (section 5.3) is purely analytic; and the third (section 5.4) consists of working some simple numerical examples. A comparison between the new method and the analytic method outlined above is presented in section 5.5.

The relations between the complex constants a, b, c, and d, the fixed points Z_{f1} and Z_{f2} and the multiplier q, and the components of the equivalent T- and π-networks were derived in Eqs. 93, 94, 95, 96, and 97. We shall therefore consider the problem solved when the complex constants or the fixed points and the multiplier have been determined from the six given and measured impedances or reflection coefficients.

Let us denote the three different given load impedances by Z_A, Z_B, and Z_C, and the corresponding measured input impedances by Z'_A, Z'_B, and Z'_C. By stereographically mapping the six points on the unit sphere, the points A, B, C, A', B', and C' are obtained on the surface of the sphere. The last six points, of course, could have been obtained also by a stereographic projection of six given reflection coefficients Γ_A, Γ_B, Γ_C, Γ'_A, Γ'_B, and Γ'_C from (-1, 0, 0) or by projection of six mixed values, for example, Z_A, Z_B, and Z_C from the top of the sphere (0, 0, 1), and Γ'_A, Γ'_B, and Γ'_C from the point (-1, 0, 0).

5.2 GEOMETRIC PART OF THE GENERAL METHOD

a. Klein's Generalization of the Pascal Theorem

In order to find the fixed points of Eqs. 5 and 8 from the six points A, B, C, A', B', and C' on the surface of the sphere, we use a generalized form of

the Pascal theorem in the plane, which has already been stated in section 3.3. (See Fig. 32.)

In 1866, Hesse (58) showed that in a plane a line cutting a conic in two real points can be represented by two points on a fixed line. The principle that has been called "Hesse's transfer principle" ("Übertragungsprincip") consists of a mapping of the two crossover points between the line and the conic stereographically mapped on the fixed line from an arbitrary point on the conic.

The transfer principle was generalized by Klein (69). He represented variables, whose original real parts were set in correspondence with the points on the fixed line, on the Riemann unit sphere (or an arbitrary second-degree surface). Thus the real or complex lines in the original plane correspond to two points on the surface of the sphere. Klein then replaces this point pair by its connecting line, so that every real or complex line in the plane is set in correspondence with one, and usually only one, real line in the three-dimensional space. This line necessarily has to cut the Riemann sphere. Now, two lines in the plane which form a real cross ratio with the two tangents through the crossover point of the two lines to the fixed conic correspond in three dimensions to two lines that cut and form the same cross ratio with the two tangents through the crossover point to the fixed sphere. This property yields the result that if the fixed conic in the plane and the Riemann sphere are considered to be an absolute curve and an absolute surface of Cayley-Klein models of non-Euclidean hyperbolic spaces, then two non-Euclidean perpendicular lines in the plane correspond to two non-Euclidean perpendicular lines that cut in three dimensions.

By using the property of the perpendicular lines Klein generalized the Pascal theorem to three dimensions. The generalized formulation states: The non-Euclidean perpendiculars to opposite sides of a space hexalateral inscribed in a second-degree surface (for simplicity, the unit sphere) have a common non-Euclidean perpendicular. In Fig. 32 the perpendiculars to opposite sides are lines through the points P_1, P_2, and P_3, and they are all perpendicular to the plane of the figure. In the general case, with the points A, B, C, A', B', and C' arbitrarily located on the surface of the sphere, these perpendiculars are, of course, no longer parallel. Then the common perpendicular through P_1, P_2, and P_3 (see Fig. 32) will be changed into a line in three-dimensional space. Let us call this line "the Pascal line," or better still, "the inner axis."

In projection geometry the "dual" of a configuration, composed of straight lines and crossover points, is obtained, in two dimensions, by exchanging lines for points, and points for lines (56). The "dual" of the Pascal theorem is called the "Brianchon theorem." This theorem states that if a hexagon is circumscribed about a nondegenerate conic, the lines joining the pairs of opposite vertices are concurrent. A generalization of the Brianchon theorem to three dimensions yields a line that is the polar of the Pascal space line or the inner axis. Let us call this line "the outer axis."

b. Geometric Construction of the Inner Axis

According to the generalized Pascal theorem, the inner axis can be constructed as follows: Assume that the space hexalateral inscribed in the Riemann unit sphere is AB'CA'BC'A. Construct the opposite sides $\overline{AB'}$ and $\overline{BA'}$ and the non-Euclidean perpendicular to the two sides. Repeat the procedure for $\overline{AC'}$ and $\overline{CA'}$ (or $\overline{BC'}$ and $\overline{CB'}$). Construct the common perpendicular to the two perpendiculars that are obtained. This is the inner axis.

The geometric construction of a common non-Euclidean perpendicular to two lines in space that cut the sphere can be carried out in the following way, according to a method of Klein published by Wedekind (103). Through the line $\overline{AB'}$ two planes are laid, one of which passes through A' and the other through B. The non-Euclidean (elliptic) angle between these planes is then bisected so that the plane H_1, passing through $\overline{AB'}$ and cutting $\overline{BA'}$, is obtained. The procedure is repeated for the planes BA'A and BA'B', which yields a plane H_2. The line that is cut out by the planes H_1 and H_2 is the desired perpendicular.

c. Determination of the Fixed Points and the Multiplier

The fixed points of the linear fractional transformation, Eq. 5, are obtained by stereographically mapping the crossover points between the inner axis and the surface of the unit sphere.

The multiplier of the transformation is obtained by first selecting an arbitrary point E on the surface of the sphere. We then connect, for example, A and its image point, A' with E, and construct the non-Euclidean perpendiculars to $\overline{AE}$ and the inner axis, and to $\overline{A'E}$ and the inner axis. The hyperbolic distance between the two crossover points between the perpendiculars and the inner axis is λ', and the two planes through the perpendiculars and the inner axis form the non-Euclidean (elliptic) angle λ''. The multiplier is obtained from Eq. 9. Since the fixed points and the multiplier are known, the equivalent network is obtained from Eqs. 93-97.

The geometric constructions that have been described for finding the fixed points and the multiplier of the impedance transformation can be performed by ruler and compass. Since most of the constructions are performed in three dimensions, the amount of work is extensive. However, the basic aim of the geometric part of the general method is not to create a constructive geometric method, but to give a graphic picture of how it is possible to generalize the simple two-dimensional constructions corresponding to impedance transformations through bilateral lossless two-port networks to three-dimensional constructions for impedance transformations through bilateral lossy two-port networks. In section 5.3 the geometric constructions will be put into analytic form. Thus a geometric-analytic method is created for finding the fixed points and the multiplier of the transformation from three arbitrary impedance or reflection-coefficient measurements.

5.3 ANALYTIC PART OF THE GENERAL METHOD

In the analytic part of the general method we shall put the geometric constructions of section 5.2 into analytic form. We shall apply a theory of Klein, which was described in his lectures on the hypergeometric function (67).

a. Representation by Quadratic Equations of Lines That Cut the Sphere

Following Klein (67), if we reverse the signs of the coordinates of the point (x, y, z) in Eq. 77, then Z transforms into $-1/Z^*$, with the star, as before, indicating a complex conjugate quantity. Therefore, two points on a diameter are represented by R + jX and $-1/(R - jX)$ in the Z-plane. These points are the roots of the following quadratic equations:

$$[\eta - (R + jX)][(R - jX)\,\eta + 1] = 0 \tag{98}$$

or

$$(R - jX)\,\eta^2 + (1 - R^2 - X^2)\,\eta - (R + jX) = 0 \tag{99}$$

Klein introduces homogeneous coordinates, $\eta = \eta_1/\eta_2$, and calls the expression of the form

$$F: \quad (u - jv)\,\eta_1^2 + (1 - u^2 - v^2)\,\eta_1\eta_2 - (u + jv)\,\eta_2^2 \tag{100}$$

a "diameter form." Thus, by equating a diameter form with zero, a specific diameter on the sphere is obtained.

Klein then allows u and v in Eq. 100 to take any arbitrary complex values, so that

$$(u - jv)\,\eta_1^2 + (1 - u^2 - v^2)\,\eta_1\eta_2 - (u + jv)\,\eta_2^2 = 0 \tag{101}$$

represents any arbitrary, nonsingular quadratic equation. This is the analytic formulation of Klein's generalization of Hesse's transfer principle described in section 5.2.

b. Analytic Representation of a Line That is Non-Euclidean Perpendicular to Two Given Lines

In the geometric part we often had to construct a space line non-Euclidean perpendicular to two given space lines. This perpendicular can be found analytically by using the following method (67): Let us represent two arbitrary diameters of the sphere by the diameter forms,

$$F_1: \quad (u_1 - jv_1)\,\eta_1^2 + \left(1 - u_1^2 - v_1^2\right)\eta_1\eta_2 - (u_1 + jv_1)\,\eta_2^2 \tag{102}$$

$$F_2: \quad (u_2 - jv_2)\,\eta_1^2 + \left(1 - u_2^2 - v_2^2\right)\eta_1\eta_2 - (u_2 + jv_2)\,\eta_2^2 \tag{103}$$

According to the theory of invariants, the functional determinant,

$$G = \begin{vmatrix} \frac{\partial F_1}{\partial \eta_1} & \frac{\partial F_1}{\partial \eta_2} \\ \frac{\partial F_2}{\partial \eta_1} & \frac{\partial F_2}{\partial \eta_2} \end{vmatrix} \tag{104}$$

represents a diameter form that is perpendicular to both diameters, $F_1 = 0$ and $F_2 = 0$. If, then, we allow u_1, v_1, u_2, and v_2 to take any arbitrary complex values, $G = 0$ will represent the non-Euclidean perpendicular to the two lines $F_1 = 0$ and $F_2 = 0$.

c. Analytic Expression for the Complex Angle between Two Lines That Cut the Unit Sphere

Besides the analytic expression for a line in space and a non-Euclidean perpendicular to two given lines, we also need an analytic expression for the complex angle between any two space lines that cut the unit sphere, in order to formulate analytically the geometric part of the general method. If one end point of the first diameter is denoted (x_1, y_1, z_1) and one end point of the other diameter is denoted (x_2, y_2, z_2), then the angle between the diameters can be written

$$\phi = \cos^{-1} \frac{x_1x_2 + y_1y_2 + z_1z_2}{\sqrt{x_1^2 + y_1^2 + z_1^2}\sqrt{x_2^2 + y_2^2 + z_2^2}} \tag{105}$$

By using Eq. 75, and the u-, v-notations of Eq. 100, we obtain

$$\phi = \cos^{-1} \frac{4u_1u_2 + 4v_1v_2 + \left(1 - u_1^2 - v_1^2\right)\left(1 - u_2^2 - v_2^2\right)}{\left(1 + u_1^2 + v_1^2\right)\left(1 + u_2^2 + v_2^2\right)} \tag{106}$$

If, for the sake of simplicity, we write the forms of Eqs. 102 and 103 as

$$F_1: \quad \alpha_1\eta_1^2 + 2\beta_1\eta_1\eta_2 + \gamma_1\eta_2^2 \tag{107}$$

$$F_2: \quad \alpha_2\eta_1^2 + 2\beta_2\eta_1\eta_2 + \gamma_2\eta_2^2 \tag{108}$$

then the invariants (discriminants) and the simultaneous invariant of these forms can be written

$$\left.\begin{aligned} D_{11} &= 4\left(\beta_1^2 - \alpha_1\gamma_1\right) \\ D_{22} &= 4\left(\beta_2^2 - \alpha_2\gamma_2\right) \\ D_{12} &= 2(2\beta_1\beta_2 - \alpha_1\gamma_2 - \alpha_2\gamma_1) \end{aligned}\right\} \tag{109}$$

These invariants yield

$$\left.\begin{aligned} D_{11} &= \left(1 + u_1^2 + v_1^2\right)^2 \\ D_{22} &= \left(1 + u_2^2 + v_2^2\right)^2 \\ D_{12} &= 4u_1u_2 + 4v_1v_2 + \left(1 - u_1^2 - v_1^2\right)\left(1 - u_2^2 - v_2^2\right) \end{aligned}\right\} \tag{110}$$

If we compare Eqs. 106 and 110, we obtain

$$\phi = \cos^{-1}\frac{D_{12}}{\sqrt{D_{11}}\sqrt{D_{22}}} \tag{111}$$

If, then, we allow u_1, v_1, u_2, and v_2 to take any arbitrary values, Eq. 111 will represent the complex angle between two arbitrary lines that cut the unit sphere. The real part of the angle is the non-Euclidean (elliptic) angle between two planes, one plane passing through the first line and the common non-Euclidean perpendicular to the two lines, and the other plane passing through the second line and the common non-Euclidean perpendicular. The imaginary part of Eq. 111 is the hyperbolic distance that is cut out on the common perpendicular by the two lines.

d. Determination of the Fixed Points of the Transformation

Following the procedure outlined in the geometric part of the method, we find that the two space lines, one of which cuts the sphere in the points A and B', and the other in the points B and A', correspond to the following quadratic equations:

$$\overline{AB'}: \quad \eta_1^2 - (Z_A + Z'_B)\,\eta_1\eta_2 + Z_AZ'_B\,\eta_2^2 = 0 \tag{112}$$

$$\overline{BA'}: \quad \eta_1^2 - (Z_B + Z'_A)\,\eta_1\eta_2 + Z_BZ'_A\,\eta_2^2 = 0 \tag{113}$$

The functional determinant is

$$\begin{vmatrix} 2\eta_1 - (Z_A + Z'_B)\,\eta_2 & -(Z_A + Z'_B)\,\eta_1 + 2Z_AZ'_B\,\eta_2 \\ 2\eta_1 - (Z_B + Z'_A)\,\eta_2 & -(Z_B + Z'_A)\,\eta_1 + 2Z_BZ'_A\,\eta_2 \end{vmatrix} \tag{114}$$

Equating the determinant with zero, we obtain

$$k_1\eta_1^2 - 2k_2\eta_1\eta_2 + k_3\eta_2^2 = 0 \tag{115}$$

where

$$\left.\begin{aligned} k_1 &= (Z_A - Z'_A) - (Z_B - Z'_B) \\ k_2 &= Z_A Z'_B - Z'_A Z_B \\ k_3 &= (Z_A - Z'_A)\, Z_B Z'_B - (Z_B - Z'_B)\, Z_A Z'_A \end{aligned}\right\} \tag{116}$$

Repeating the procedure for A and C', and for C and A', we also obtain

$$k_4 \eta_1^2 - 2k_5 \eta_1 \eta_2 + k_6 \eta_2^2 = 0 \tag{117}$$

where

$$\left.\begin{aligned} k_4 &= (Z_A - Z'_A) - (Z_C - Z'_C) \\ k_5 &= Z_A Z'_C - Z'_A Z_C \\ k_6 &= (Z_A - Z'_A)\, Z_C Z'_C - (Z_C - Z'_C)\, Z_A Z'_A) \end{aligned}\right\} \tag{118}$$

The common perpendicular to Eqs. 115 and 117 is given by equating the following functional determinant with zero.

$$\begin{vmatrix} 2k_1\eta_1 - 2k_2\eta_2 & -2k_2\eta_1 + 2k_3\eta_2 \\ 2k_4\eta_1 - 2k_5\eta_2 & -2k_5\eta_1 + 2k_6\eta_2 \end{vmatrix} \tag{119}$$

Then, we obtain

$$\left.\begin{matrix} Z_{f1} \\ Z_{f2} \end{matrix}\right\} = \frac{k_7 \pm \sqrt{k_7^2 - 4k_8}}{2} \tag{120}$$

where

$$\left.\begin{aligned} k_7 &= \frac{k_1 k_6 - k_3 k_4}{k_1 k_5 - k_2 k_4} \\ k_8 &= \frac{k_2 k_6 - k_3 k_5}{k_1 k_5 - k_2 k_4} \end{aligned}\right\} \tag{121}$$

Here Z_{f1} and Z_{f2} are the fixed points of the linear fractional transformation. We denote the corresponding points on the sphere P_{f1} and P_{f2}.

e. Determination of the Multiplier of the Transformation

Following the procedure outlined in the geometric part (section 5.2), we select an arbitrary point E, determine the two non-Euclidean perpendiculars to $\overline{CE}$ and $\overline{P_{f1}P_{f2}}$, and $\overline{EC'}$ and $\overline{P_{f1}P_{f2}}$. We obtain

$$\left.\begin{aligned} k_9\eta_1^2 - 2k_{10}\eta_1\eta_2 + k_{11}\eta_2^2 = 0 \\ k_{12}\eta_1^2 - 2k_{13}\eta_1\eta_2 + k_{14}\eta_2^2 = 0 \end{aligned}\right\} \tag{122}$$

where

$$\left.\begin{aligned} k_9 &= (Z_C + Z_E) - (Z_{f1} + Z_{f2}) \\ k_{10} &= Z_C Z_E - Z_{f1} Z_{f2} \\ k_{11} &= (Z_{f1} + Z_{f2})\, Z_C Z_E - (Z_C + Z_E)\, Z_{f1} Z_{f2} \\ k_{12} &= (Z'_C + Z_E) - (Z_{f1} + Z_{f2}) \\ k_{13} &= Z'_C Z_E - Z_{f1} Z_{f2} \\ k_{14} &= (Z_{f1} + Z_{f2})\, Z'_C Z_E - (Z'_C + Z_E)\, Z_{f1} Z_{f2} \end{aligned}\right\} \tag{123}$$

From Eqs. 109 and 122, we obtain

$$\left.\begin{aligned} D_{11} &= 4\left(k_{10}^2 - k_9 k_{11}\right) \\ D_{22} &= 4\left(k_{13}^2 - k_{12} k_{14}\right) \\ D_{12} &= 2(2k_{10}k_{13} - k_9 k_{14} - k_{11}k_{12}) \end{aligned}\right\} \tag{124}$$

so that

$$\lambda = \lambda' + j\lambda'' = \underset{(\mp)}{-} \cosh^{-1} \frac{D_{12}}{\sqrt{D_{11}}\sqrt{D_{22}}} \tag{125}$$

and

$$q = e^{2\lambda} \tag{126}$$

Equation 125 is slightly different from Eq. 111 in that the real and imaginary parts of Eq. 111 have been interchanged to comply with the notations used in previous sections. The minus sign in Eq. 125 corresponds to the minus sign of Eq. 9. The quantity q in Eq. 126 is the multiplier of the transformation.

5.4 CALCULATION OF SEVERAL NUMERICAL EXAMPLES

In order to show the usefulness and the constructive features of the geometric-analytic method, three numerical examples have been worked out. In all examples the load impedances Z_A, Z_B, and Z_C and the corresponding measured input impedances Z'_A, Z'_B, and Z'_C are assumed to be known, and the fixed points and the multiplier of

the canonic form of the linear fractional transformation are determined. The first example treats of a pure resistive two-port network; the second, of a lossless lowpass network; and the third, of a cascading of the two networks in examples 1 and 2. The network in the third example, therefore, necessarily contains both resistances and reactances.

a. Example 1. Attenuator

The given values are

$$Z_A = 0 \qquad Z_B = 1/2 \qquad Z_C = 1$$

$$Z'_A = 35/18 = 1.944 \qquad Z'_B = 2.300 \qquad Z'_C = 57/22 = 2.590$$

All six impedances are real so that a simple figure, Fig. 43, can be drawn, showing the stereographic mapping of the given points on the unit circle in the xz-plane. The

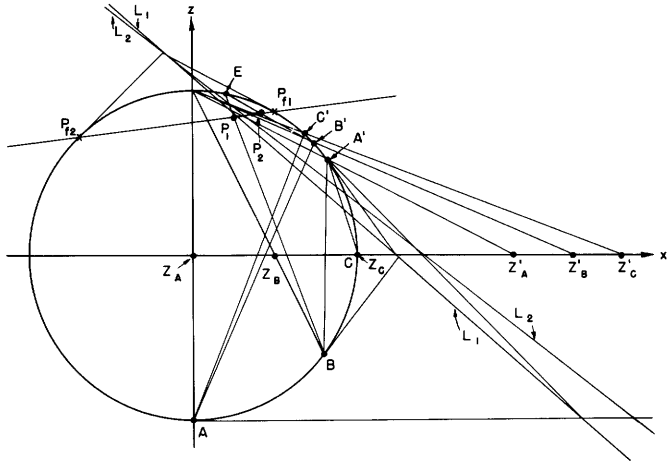

Fig. 43. Example 1. Attenuator.

non-Euclidean perpendiculars to $\overline{AB'}$ and $\overline{BA'}$, and to $\overline{AC'}$ and $\overline{CA'}$ in Fig. 43 are expressed in analytic form by using Eqs. 115-118. Thus

$$\frac{13}{5}\eta_1^2 - 35\eta_1\eta_2 + \frac{161}{4}\eta_2^2 = 0$$

and

$$\eta_1^2 - 11\eta_1\eta_2 + \frac{57}{4}\eta_2^2 = 0$$

The first perpendicular, L_1, cuts the unit circle in points corresponding to the roots $Z_1 = 12.2$ and $Z_2 = 1.27$ in the Z-plane. The second perpendicular, L_2, has the corresponding values $Z_1 = 9.5$ and $Z_2 = 1.5$. From Eqs. 119-121, the common non-Euclidean

perpendicular to these perpendiculars is

$$\frac{64}{5}\eta_1^2 - \frac{64}{5}\eta_1\eta_2 - 112\eta_2^2 = 0$$

which has the roots $Z_1 = 3.5$ and $Z_2 = -2.5$. These impedance values constitute the fixed points of the transformation, and hence $Z_{f1} = 3.5$ and $Z_{f2} = -2.5$.

In order to find the multiplier, an arbitrary point, here $Z_E = 10$, is selected. From Fig. 43, we find that the non-Euclidean perpendicular to $\overline{BE}$ and $\overline{P_{f1}P_{f2}}$ is a line through P_1 perpendicular to the plane of the figure. Similarly, the perpendicular to $\overline{B'E}$ and $\overline{P_{f1}P_{f2}}$ is a line through P_2 perpendicular also to the plane of the figure. Thus both perpendiculars are situated in the same plane through $\overline{P_{f1}P_{f2}}$, indicating that the transformation is hyperbolic, since $\lambda'' = 0$. The multiplier is real. The hyperbolic distance $\overline{P_1P_2}$ is λ'. From Eqs. 122-126, we obtain the perpendiculars through P_1 and P_2. Thus

$$\frac{113}{5}\eta_1^2 - 127\eta_1\eta_2 + \frac{1045}{4}\eta_2^2 = 0$$

and

$$19\eta_1^2 - 55\eta_1\eta_2 + \frac{775}{4}\eta_2^2 = 0$$

We also have

$$D_{11} = -(24\sqrt{13})^2$$

$$D_{22} = -(30\sqrt{13})^2$$

$$D_{12} = -36 \cdot 25 \cdot 13$$

so that

$$\lambda = \lambda' = -\cosh^{-1} 1.25 = -0.692$$

Finally, we obtain

$$q = e^{2\lambda'} = 0.25$$

This is the desired multiplier. From Eq. 94, we obtain the linear fractional transformation

$$Z' = \frac{\frac{11}{8}Z + \frac{35}{16}}{\frac{1}{4}Z + \frac{9}{8}}$$

The components of the equivalent T-network are obtained from Eq. 95:

$$Z_1 = 3/2, \quad Y_2 = 1/4, \quad \text{and} \quad Z_3 = 1/2$$

b. Example 2. Lossless Lowpass Network

The given values are

$$Z_A = -j \qquad Z_B = 0 \qquad Z_C = j$$

$$Z'_A = j/2 \qquad Z'_B = 1.4j \qquad Z'_C = 5j$$

All six impedances are imaginary (or zero) so that a simple figure, Fig. 44, can be drawn, showing the stereographic mapping of the given points on the unit circle in the yz-plane. The non-Euclidean perpendiculars, L_1 and L_2, to $\overline{AB'}$ and $\overline{BA'}$, and to $\overline{AC'}$ and $\overline{CA'}$ are expressed in analytic form by using Eqs. 115-118. Thus

$$-\frac{j}{10}\eta_1^2 - \frac{14}{5}\eta_1\eta_2 + \frac{7j}{10}\eta_2^2 = 0$$

and

$$\frac{5j}{2}\eta_1^2 - 11\eta_1\eta_2 + \frac{19j}{2}\eta_2^2 = 0$$

with the Z-plane roots $Z_1 = 27.75j$, $Z_2 = 0.25j$, and $Z_1 = 0.74j$, $Z_2 = -5.14j$. From Eqs. 119-121, the common non-Euclidean perpendicular to these perpendiculars is

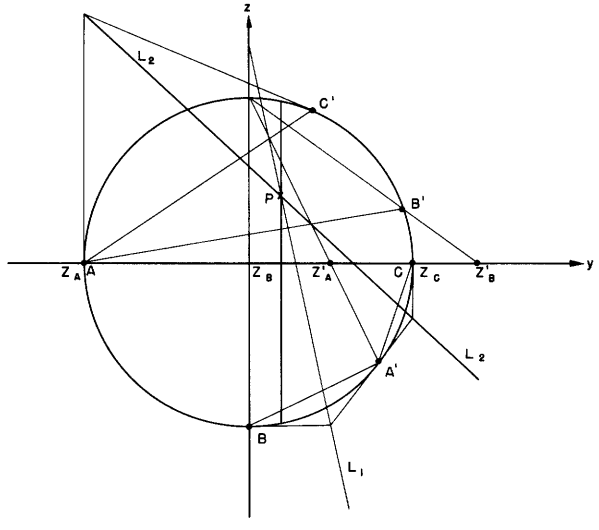

Fig. 44. Example 2. Lossless two-port network.

$$\eta_1^2 - \frac{2}{3}\eta_1\eta_2 - \frac{7}{3}\eta_2^2 = 0$$

The Z-roots are $Z_1 = Z_{f1} = j/3 + 2\sqrt{5}/3$, and $Z_2 = j/3 - 2\sqrt{5}/3$.

In order to find the multiplier, an arbitrary point, here $Z_E = j$, is selected. From Fig. 44, we find that the non-Euclidean perpendicular to $\overline{AE}$ and $\overline{P_{f1}P_{f2}}$ (the latter being a line perpendicular to the plane of the figure through P) is a line through P. Similarly, the perpendicular to $\overline{EA'}$ and $\overline{P_{f1}P_{f2}}$ is a line through P. Thus both perpendiculars are situated in a plane non-Euclidean perpendicular to $\overline{P_{f1}P_{f2}}$, indicating that the transformation is elliptic, since $\lambda' = 0$. The multiplier has an absolute value of unity. The transformation is a non-Euclidean rotation around P. The non-Euclidean (elliptic) angle between the two perpendiculars through P is λ''. From Eqs. 122-126, we obtain the equations for the perpendiculars:

$$\eta_1^2 - 10j\eta_1\eta_2 - \eta_2^2 = 0$$

and

$$-\eta_1^2 - \frac{22}{5}j\eta_1\eta_2 - \frac{19}{5}\eta_2^2 = 0$$

We also obtain

$$D_{11} = -96$$

$$D_{22} = -(12\sqrt{6}/5)^2$$

$$D_{12} = -3 \cdot \frac{64}{5}$$

so that

$$\lambda = \lambda'' = -\cos^{-1}\frac{2}{3} = -48.2°$$

Finally, we obtain

$$q = e^{2\lambda''} = \left(\frac{2}{3} - j\frac{\sqrt{5}}{3}\right)^2 = -\frac{1}{9} - j\frac{4\sqrt{5}}{9}$$

This is the multiplier. From Eq. 93 we obtain the linear fractional transformation

$$Z' = \frac{\frac{1}{2}Z + \frac{7j}{6}}{\frac{j}{2}Z + \frac{5}{6}}$$

The components of the equivalent T-network are obtained from Eq. 94:

$$Z_1 = j, \quad Y_2 = j/2, \quad \text{and} \quad Z_3 = j/3$$

c. Example 3. RLC Network

In order to apply the geometric-analytic method to an RLC network, the networks of examples 1 and 2 are cascaded. The resultant transformation is

$$Z' = \frac{\left(\frac{11}{16} + j\,\frac{35}{32}\right)Z + \left(\frac{176}{96} + j\,\frac{77}{48}\right)}{\left(\frac{1}{8} + j\,\frac{9}{16}\right)Z + \left(\frac{15}{16} + j\,\frac{7}{24}\right)}$$

It has the following fixed points and multiplier:

$$Z_{f1} = 2.615 - j0.1479$$

$$Z_{f2} = -1.3508 + j0.8734$$

$$\lambda = -0.7904 - j0.9130$$

$$q = -0.0520 - j0.1991$$

The resultant T-network (see Fig. 45), from Eq. 94, has the following components:

$$Z_1 = \frac{59}{34} + j\,\frac{16}{17} = 1.735 + j0.941$$

$$Y_2 = \frac{1}{8} + j\,\frac{9}{16} = 0.125 + j0.562$$

$$Z_3 = \frac{8}{17} + j\,\frac{11}{51} = 0.470 + j0.216$$

Now let us attempt to find the fixed points and the multiplier from the given values. We obtain

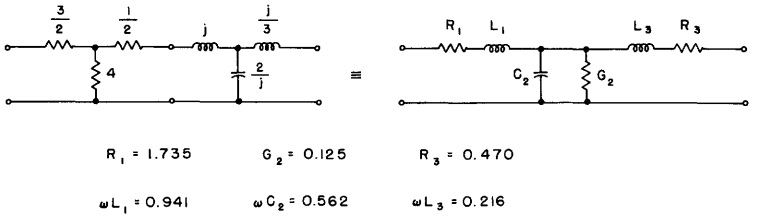

Fig. 45. Example 3. RLC network.

$$Z_A = 1 + 2j \qquad Z'_A = \frac{31 + 391j}{-6 + 106j}$$

$$Z_B = 2 - 3j \qquad Z'_B = \frac{311 + 83j}{138 + 50j}$$

$$Z_C = 4 + j \qquad Z'_C = \frac{167 + 320j}{42 + 128j}$$

With the notations of section 5.3 (a desk calculator was used) we obtain:

$$k_1 = (Z_A - Z'_A) - (Z_B - Z'_B) = -2.476 + j5.310$$

$$k_2 = Z_A Z'_B - Z'_A Z_B = -3.257 + j16.16$$

$$k_3 = (Z_A - Z'_A) Z_B Z'_B - (Z_B - Z'_B) Z_A Z'_A = -11.079 + j42.30$$

$$k_4 = (Z_A - Z'_A) - (Z_C - Z'_C) = -4.017 + j1.0624$$

$$k_5 = Z_A Z'_C - Z'_A Z_C = -11.623 + j8.188$$

$$k_6 = (Z_A - Z'_A) Z_C Z'_C - (Z_C - Z'_C) Z_A Z'_A = -28.05 + j9.195$$

$$k_7 = \frac{k_1 k_6 - k_3 k_4}{k_1 k_5 - k_2 k_4} = 1.265 + j0.725$$

$$k_8 = \frac{k_2 k_6 - k_3 k_5}{k_1 k_5 - k_2 k_4} = -3.404 + j2.484$$

$$\left.\begin{matrix} Z_{f1} \\ Z_{f2} \end{matrix}\right\} = \frac{k_7 \pm \sqrt{k_7^2 - 4k_8}}{2} = \begin{cases} 2.615 - j0.1480 \\ -1.3510 + j0.8735 \end{cases}$$

These values check with the values that were calculated directly from the linear fractional transformation.

With the notations of section 5.3, we select

$$Z_E = 9 + 7j$$

$$Z_C = 4 + j; \qquad Z'_C = \frac{167 + 320j}{42 + 128j}$$

and obtain

$$k_9 = (Z_C + Z_E) - (Z_{f1} + Z_{f2}) = 11.735 + j7.275$$

$$k_{10} = Z_C Z_E - Z_{f1} Z_{f2} = 32.40 + j34.52$$

$$k_{11} = (Z_{f1} + Z_{f2}) Z_C Z_E - (Z_C + Z_E) Z_{f1} Z_{f2} = 73.96 + j62.77$$

$$k_{12} = (Z'_C + Z_E) - (Z_{f1} + Z_{f2}) = 10.379 + j5.837$$

$$k_{13} = Z'_C Z_E - Z_{f1} Z_{f2} = 30.26 + j12.085$$

$$k_{14} = (Z_{f1} + Z_{f2}) Z'_C Z_E - (Z'_C + Z_E) Z_{f1} Z_{f2} = 79.33 + j31.32$$

We also obtain

$$D_{11} = 4\left(k_{10}^2 - k_9 k_{11}\right) = -2211 + j3849$$

$$D_{22} = 4\left(k_{13}^2 - k_{12} k_{14}\right) = 515.6 - j227.4$$

$$D_{12} = 2(2k_{10}k_{13} - k_9 k_{14} - k_{11} k_{12}) = 44.65 + j1688$$

so that

$$\lambda = \lambda' + j\lambda'' = -0.7905 - j0.9130$$

Finally, we obtain

$$q = e^{2\lambda} = -0.0519 - j0.1991$$

These values also check with the values that were calculated directly from the linear fractional transformation.

5.5 COMPARISON OF THE GEOMETRIC-ANALYTIC METHOD WITH A PURE ANALYTIC METHOD

In section 5.1 a pure analytic method for determining the equivalent T- or π-network from three arbitrary impedance measurements was outlined. It consists of inserting the three terminating impedances Z_A, Z_B, and Z_C, and the corresponding measured impedances Z'_A, Z'_B, and Z'_C into the linear fractional transformation (Eq. 5) and solving for the complex constants a, b, c, and d. Equation 5 can be written

$$aZ + b - cZZ' = dZ' \tag{127}$$

so that

$$\left.\begin{aligned} aZ_A + b - cZ_AZ'_A &= dZ'_A \\ aZ_B + b - cZ_BZ'_B &= dZ'_B \\ aZ_C + b - cZ_CZ'_C &= dZ'_C \end{aligned}\right\} \tag{128}$$

The complex constants a, b, c, and d are obtained by Cramer's rule and by the use of the reciprocity condition ad - bc = 1. The positive values of the constants are used.

This method was applied to example 3 in section 5.4, in which the values of the constants a, b, c, and d are

$$a = \frac{11}{16} + j\frac{35}{32} = 0.6875 + j\,1.09375$$

$$b = \frac{175}{96} + j\frac{77}{48} = 1.82292 + j\,1.60417$$

$$c = \frac{1}{8} + j\frac{9}{16} = 0.12500 + j0.5625$$

$$d = \frac{15}{16} + j\frac{7}{24} = 0.9375 + j0.291667$$

The values obtained (a desk calculator was used) by using the pure analytic method are

$$a = 0.687516 + j\,1.093728$$

$$b = 1.82286 + j\,1.60416$$

$$c = 0.1250071 + j0.562487$$

$$d = 0.937485 + j0.291647$$

A comparison of the two sets of values shows excellent agreement.

The amount of work involved in calculating a numerical example by the pure analytic method is roughly the same as calculation of the same example by the geometric-analytic method presented in Section V would entail. The new method, however, has the advantage of giving a visual geometric picture of the different operations of the method.

VI. GENERAL METHOD OF CASCADING BILATERAL TWO-PORT NETWORKS BY MEANS OF THE SCHILLING FIGURE

6.1 INTRODUCTION: THE SCHILLING FIGURE

It was shown in Section V how the Klein generalization of the well-known Pascal theorem to three dimensions can be used for analyzing a bilateral two-port network from three arbitrary impedance or reflection-coefficient measurements. Another important problem in network theory, that of cascading bilateral two-port networks, can be studied by using the Schilling generalization of the Hamilton theorem, a well-known theorem in spherical trigonometry (67). Hamilton's theorem states:

> "If, on a sphere, we denote the fixed diameters passing through the corners of a spherical triangle $A_1A_2A_3$ by OA_1, OA_2, and OA_3, and if we rotate the sphere consecutively around each of the diameters through angles equal to twice the (inner) angles of the triangle, then the sphere and the entire space return to their original positions."

Instead of the three diameters we may assume that we have three arbitrary straight lines L_1, L_2, and L_3, cutting the sphere. We denote the three non-Euclidean perpendiculars to the lines by L_{12}, L_{31}, and L_{23}. The non-Euclidean distance that is cut out on L_1 by L_{12} and L_{31} is λ_1'; the non-Euclidean angle between planes through L_{12} and L_1, and L_{13} and L_1 is λ_1''. Similar notations are introduced for L_2 and L_3. By using these notations, Schilling generalized the Hamilton theorem to the following form:

> "If the three straight lines L_1, L_2, and L_3 are used as axes of three consecutive spiral movements, specified by the three quantities $2(\lambda_1' + j\lambda_1'')$, $2(\lambda_2' + j\lambda_2'')$, and $2(\lambda_3' + j\lambda_3'')$, then the sphere and the entire space return to their original positions."

The geometric configuration of the lines L_1, L_2, and L_3 and their non-Euclidean perpendiculars L_{12}, L_{23}, and L_{31} was found by Schilling (88), a pupil of Klein, in 1891, and it was, therefore, called the "Schilling figure" by Klein (67, 96). It has found extensive application in the theories of the hypergeometric function (67) and of the Schwarzian s-function (89). The lines L_1, L_2, and L_3 form a "core" (German: "Kern") and the perpendiculars L_{12}, L_{23}, and L_{31} form a "polar core."

6.2 GEOMETRIC TREATMENT

The Schilling figure can be used directly for finding the resultant network of two cascaded two-port networks. The procedure is as follows: Map the fixed points of the given networks stereographically on the surface of the Riemann unit sphere. Draw the inner axes L_1 and L_2 connecting the fixed point pairs. Find the non-Euclidean perpendicular L_{12} to L_1 and L_2. Construct two lines L_{23} and L_{31} that are non-Euclidean perpendicular to L_2 and L_1 so that L_{23} and L_{12}, and L_{31} and L_{12} are separated non-Euclidean distances and form non-Euclidean angles given by half of the real and imaginary parts of the exponents of the two multipliers of the two given networks. Find the

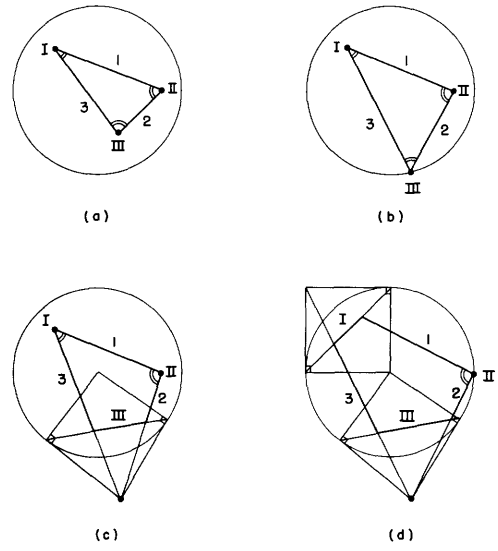

Fig. 46. Use of the Schilling figure for cascading lossless two-port networks:
(a) elliptic-elliptic-elliptic transformations;
(b) elliptic-elliptic-parabolic transformations;
(c) elliptic-elliptic-hyperbolic transformations;
(d) hyperbolic-parabolic-hyperbolic transformations.

perpendicular L_3 to L_{23} and L_{31}. This line cuts the absolute surface of the three-dimensional Cayley-Klein model in points that correspond to the fixed points of the resultant network. The distance between L_{23} and L_{31} along L_3, and the angle between planes through L_3 and L_{23}, and through L_3 and L_{31}, yield the multiplier of the resultant network.

In the special case of lossless two-port networks, the inner axes are all perpendicular to or immersed in the yz-plane that contains the Γ-plane (see Fig. 8). Therefore, all sides of the Schilling figure are also perpendicular to or immersed in the yz-plane. Figure 46 shows some illustrative examples of the use of the Schilling figure for cascading lossless two-port networks. (In the figures L_1, L_2, L_3, L_{12}, L_{23}, and L_{31} are denoted I, II, III, 1, 2, and 3.)

Works by Van Slooten, Deschamps, and de Buhr on cascading lossless two-port networks by means of the Cayley-Klein diagram are discussed in Appendix 4. Recently, a purely geometric work on the cascading of lossy two-port networks was published by de Buhr (38). He utilizes the unit sphere for tutorial purposes and performs all geometric constructions in the plane – a rather complicated method.

6.3 ANALYTIC TREATMENT

The geometric constructions for finding the fixed points and the multiplier of a resultant network of two cascaded two-port networks by using the Schilling figure can be

performed analytically by means of the formulas of section 5.3 that were derived by means of the theory of invariance of quadratic forms and complex spherical trigonometry.

A detailed investigation of the use of the Schilling figure in network theory will be published elsewhere.

VII. GRAPHICAL METHODS OF DETERMINING THE EFFICIENCY OF TWO-PORT NETWORKS BY MEANS OF NON-EUCLIDEAN HYPERBOLIC GEOMETRY

7.1 USE OF MODELS OF TWO-DIMENSIONAL HYPERBOLIC SPACE

In an early work Weissfloch (106) showed that it is possible to represent the real power transfer from a generator with constant emf, E, and constant generator impedance, $Z_G = R_G + jX_G$, to an arbitrary load, $Z_2 = R_2 + jX_2$, by a simple geometric construction in the complex load impedance plane. He found that the loci of constant $P_2/P_{2\,max}$ were circles with their centers on a line parallel to the real axis through the point $(O, -jX_G)$. (See Fig. 47.) The circles all have the property that $R_a R_b = R_G^2$, where R_a, R_b, and R_G are indicated in Fig. 47.

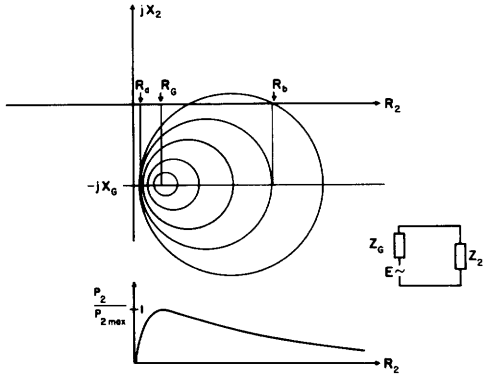

Fig. 47. Curves for constant $P_2/P_{2\,max}$.

When a bilateral lossy two-port network is inserted between the generator and the load, Weissfloch (108) found a similar set of circles within a circle called the "image circle" in the complex input impedance plane. The image circle represents the input impedance locus of the network terminated in pure reactances, so that the circle is the image of the imaginary axis (see Fig. 48). The circles inside the image circle were calibrated in $1 - \eta$ by Weissfloch (η is the efficiency of the network). The image circle corresponds to $\eta = 0$, and the center of the pencil of circles corresponds to $1 - \eta_{max}$. (See also references 84, 110, and 12.) A similar circle diagram for the circuit efficiency is described by Altar (1).

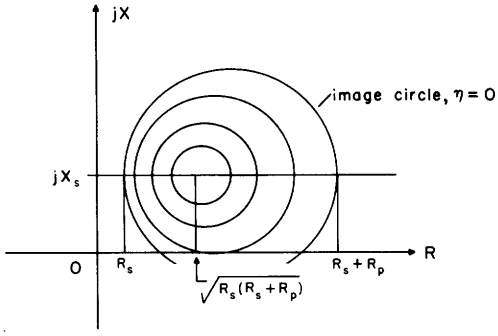

Fig. 48. The image circle and efficiency circles in the Z-plane.

Wheeler and Dettinger (105) found that if the image circle is transferred to the Smith chart in such a way that it is centered around the center of the chart by some lossless transformations, then the radius of the new image circle equals the efficiency of the lossy network. A simple geometrical construction made by Mathis (76) yields the reflection coefficient Γ_a that corresponds to the input impedance of a bilateral lossy two-port network terminated in its conjugate image impedance match. See Fig. 49. (In this figure the circle Γ' is the image circle.) A similar construction by Altschuler (2) for finding the maximum

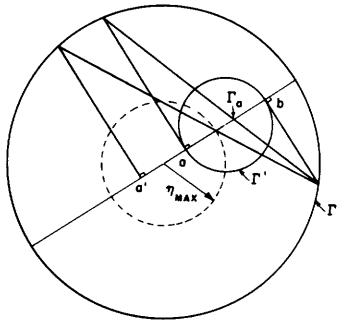

Fig. 49. The constructions of Mathis and Altschuler for determining Γ_a and η_{max}.

efficiency η_{max} is also shown in Fig. 49. We shall now give simple geometric explanations for these constructions (6).

Let us assume that the Γ-circle in Fig. 49 is the absolute curve of a Poincaré model of hyperbolic geometry (see Appendix 1). In this model the pencil of circles, of which the circles Γ and Γ' in Fig. 49 are members, is composed of coaxial circles that have Γ_a as common center. To find Γ_a, we have to divide the distance $\overline{ab}$ into two equal hyperbolic distances. This can be done by means of the butterfly-shaped figure (introduced in Section III) which is shown in Fig. 50a. Two lines of the butterfly figure are non-Euclidean perpendicular to the line through a and b. The hyperbolic distances $\overline{ac}$ and $\overline{cb}$ are equal, because the cross ratios (uacv) and (ucbv) are equal and the hyperbolic distance is, by definition, proportional to the logarithm of the cross ratio of the end points and the two points cut out on the absolute curve. The butterfly figure, which was introduced into network theory by Van Slooten (99), can be thought of as forming part of a complete quadrangle.

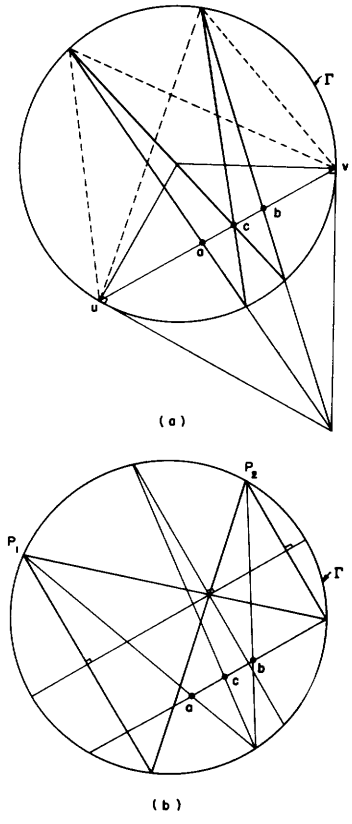

Fig. 50. Division of a hyperbolic distance into two equal parts.

The division of $\overline{ab}$ in Fig. 50a can be performed completely inside the circle Γ if the butterfly figure is centered around a diameter, as shown in Fig. 50b. A hyperbolic distance $\overline{P_1P_2}$ can be displaced along a straight line to $\overline{P_3P_4}$ by the construction shown in Fig. 27, which is also performed by means of a butterfly figure.

Figures 50 and 27 give simple geometric explanations of the constructions by Mathis and Altschuler (see Fig. 51a). From Fig. 51a it is evident why Altschuler starts out from the point a' at the same distance as a from the center of Γ and opposite point a. Figure 51b, finally, shows a more symmetric construction for moving the image circle Γ' to the center of the circle Γ.

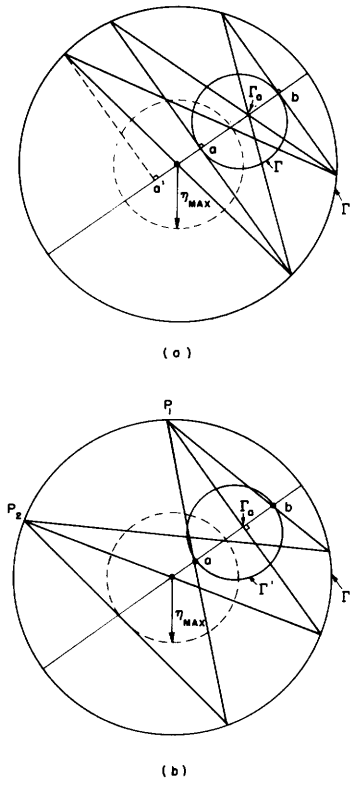

Fig. 51. Use of the butterfly figure for determining Γ_a and η_{max}.

If a copy of the ingenious hyperbolic protractor invented by Deschamps (48, 49) is available, it can, of course, be used directly for determining Γ_a and η_{max}.

7.2 USE OF THE CAYLEY-KLEIN MODEL OF THREE-DIMENSIONAL HYPERBOLIC SPACE

It was shown in section 7.1 how a method, introduced by Altschuler (2), for finding the maximum efficiency of an arbitrary bilateral two-port network that is terminated in its conjugate image impedance match could be given a simple geometric explanation. We shall now show how the efficiency of a two-port network, terminated in an arbitrary load, can be obtained by similar graphical constructions by means of the Cayley-Klein model of three-dimensional hyperbolic space (10).

If we map the complex impedance plane stereographically on the Riemann unit sphere (see Fig. 8), the image circle transforms into a circle on the right hemisphere. This circle is moved until it is symmetric with both the xz-plane and xy-plane. This can be done in two steps, each of which corresponds to a lossless network. In the first step, the image circle is transformed so that it is symmetric with the xz-plane. Several methods are possible, the simplest being those of Weissfloch (108) and of Wheeler and Dettinger (105). Weissfloch extracts a series reactance, corresponding to a parabolic

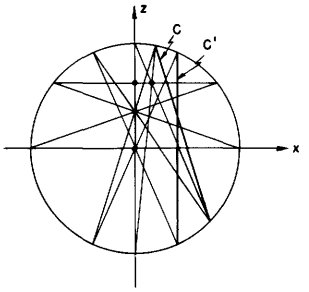

Fig. 52. Graphical construction C → C', which corresponds to an ideal transformer.

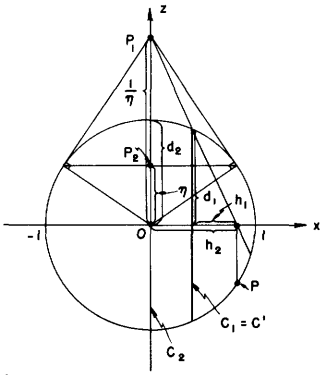

Fig. 53. Graphical determination of the efficiency η.

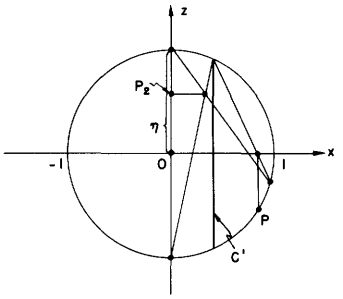

Fig. 54. Graphical determination of the efficiency η.

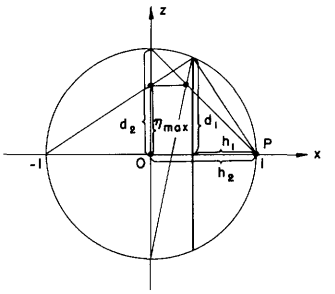

Fig. 55. Graphical determination of the maximum efficiency η_{max}.

transformation that has its fixed point at the top of the sphere. Wheeler and Dettinger extract a piece of uniform lossless transmission line, which corresponds to an elliptic transformation that has its axis of rotation coalescing with the x-axis. In Fig. 52 the transformed image circle is shown in the xz-plane as a straight line C. The symmetry to the xy-plane is now easily obtained by a hyperbolic transformation along the z-axis; this corresponds to an ideal transformer. The projection C is transformed into C' (see Fig. 52).

The total power generated and the power at the output of a two-port network were computed by Altar (1) by means of relations that connected them with the geometric concept of "power" of a point P with respect to a circle. If a and b are the segments of a chord that is divided at P, the product ab is called the "power" of point P relative to the circle. The power is only a function of the position of P and the circle but not the chord chosen. Altar showed that the efficiency of the network could be expressed as the ratio of two powers. The idea was acted upon by Deschamps (46), who introduced the concept of "pseudo distance." On a flat map the pseudo distance C(W) between a circle C with a radius R and a point W at a distance d from the center of the circle is

$$C(W) = \frac{d^2 - R^2}{2R} \tag{129}$$

Now, the ratio of two pseudo distances from a point P to two circles C_1 and C_2 is invariant by inversion; therefore it is not influenced by transformations like those that we have already performed. In Fig. 53 we interpret the circle C_1 as C' and C_2 as the great circle in the yz-plane. An arbitrary load will, after transformation through the network, correspond to a point on the sphere to the right of C'. For the sake of simplicity, let us select the point P shown in Fig. 53. Using the notations of this figure, we can write the efficiency η of the two-port network:

$$\eta = \frac{h_1}{d_1} \cdot \frac{d_2}{h_2} \tag{130}$$

where $d_2 = 1$, because it is the radius of the unit circle. The use of similar triangles immediately yields a distance $\overline{OP_1} = 1/\eta$ on the z-axis. The polar to P_1 cuts the z-axis at P_2, so that $\overline{OP_2} = \eta$. In Fig. 54 a simple construction is shown for obtaining P_2 without any constructions outside the unit circle.

It is interesting to check the fact that if the point P is situated in (1, 0) in the xz-plane, $\eta = \eta_{max}$; this is evident from Fig. 55. The point P_2 is simply the crossover point between the z-axis and a line joining (−1, 0) and the upper point of C'. Therefore,

$$\eta = \eta_{max} = \frac{h_1}{d_1} \tag{131}$$

The yz-plane contains the complex reflection-coefficient plane. Figure 55 reveals that η_{max} is the radius of a circle which is C' stereographically mapped on the yz-plane from the point (−1, 0). This checks nicely with the method of Wheeler and Dettinger (105).

VIII. ELEMENTARY NETWORK THEORY FROM AN ADVANCED GEOMETRIC STANDPOINT

8.1 CLASSIFICATION OF BILATERAL TWO-PORT NETWORKS

It has been shown in previous sections how impedance transformation through bilateral two-port networks can be performed in the three-dimensional Cayley-Klein model by means of a geometric configuration consisting of the inner axis and two non-Euclidean perpendiculars to that axis. The position of the configuration in the model can be taken as a means of classifying two-port networks. The following theorems are valid:

1. If the inner axis is imbedded in the yz-plane (see Fig. 8) and the transformation is hyperbolic (i.e., the two perpendiculars are in a plane through the inner axis), or if the inner axis is perpendicular to the yz-plane and the transformation is elliptic (i.e., the two perpendiculars are in a plane non-Euclidean perpendicular to the inner axis), then the network is reactive. In the transitional case between the two cases that have been mentioned, a parabolic transformation, the inner axis is tangent to the unit sphere.

2. If the inner axis is imbedded in the xz-plane and the transformation is hyperbolic, or if the inner axis is perpendicular to the xz-plane and the transformation is elliptic, then the network is resistive (composed of positive and negative resistances).

3. If the inner axis is perpendicular to the z-axis, then the network is symmetric.

8.2 SPLITTING OF A TWO-PORT NETWORK INTO RESISTIVE AND REACTIVE PARTS

The common method in splitting a bilateral two-port network into resistive and reactive parts is to perform three measurements of the input impedance, with the output terminated in reactances. Three points on the great circle in the yz-plane (see Fig. 8), corresponding to the imaginary axis in the complex impedance plane, are then transformed into three points on the right hemisphere. Through these three points the image circle of the great circle can be drawn.

The first operation is to find a transformation by which the image circle is moved until it is symmetric with the xz-plane. This can be done in several ways, the simplest being the methods of Weissfloch (108) and of Wheeler-Dettinger (105), which were described in section 7.1. In Figs. 56, 57, and 58 the transformed image circle is shown in the xz-plane as a straight line, C.

The second operation is to extract an attenuator so that C is transformed into the projection in the xz-plane of the great circle in the yz-plane. The transformation is hyperbolic. Once more, several methods are possible. Weissfloch (108) utilizes an L-network composed of the series resistance R_s and the shunt resistance R_p. In Fig. 56 the inner axes, denoted l.t.t.i.i. (line that transforms into itself), projections of the isometric circles in the impedance plane, and the points that yield R_s and R_p are graphically constructed. If the attenuator is composed of a symmetric T-network, the corresponding constructions will be those shown in Fig. 57. In Fig. 58 a procedure discussed

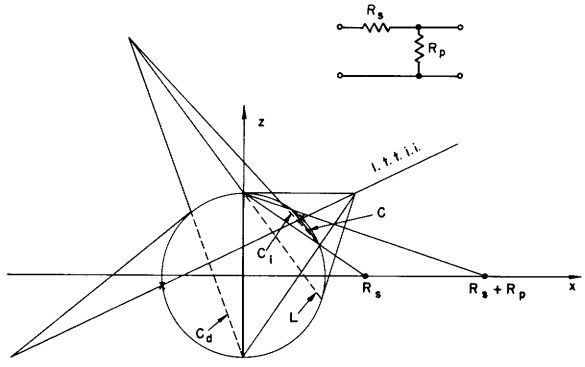

Fig. 56. Transformation through attenuator (L-network).

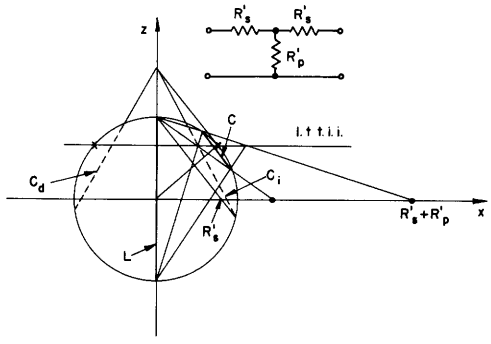

Fig. 57. Transformation through attenuator (symmetric T-network).

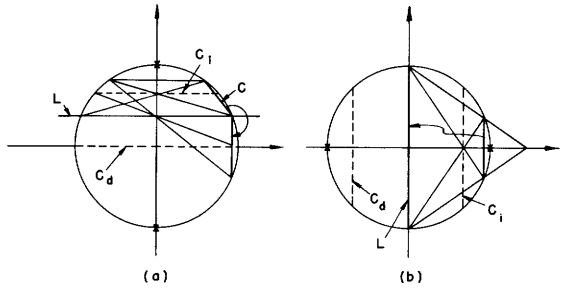

Fig. 58. Transformation through ideal transformer and ideal reflection-coefficient transformer.

by Altschuler (3) is shown. He divides the operation into two steps (Figs. 58a and b), a hyperbolic transformation along the z-axis, corresponding to an ideal transformer, and a hyperbolic transformation along the x-axis, corresponding to an ideal reflection-coefficient transformer.

These two operations have moved the three points on the original image circle to the great circle in the yz-plane. In the third operation these points are transformed into the original points on the same circle by a nonloxodromic transformation, corresponding to a lossless two-port network. This part of the problem is a special case of the general problem of analyzing a two-port network from three arbitrary impedance measurements, treated in Section V. Thus the lossless network can be obtained by using Van Slooten's method of utilizing the two-dimensional Pascal theorem (99).

8.3 COMPARISON OF THE ITERATIVE IMPEDANCE AND THE IMAGE IMPEDANCE METHODS

In the early days of network theory two different methods of transforming impedances by the linear fractional transformation,

$$Z' = \frac{aZ + b}{cZ + d}, \qquad ad - bc = 1 \tag{132}$$

were developed. These methods were called the "iterative impedance method" and the "image impedance method" (53, 54, 57).

In the first method the input impedance Z' is expressed in the output impedance Z by the linear fractional transformation

$$Z' = \frac{Z \dfrac{Z_{f1}\, e^{-\lambda} - Z_{f2}\, e^{\lambda}}{Z_{f1} - Z_{f2}} + \dfrac{Z_{f1} Z_{f2}}{Z_{f1} - Z_{f2}} (e^{\lambda} - e^{-\lambda})}{Z \dfrac{e^{-\lambda} - e^{\lambda}}{Z_{f1} - Z_{f2}} + \dfrac{Z_{f1}\, e^{\lambda} - Z_{f2}\, e^{-\lambda}}{Z_{f1} - Z_{f2}}} \tag{133}$$

in which the iterative impedances Z_{f1} and Z_{f2}, the fixed points of the transformation, are expressed in the complex constants a, b, c, and d of Eq. 132 by Eq. 7 and the multiplier, $q = e^{2\lambda}$, is obtained from Eq. 9. Equation 133 is the same as Eq. 94, derived in Section V. In the Cayley-Klein model of three-dimensional hyperbolic space, Eq. 132 can be interpreted as a spiral (loxodromic) movement of the surface of the unit Riemann sphere around an inner axis through the fixed points Z_{f1} and Z_{f2}. The movement can be split into a stretching and a rotation, given by the real part λ' and the imaginary part λ'' of λ, respectively.

A similar geometric interpretation is valid for the image impedance method. For that case, Eq. 132 can be written

$$Z' = \frac{Z\sqrt{\frac{Z_i'}{Z_i}}\cosh\theta + \sqrt{Z_i Z_i'}\sinh\theta}{Z\frac{1}{\sqrt{Z_i Z_i'}}\sinh\theta + \sqrt{\frac{Z_i}{Z_i'}}\cosh\theta} \tag{134}$$

with

$$Z_i = \sqrt{Z_o Z_s} \tag{135}$$

$$Z_i' = \sqrt{Z_o' Z_s'} \tag{136}$$

and

$$\tanh\theta = \sqrt{\frac{Z_s}{Z_o}} = \sqrt{\frac{Z_s'}{Z_o'}} \tag{137}$$

where Z_i and Z_i' are the image impedances at the output and the input, Z_o and Z_o' are open-circuit impedances, Z_s and Z_s' are short-circuit impedances, and θ is the image propagation function, also called the "image transfer constant." A comparison of Eqs. 134 and 132 yields

$$Z_i = \sqrt{\frac{bd}{ac}} \quad , \quad Z_i' = \sqrt{\frac{ab}{cd}} \quad , \quad \tanh\theta = \sqrt{\frac{bc}{ad}} \tag{138}$$

Let us study a simple example consisting of the unsymmetric resistive network shown in Fig. 59. The six impedances $Z_{f1} = 2$, $Z_{f2} = -1$, $Z_o' = 3$, $Z_s' = 1$, $Z_o = -2$, and $Z_s = -2/3$ are stereographically mapped on the unit sphere (unit circle), as shown in Fig. 60. The sphere (circle) is considered as the absolute surface (curve) of a three- (two-) dimensional Cayley-Klein model.

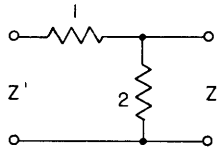

Fig. 59. Simple example of resistive network.

Equations 135 and 136 yield simple constructions for the image impedances $Z_i = 2\sqrt{3}/3$ and $Z_i' = \sqrt{3}$. See Fig. 60. Equation 137 is essentially the equation for an ideal transformer. Therefore, the hyperbolic distances $\overline{OS}$ and $\overline{O'S'}$ in Fig. 60 are equal; here $\tanh\theta = \sqrt{3}/3$. From Eqs. 136, 137, 138, 7, and 132 we obtain

$$\sqrt{-Z_s Z_o} = \sqrt{-Z_s' Z_o} = \sqrt{Z_i Z_i'} = \sqrt{-Z_{f1} Z_{f2}} \quad (=\sqrt{2}) \tag{139}$$

Therefore, the straight lines $\overline{Z_s Z_o'}$, $\overline{Z_s' Z_o}$, $\overline{(-Z_i)Z_i'}$, and $\overline{Z_{f1} Z_{f2}}$ must all pass through

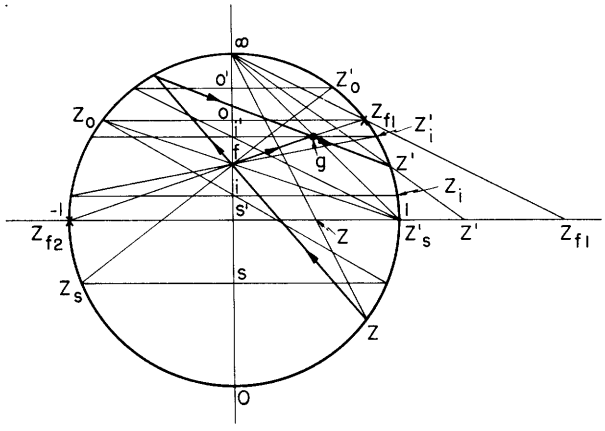

Fig. 60. Iterative impedance method.

the point f in Fig. 60. This yields, for example, a simple construction for finding Z_o, when Z'_s, Z'_o, and Z_s are known.

Equation 134 can be split as follows.

$$Z_a = \frac{Z'_i}{Z_i} Z \tag{140a}$$

$$Z' = \frac{Z_a \cosh \theta + Z'_i \sinh \theta}{Z_a \frac{\sinh \theta}{Z'_i} + \cosh \theta} \tag{140b}$$

$$Z_b = \frac{1}{Z_i} Z \tag{141a}$$

$$Z_c = \frac{Z_b \cosh \theta + \sinh \theta}{Z_b \sinh \theta + \cosh \theta} \tag{141b}$$

$$Z' = Z'_i Z_c \tag{141c}$$

$$Z_d = \frac{Z \cosh \theta + Z_i \sinh \theta}{Z \frac{\sinh \theta}{Z_i} + \cosh \theta} \tag{142a}$$

$$Z' = \frac{Z'_i}{Z_i} Z_d \tag{142b}$$

Equations 140a, 141a, 141c, and 142b represent ideal transformers that correspond to hyperbolic transformations (stretchings) along the vertical axis through the fixed points zero and infinity. Equations 140b, 141b, and 142a represent symmetric two-port networks

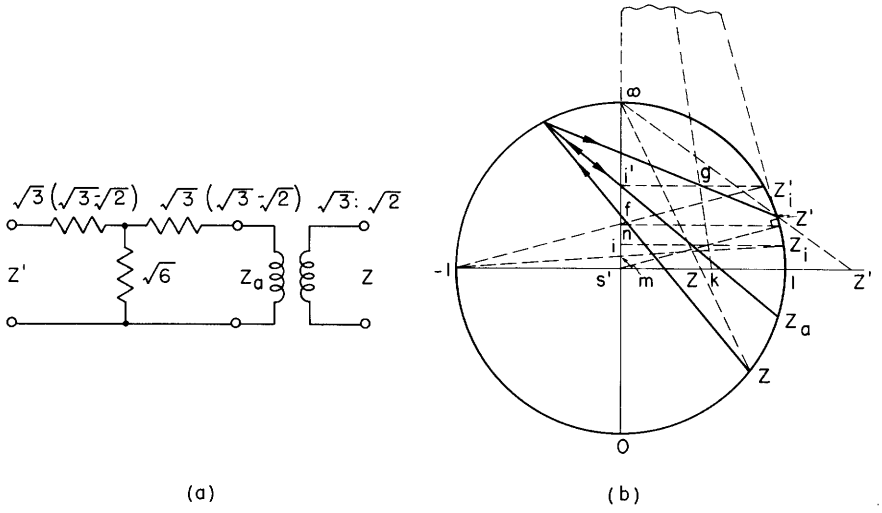

(a) (b)

Fig. 61. Image impedance method. Example 1.

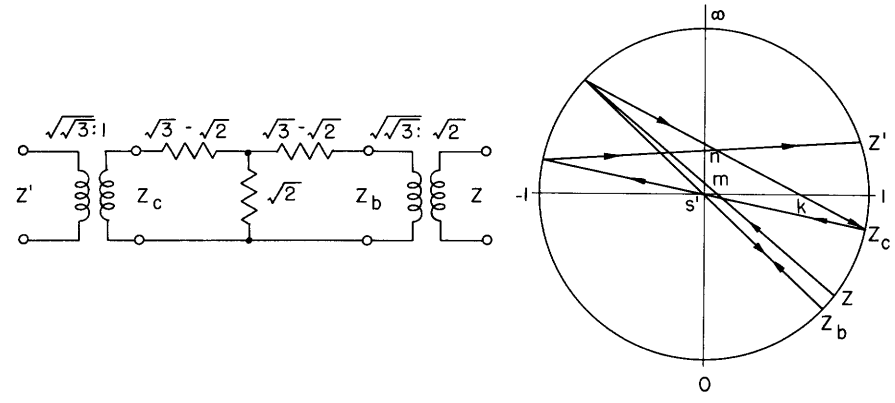

(a) (b)

Fig. 62. Image impedance method. Example 2.

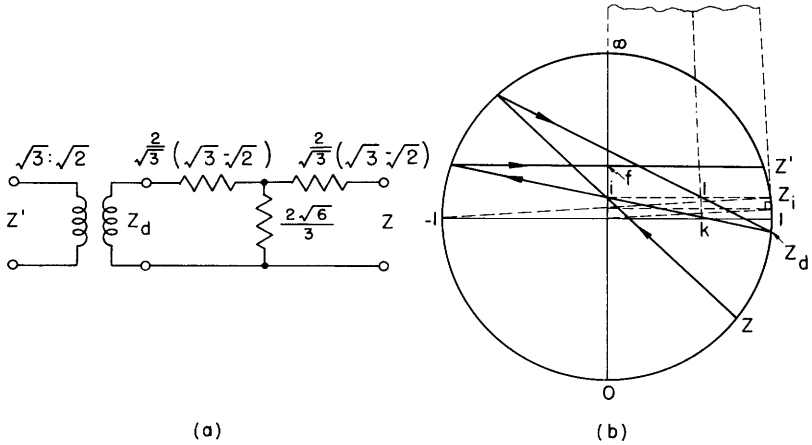

(a) (b)

Fig. 63. Image impedance method. Example 3.

(a=d) that, in our case, correspond to hyperbolic transformations (a + d > 2) along horizontal axes through the fixed points $\pm Z_i'$, ± 1, and $\pm Z_i$. The equivalent networks corresponding to Eqs. 140, 141, and 142 are shown in Figs. 61a, 62a, and 63a.

Finally, let us perform a transformation of the impedance $Z = 0.5$ to $Z' = 1.4$ by the iterative impedance method and the image impedance method. We know that the point $Z = 0$ is transformed into $Z' = Z_s'$ so that, according to the first method, f is transformed into g in Fig. 60. The hyperbolic distance $\overline{fg}$ is $\lambda' = \ln \frac{1}{2}$. Therefore, Z' is obtained from Z by two perspectivities with f and g as centers (see Section III). Transformations by the image impedance method are shown in Figs. 61b, 62b, and 63b. According to Fig. 61a and b, $Z \rightarrow Z'$ by two perspectivities through f and i', corresponding to the ideal transformer, followed by two perspectivities through i' and g, corresponding to the symmetric network. From Fig. 62a and b, we obtain six perspectivities through m and s' (first ideal transformer), s' and k (symmetric network = ideal reflection-coefficient transformer), and s' and n (second ideal transformer). From Fig. 63a and b, finally, we obtain four perspectivities through i and ℓ (symmetric network), and i and f (ideal transformer). Obviously, if the two-port network is symmetric, $Z_{f1} = Z_i = Z_i'$ and $Z_{f2} = -Z_i = -Z_i'$, and the two methods coalesce.

If the network is composed of both lossy and lossless components, the geometric constructions have to be performed in three dimensions.

IX. CONCLUSION

Impedance transformations through bilateral lossy two-port networks, composed of positive and negative resistances and positive and negative reactances, form a group, since a transformation through a cascade of such networks and the inverse transformation belong to the group. The transformation group is characterized by the property that by a transformation belonging to it, an entire complex plane is transformed into itself, or, which is the same thing, the surface of the Riemann unit sphere is transformed into itself. We may obtain a subgroup of this group by specifying that in performing the transformation a circle (straight line) be transformed into itself. Examples of such subgroups are: impedance transformations through bilateral lossless two-port networks composed of positive and negative reactances, in the performance of which the imaginary axis of the Z-plane, or the unit circle of the Γ-plane, is transformed into itself (see section 2.6); or impedance transformations through resistive two-port networks composed of positive and negative resistances, in the performance of which the real axis of the Z-plane is transformed into itself.

It is possible to find transformation groups which have all groups that are mentioned above as subgroups. Such a transformation is, for example, the conformal three-dimensional transformation which has recently been used by the writer as the basis of a geometric-analytic theory of noisy two-port networks. This theory will be published in a report entitled, "Theory of Noisy Two-Port Networks," Technical Report 344, Research Laboratory of Electronics, M.I.T., June 14, 1958.

This group description of impedance and power transformations checks well with the famous "Erlangen Program" of Klein (62). In the present work various models of non-Euclidean hyperbolic geometry have been used. In discussing non-Euclidean geometry we may base our treatment on the following alternatives:

1. a set of postulates;
2. the differential geometry method (Riemann);
3. the theory of groups (Lie); or
4. the projective measure of length and angle.

The author selected the fourth alternative in this research work as being the most appropriate for an introductory investigation of the use of modern (higher) geometry in electrical engineering.

APPENDIX 1

MODELS OF TWO- AND THREE-DIMENSIONAL NON-EUCLIDEAN HYPERBOLIC AND ELLIPTIC SPACES

It was stated in section 1.2 that Klein divided non-Euclidean geometry into hyperbolic, or Gauss-Bolyai-Lobachevsky, geometry, and elliptic, or Riemann, geometry. Hyperbolic geometry is characterized by the properties that through a point outside a straight line two parallel lines can be drawn, that the sum of the angles of a triangle is less than π, and that this geometry is valid on a surface of constant negative curvature. Elliptic geometry is characterized by the properties that through a point outside a straight line no parallel line can be drawn, that the sum of the angles of a triangle is greater than π, and that this geometry is valid on a surface of constant positive curvature.

1. HYPERBOLIC GEOMETRY MODELS

a. Two-Dimensional Models

i. The pseudosphere

The pseudosphere, which originates if a tractrix is rotated around its asymptote (see Fig. A-1) is the simplest surface with constant negative curvature. This important adjunct was combined with hyperbolic geometry by Beltrami (4), in 1868. The pseudosphere has recently been thoroughly discussed by Schilling (92, 93), who also transforms the surface into the complex plane. The pseudosphere has a singular line. It has been shown by Hilbert (59) that in Euclidean space there is no analytic surface of constant negative curvature that does not have a singular line.

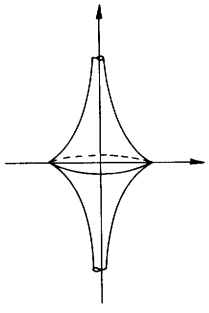

Fig. A-1. Tractrix.

ii. The hyperboloid

Another surface of constant negative curvature which is imbedded in three-dimensional space is the hyperboloid, which has been discussed by Schilling (93) and M. Riesz (83). Besides studying the hyperbolic geometry model and the Cayley-Klein and the Poincaré models, Riesz devotes a considerable part of his presentation to a thorough investigation of the properties and movements of the three-dimensional space with Lorentz metric, in which space the hyperboloid is imbedded. For further information on the hyperboloid, see the references in the work of M. Riesz (83).

iii. The Cayley-Klein diagram

This model was introduced by Beltrami (4) in 1868. However, it did not come into practical use until 1871, when Klein (63) introduced it as a projective model with a conic as the absolute or fundamental curve. Klein based his work, to a large extent, on the

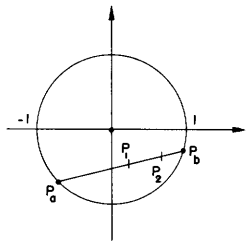

Fig. A-2. Two-dimensional Cayley-Klein model.

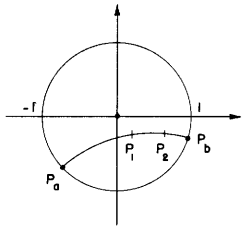

Fig. A-3. Two-dimensional Poincaré model.

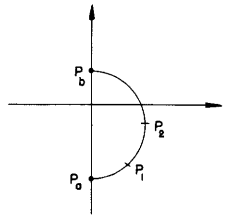

Fig. A-4. Two-dimensional Poincaré model.

works of Cayley (41); therefore the model is usually called the "Cayley-Klein diagram." An example of this model is shown in Fig. A-2. The unit circle in the figure corresponds to the absolute curve (infinity). A straight line is a chord. The hyperbolic distance between two points P_1 and P_2 is defined as half of the logarithm of the cross ratio between P_1, P_2, and the two points, P_a and P_b, cut out of the absolute curve by a straight line through P_1 and P_2.

iv. The Poincaré model

Although it was known to Beltrami (4), this model has been named after Poincaré because he used it extensively in his investigations on automorphic functions (79). Examples of this model are shown in Figs. A-3 and A-4. In Fig. A-3 the unit circle is the absolute curve (infinity), and in Fig. A-4 the absolute curve is a straight line. In both figures a straight line is represented by an arc of a circle which cuts the absolute curve orthogonally.

b. Three-Dimensional Models

i. The hyperhyperboloid

The hyperhyperboloid is imbedded in four-dimensional space; thus it is of little interest from the engineer's point of view. However, in many cases the calculations and constructions can be made in three dimensions and formally extended to four dimensions (83).

ii. The Cayley-Klein model

This model is a direct generalization of the Cayley-Klein diagram to three dimensions. It has been thoroughly studied by Schilling (96) who, for the sake of simplicity, uses the unit sphere as the absolute surface.

iii. The Poincaré model

This model is a direct generalization of the two-dimensional Poincaré model to three dimensions.

2. ELLIPTIC GEOMETRY MODELS

a. Two-Dimensional Models

i. The sphere

The sphere is the simplest surface of constant positive curvature. However, an assumption that two points on a diameter of the sphere together form a single "point" has to be made in order for the sphere (hemisphere) to constitute an ideal model of two-dimensional elliptic geometry. A similar assumption, incidentally, has to be made in connection with the hyperboloid discussed above.

ii. The projective plane

A central projection of the hemisphere on a plane parallel to the plane that limits the hemisphere and is tangent to it yields a model of elliptic geometry in the form of a one-sided projective plane.

iii. Closed surfaces

Two closed surfaces without singularities were found by Boy (29) and by Schilling (90). These surfaces possess all the properties of the projective plane.

b. Three-Dimensional Models

i. The hypersphere

The hypersphere is imbedded in four dimensions.

ii. Three-dimensional elliptic space

This space has been thoroughly discussed by Schilling (95).

iii. Two Riemann spheres

An interesting model of three-dimensional elliptic space consists of two Riemann spheres imbedded in Euclidean space. The natural analytic tool to be used is the theory of quaternions. See the works of Study (102) and others (64).

M. Riesz (83) makes the interesting observation that parabolic geometry is valid on a paraboloid. Thus elliptic geometry is valid on the sphere, parabolic geometry on the paraboloid, and hyperbolic geometry on the hyperboloid.

For additional expository references concerning non-Euclidean models, see references 65, 66, 60, 43, 28.

In order to show the interconnections of the three-dimensional models, we have to use a four-dimensional space. Some of the projections performed, however, result in three-dimensional models. These models, which are direct generalizations of the two-dimensional models that have been described, can be used for geometric constructions.

3. ANALYTIC TREATMENT

An attempt to show how the models of two- and three-dimensional hyperbolic and elliptic spaces are interconnected analytically has lately been made by the writer in a recent research work (14). The treatment consists basically of an analytic interpretation of the geometric constructions described in the geometric treatment that has been given in this report.

APPENDIX 2
INTERCONNECTIONS OF THE NON-EUCLIDEAN GEOMETRY MODELS

1. GEOMETRIC TREATMENT

In order to study the interconnections of some of the two-dimensional non-Euclidean geometry models, let us select a simple example.

$$Z' = k^2 Z = e^{2\psi} Z \quad , \quad k = 2 \tag{A-1}$$

If the Z's in Eq. A-1 represent complex impedances, the transformation is performed by an ideal transformer. If we use the well-known transformation,

$$\Gamma' = \frac{Z' - 1}{Z' + 1} \quad , \quad \Gamma = \frac{Z - 1}{Z + 1} \tag{A-2}$$

where Γ' and Γ are complex reflection coefficients, Eq. A-1 transforms into

$$\Gamma' = \frac{\Gamma \cosh \psi + \sinh \psi}{\Gamma \sinh \psi + \cosh \psi} = \frac{\frac{5}{4}\Gamma + \frac{3}{4}}{\frac{3}{4}\Gamma + \frac{5}{4}} \tag{A-3}$$

If the complex impedance plane, $Z = R + jX$, is stereographically mapped on the Riemann unit sphere, the reflection-coefficient plane, $\Gamma = \Gamma_z + j\Gamma_y$, falls in the yz-plane. It is shown in section 2.2 that Eq. A-2 corresponds on the sphere to a rotation of the projection center from (0, 0, 1) to (-1, 0, 0). In Fig. A-5 the point Z = 1 corresponds to $\Gamma = 0$,

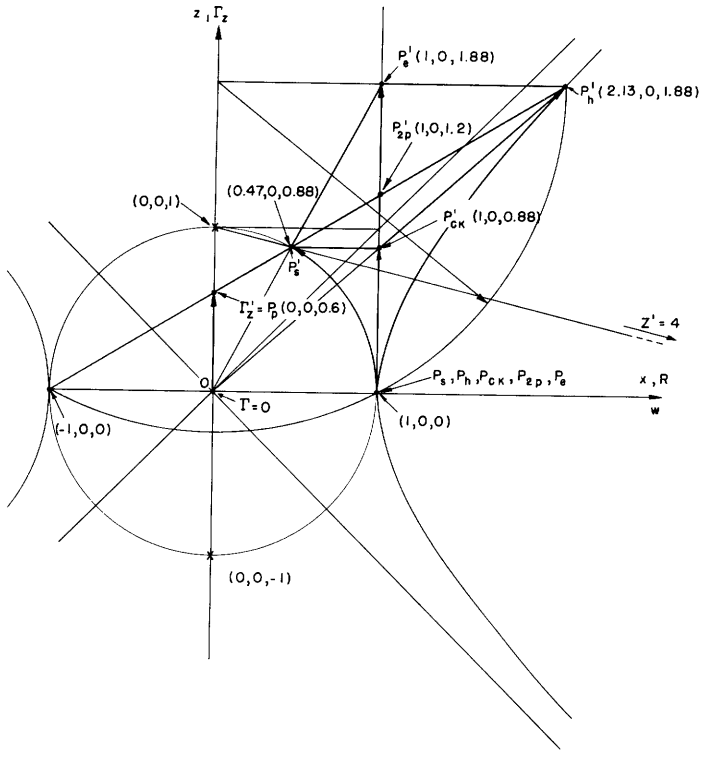

Fig. A-5. Connections between different non-Euclidean geometry models.

and $Z' = 4$, obtained from Eq. A-1, corresponds to $\Gamma'_z = 0.6$. The ideal transformer performs a stretching (hyperbolic transformation) of the surface of the sphere directed from the fixed point (0, 0, -1) toward the fixed point (0, 0, 1), so that (1, 0, 0) is transformed into (0.47, 0, 0.833).

We now consider a unit hyperboloid with the x-axis used as the symmetry axis. Thus, in Fig. A-5 we obtain a unit hyperbola. M. Riesz (83) has shown that if in Fig. A-5 the point, $\Gamma'_z = P_p$, which may be considered as lying in a two-dimensional Poincaré model in the yz-plane, with the unit circle as the absolute curve, is stereographically mapped on the hyperboloid from (-1, 0, 0), so that the point P'_h is obtained, then a central line $\overline{OP'_h}$ cuts the vertical plane parallel to the yz-plane through the point (1, 0, 0) in a point P'_{CK}, which may be considered to be a point of a two-dimensional Cayley-Klein model. The Cayley-Klein diagram may also be obtained by an orthographic projection of the sphere on this vertical plane through (1, 0, 0). An orthographic projection of P'_h on the same plane yields a point P'_e, which may also be obtained by a central projection of the point P'_s on the surface of the sphere. Therefore P'_e lies in an elliptic projective plane. Thus the hyperbolic Cayley-Klein diagram (point P'_{CK}), the ordinary parabolic (Euclidean) plane (point P'_{2p}), and the elliptic projective plane (point P'_e) are represented in the same vertical plane. By varying Z' (Γ'_z), we immediately obtain a geometric picture of how the points P'_s, P'_{CK}, P'_{2p}, P'_e, and P'_h vary. The example selected, $Z = 1 \rightarrow Z' = 4$, is indicated by arrows in Fig. A-5.

APPENDIX 3
HISTORICAL NOTE ON NON-EUCLIDEAN GEOMETRY

The evolution of non-Euclidean geometry followed two different lines of development. The oldest started with Euclid's fifth postulate ("parallel postulate") which states: "That, if a straight line falling on two straight lines makes the interior angles on the same side less than two right angles, the two straight lines, if produced indefinitely, meet on that side on which are the angles that are less than the two right angles."

For approximately 2000 years, attempts were made to derive the fifth postulate from the first four postulates of Euclid, but without success. C. F. Gauss (1777-1855) was the first to invent a geometry that substituted for Euclid's fifth postulate another hypothesis but retained all the others. Some of this geometry, which Gauss called "non-Euclidean," was formulated as early as 1792, but he resolved not to publish it during his lifetime. In this geometry the sum of the angles of a triangle is always less than π, and through a point outside a straight line two parallel lines can be drawn. This new geometry was invented independently in 1823 by J. Bolyai (1802-1860) and published in 1832, and by N. I. Lobachevsky (1793-1856), who presented his researches to the Kasan Scientific Society in 1826 but did not secure publication until 1829.

In both the Euclidean and the Gauss-Bolyai-Lobachevsky geometries the assumption is made that the straight line is of infinite extent. B. Riemann (1826-1866) recognized another possibility. In his famous trial lecture, read before the philosophical faculty of the University of Göttingen, on June 10, 1854, he described a geometry in which a straight line is finite and closed. In this geometry the sum of the angles of a triangle is always greater than π, and through a point outside a straight line no parallel line can be drawn. Riemann's lecture (80) was not published until 1868, after his death. It has been translated into English by Clifford (81), and it has been republished and commented upon by Weyl (82).

The second line of development of non-Euclidean geometry grew out of the "projective geometry" of Desargues, and others which was brought to fruition in 1822 by J. V. Poncelet (1788-1867). He showed that in Euclidean geometry the formula for distance is closely related to a degenerate quadratic form that corresponds to the imaginary circular points. This "absolute," or "fundamental," expression serves as a basis for all Euclidean measure. In 1859, in the sixth of a series of papers (41), entitled "Memoirs upon Quantics," A. Cayley (1821-1895) selected as a basis, instead of the imaginary circular points, an arbitrary quadratic form, and defined, in correspondence with it, distance and angle in such a way that the Euclidean quantities were obtained when the quadratic form degenerated into the imaginary circular points. As Cayley was not aware of the works on non-Euclidean geometry that have been mentioned, it became the important contribution of F. Klein (1849-1925) to show that non-Euclidean geometry could be treated in a simple way by using projective geometry. Klein (63) published his results in 1871.

For excellent surveys of non-Euclidean geometry, see references 65, 66, 28, and 77.

APPENDIX 4
SURVEY OF THE USE OF NON-EUCLIDEAN GEOMETRY IN ELECTRICAL ENGINEERING

In 1931, König (71) mapped the complex impedance plane stereographically on a sphere. In order to be able to use a transmission-line equivalent network for a given network, he restricts himself to the study of symmetric networks. He considers an impedance transformation through a bilateral, lossy, symmetric two-port network as corresponding to a spiral movement of the surface of the sphere. By selecting the radius of the sphere equal to the absolute value of the image impedance of the network, the axis of the spiral movement is made to pass through the center of the sphere. König splits the transformation, which is called a "loxodromic" transformation, into a pure rotation around the axis, corresponding to an elliptic transformation, and a pure stretching along the axis, corresponding to a hyperbolic transformation. The amount of rotation and stretching is given by the multiplier of the canonic form of the linear fractional transformation representing the network. If the sphere is used as the absolute surface of a three-dimensional Cayley-Klein model, the transformation can easily be performed by using non-Euclidean geometry methods. Apparently, König was not aware of this convenient tool. In the special case which he used, the rotation was easily performed, since the axis of the transformation passes through the center of the sphere, so that it merely consists of a rotation through a given Euclidean angle. But the stretching, which consists basically of a translation of a point on the axis through a given hyperbolic distance, was more difficult to perform. König had to use a calibration curve that enabled him to convert a hyperbolic distance into a Euclidean distance. After adding two Euclidean distances, he then had to reconvert. Although he did not make any use of non-Euclidean geometry in his treatment of lossy two-port networks, König's paper is mentioned here because of his use of the sphere and his splitting of the transformation, which entitle him to be called a forerunner of the application of non-Euclidean geometry to electrical engineering.

Among the forerunners we may also count Weissfloch, who during 1942-43 created a powerful circle geometric theory for impedance and reflection-coefficient transformations by the linear fractional transformation (110).

In a study of the synthesis of finite one-port networks Brune (31, 40), in 1931, momentarily considered the right half of a complex plane to be a Poincaré model of two-dimensional hyperbolic space. Brune used the model for a transfer and an interpretation of a generalized form of the Schwarzian lemma for the case of positive functions.

1. IMPEDANCE TRANSFORMATIONS BY MODELS OF TWO-DIMENSIONAL HYPERBOLIC SPACE

Van Slooten, who published a thesis in 1946 on "Geometric Considerations in Connection with the Theory of Four-Terminal Networks" (99), seems to have been the first to introduce non-Euclidean geometry constructively into electrical engineering. This

work is written in Dutch, but it is accompanied by an extensive summary in English with references to figures in the text. Van Slooten sets the impedance transformations through bilateral lossless two-port networks in correspondence with movements in models of two-dimensional hyperbolic space. One of Van Slooten's research objectives is to find the resultant network of two cascaded lossless networks. This corresponds to finding the resultant movement to two known movements in the hyperbolic plane. Van Slooten begins with a study of the Poincaré model but does not succeed in finding the resultant movement. He therefore converts the Poincaré model into the Cayley-Klein model. In this model he succeeds in finding the desired construction.

In order to compress the complex impedance plane into a practical area, Steiner (100), also in 1946, mapped the plane stereographically on the Riemann unit sphere and performed an orthographic projection on the yz-plane (the x- and y-axes are assumed to coincide with the real and imaginary axes of the complex impedance plane, see Fig. A-5). By the two projections the impedance plane is transformed into the two-dimensional Cayley-Klein model in the reflection-coefficient plane (see Section III and Appendix A-2). Steiner applies the diagram to network problems, but nowhere does he mention non-Euclidean geometry.

Not knowing of the work of Van Slooten and Steiner, Deschamps introduced the two-dimensional Cayley-Klein model, in 1951, in order to facilitate polarization-ratio transformations (44). The model was obtained by an orthographic projection of the Poincaré sphere. It was used in a geometrical method of analyzing the effects of site reflections on direction-finding systems (45). Later he developed some powerful tools for working with hyperbolic geometry, in that he showed how a hyperbolic distance can be measured by means of an ingenious hyperbolic protractor of his own design (48), and how a non-Euclidean (elliptic) angle can be measured by transforming it to the center of the Cayley-Klein model (where the non-Euclidean angle equals the Euclidean angle). Deschamps (49) worked a series of examples showing the usefulness of these tools; he also gave a thorough discussion of the Poincaré models. Using two-dimensional hyperbolic models, he showed simple graphical constructions for finding the scattering matrix of a two-port network (50, 51). The same problem was solved by Storer, Sheingold, and Stein (101) in a paper that was based on an URSI address and some Federal Telecommunications Laboratories reports by Deschamps. However, Storer, Sheingold, and Stein carefully avoided the use of non-Euclidean geometry and based their proofs on inversion methods. With the use of inversion they developed a graphical method for transforming a reflection coefficient through a bilateral lossy two-port network. The method consists basically of a geometric interpretation of an analytic formula. Their method was criticized by Deschamps (47), who pointed out that the simpler method, with the use of the hyperbolic protractor and the elliptic angle construction, can be performed inside the unit circle, and, therefore, there is no need for an alternative construction such as theirs. Despite this criticism, the inversion method has gained a thorough hearing in a recent textbook (61).

The Poincaré models of two-dimensional hyperbolic space were used by Rybner (84)

in some circle geometric constructions. Dukes (52) used the Deschamps methods in transforming an impedance through a two-port network. Recently, the Poincaré model with the unit sphere as the absolute curve was used by Kyhl (72) in a study of periodically loaded transmission lines.

In a series of six papers (the first one is in two parts) de Buhr (32-37) made a thorough study of performing impedance transformations through two-port networks geometrically by straightedge and compass. In his treatment he frequently makes use of both the two-dimensional Poincaré models and the Cayley-Klein model. Evidently, de Buhr is not familiar with Van Slooten's work and only partially familiar with Deschamps' (he refers to two of Deschamps' papers in his first paper). Some of de Buhr's constructions are very interesting. As an example, an elegant method for finding the resultant transformer of two cascaded lossless transformers can be mentioned (36). In his sixth paper (37) de Buhr describes a graphical method for transforming complex impedances through lossless two-port networks. The author (9) found this method independently by a simple extension of a method of Van Slooten.

2. IMPEDANCE TRANSFORMATIONS BY MODELS OF THREE-DIMENSIONAL HYPERBOLIC SPACE

In his thesis Van Slooten (99) states that just as the Cayley-Klein model of two-dimensional hyperbolic space is suitable for impedance transformations through bilateral lossless two-port networks, so should the Cayley-Klein model of three-dimensional hyperbolic space be applicable for impedance transformations through lossy two-port networks. He adds, however, that the use of the three-dimensional model seems to be too complicated to be of any use in technique.

Steiner (100) makes a similar statement, saying that, in practice, one cannot work with the Riemann sphere itself.

Deschamps, in a basic paper (46), extends the circular transformations on the sphere to the surrounding space E^3. Points of this space are set in correspondence with Hermitian forms of a wave vector. In the space E^3 Deschamps introduces a metric which is related to a metric in a four-dimensional Minkowski space. After mentioning the three-dimensional Cayley-Klein model, Deschamps discusses the conventional spherical geometry and the two-dimensional Cayley-Klein model briefly.

Some constructive applications of the three-dimensional Cayley-Klein model for impedance and power transformations through bilateral lossy two-port networks are presented in the present research work.

ACKNOWLEDGMENT

The present work was started at the Royal Institute of Technology, Stockholm, Sweden, in the summer of 1954, and it was continued during the author's spare time while he was a guest at Instituto Nacional de la Investigación Científica, Mexico D.F., Mexico, in the winter of 1954-1955. Most of the work was carried out at the Research Laboratory of Electronics, Massachusetts Institute of Technology, during the periods September 1955 to May 1956 and October 1956 to June 1957.

The author wishes to express his gratitude to the Swedish Government Technical Research Council, Stockholm, Sweden, and to Telefonaktiebolaget L. M. Ericsson, Stockholm, Sweden, for grants that made possible the trips to Mexico and to the United States in 1954-1956. He also wishes to thank Professor Jerome B. Wiesner, Director of the Research Laboratory of Electronics, M.I.T., for giving him the opportunity to use the facilities of the laboratory.

The author wants to express his appreciation to Professor Samuel J. Mason for his encouragement and his kindness in reading several papers during the early stages of the present work. Dr. Mason has also kindly permitted the author to publish his unpublished "triangular method," which was discussed in section 2.8.

Finally, the author wishes to express his thanks to the Joint Computing Group, associated with the Research Laboratory of Electronics, M.I.T., for valuable help in performing the numerical computations of sections 5.4 and 5.5.

References

1. W. Altar, Q-circles, A means of analysis of resonant microwave systems, Proc. IRE 35, 355-361; 478-484 (April, May 1947).
2. H. M. Altschuler, Maximum efficiency of four-terminal networks, Proc. IRE 43, 1016 (Aug. 1955).
3. H. M. Altschuler, A method of measuring dissipative four-poles based on a modified Wheeler network, Trans. IRE, vol. MTT-3, no. 1, pp. 30-36 (Jan. 1955).
4. E. Beltrami, Saggio di Interpretazione della Geometria Non-Euclidea, Giorn. Mat. 6, 284-312 (1868); Opere Matematiche (Ulrico Hoepli, Milano, 1902), Vol. 1, pp. 374-405.
5. E. F. Bolinder, Impedance and polarization-ratio transformations by a graphical method using the isometric circles, Trans. IRE, vol. MTT-4, no. 3, pp. 176-180 (July 1956).
6. E. F. Bolinder, Maximum efficiency of four-terminal networks, Proc. IRE 44, 941 (July 1956).
7. E. F. Bolinder, Study of the exponential line by the isometric circle method and hyperbolic geometry, Acta Polytechnica No. 214, Electrical Engineering Series 7, No. 8 (1957).
8. E. F. Bolinder, Some applications of the isometric circle method to impedance transformations through lossless two-port networks, Paper presented at URSI-USA Meeting, Washington, D.C., May 22-25, 1957; Acta Polytechnica No. 232, Electrical Engineering Series 8, No. 6 (1957).
9. E. F. Bolinder, Graphical methods for transforming impedances through lossless networks by the Cayley-Klein diagram, Acta Polytechnica No. 202, Electrical Engineering Series 7, No. 5 (1956).
10. E. F. Bolinder, Graphical method for determining the efficiency of two-port networks, Proc. IRE 45, 361 (March 1957).
11. E. F. Bolinder, Impedance transformations by extension of the isometric circle method to the three-dimensional hyperbolic space, J. Math. Phys. 36, 49-61 (April 1957).
12. E. F. Bolinder, Survey of some properties of linear networks, Trans. IRE, vol. CT-4, no. 3, pp. 70-78 (Sept. 1957).
13. E. F. Bolinder, Note on impedance transformations by the isometric circle method, Trans. IRE, vol. MTT-6, no. 1, pp. 111-112 (Jan. 1958).
14. E. F. Bolinder, A survey of the use of non-Euclidean geometry in electrical engineering, J. Franklin Inst. 265, 169-186 (March 1958).
15. E. F. Bolinder, General method of analyzing bilateral two-port networks from three arbitrary impedance measurements, Ericsson Technics 14, No. 1, 3-37 (1958).
16. E. F. Bolinder, Impedance transformations by the isometric circle method, Quarterly Progress Report, Research Laboratory of Electronics, M.I.T., April 15, 1956, pp. 123-126.
17. E. F. Bolinder, Impedance transformations in the three-dimensional hyperbolic space, Quarterly Progress Report, Research Laboratory of Electronics, M.I.T., April 15, 1956, pp. 126-128.
18. E. F. Bolinder, Use of 4×4 real matrices in microwave theory, Quarterly Progress Report, Research Laboratory of Electronics, M.I.T., July 15, 1956, pp. 83-85.
19. E. F. Bolinder, Cascading of two terminal-pair networks by the isometric circle method, Quarterly Progress Report, Research Laboratory of Electronics, M.I.T., July 15, 1956, pp. 85-87.

20. E. F. Bolinder, Impedance transformations of the nonloxodromic type, Quarterly Progress Report, Research Laboratory of Electronics, M.I.T., July 15, 1956, pp. 87-89.

21. E. F. Bolinder, Analysis of bilateral, two terminal-pair networks in the three-dimensional hyperbolic space, Quarterly Progress Report, Research Laboratory of Electronics, M.I.T., Oct. 15, 1956, pp. 131-133.

22. E. F. Bolinder, Geometric interpretation of the Gewertz stability condition using the isometric circles, Quarterly Progress Report, Research Laboratory of Electronics, M.I.T., Jan. 15, 1957, pp. 146-148.

23. E. F. Bolinder, The isometric circle method in analytic form, Quarterly Progress Report, Research Laboratory of Electronics, M.I.T., Jan. 15, 1957, pp. 149-152.

24. E. F. Bolinder, Graphical determination of the efficiency of bilateral, two terminal-pair networks, Quarterly Progress Report, Research Laboratory of Electronics, M.I.T., Jan. 15, 1957, pp. 152-154.

25. E. F. Bolinder, Use of non-Euclidean geometry models in microwave theory, Quarterly Progress Report, Research Laboratory of Electronics, M.I.T., April 15, 1957, pp. 153-161.

26. E. F. Bolinder, Elementary network theory from an advanced geometric standpoint, Quarterly Progress Report, Research Laboratory of Electronics, M.I.T., April 15, 1957, pp. 161-165.

27. E. F. Bolinder, Analysis of bilateral, two-port networks by three arbitrary impedance or reflection-coefficient measurements, Quarterly Progress Report, Research Laboratory of Electronics, M.I.T., July 15, 1957, pp. 160-163.

28. R. Bonola, Non-Euclidean Geometry: A Critical and Historical Study of Its Developments, English translation with appendices by H. S. Carslaw (Dover Publications, Inc., New York, 1955).

29. W. Boy, Über die Curvatura integra und die Topologie geschlossener Flächen, Math. Ann. 57, 151-184 (1903).

30. L. Brillouin, Wave Propagation in Periodic Structures (Dover Publications, Inc., New York, 2d edition, 1953).

31. O. Brune, Synthesis of a finite two-terminal network whose driving-point impedance is a prescribed function of frequency, J. Math. Phys. 10, 191-236 (1930-31).

32. J. de Buhr, Eine neue Methode zur Bearbeitung linearer Vierpole, FTZ 8, I: 200-204 (April 1955); II: 335-340 (June 1955).

33. J. de Buhr, Die zeichnerische Bestimmung der geometrischen Kenngrössen verlustloser, linearer Vierpole, AEÜ 9, 350-354 (Aug. 1955).

34. J. de Buhr, Die geometrische Darstellungsweise kombinierter linearer Vierpole, AEÜ 9, 561-570 (Dec. 1955).

35. J. de Buhr, Die geometrische Darstellungsweise des Parallel- und des Serienblindwiderstandes als verlustfreie sogenannte parabolische Vierpole, NTZ 8, 636-641 (Dec. 1955).

36. J. de Buhr, Die geometrische Vierpol-Darstellung des Doppeltransformators, AEÜ 10, 45-49 (Jan. 1956).

37. J. de Buhr, Die geometrische elementarste Darstellungsform verlustloser linearer Vierpole, NTZ 9, 80-84 (Feb. 1956).

38. J. de Buhr, Die geometrische Darstellungsweise hintereinander geschalteter allgemeiner, verlustbehafteter Vierpole, AEÜ 11, 173-176 (April 1957).

39. E. Cartan, Lecons sur la Géométrie Projective Complexe (Gauthier-Villars, Paris, 1931).

40. W. Cauer, Theorie der Linearen Wechselstrom-Schaltungen, 2 Auflage, herausgegeben und aus dem Nachlass ergänzt von W. Klein und F. M. Pelz (Akademie-Verlag, Berlin, 1954).

41. A.Cayley, Sixth memoir upon quantics, Trans. Roy. Soc. (London) 149, 61-90 (1859); Collected Mathematical Papers (Cambridge University Press, London, 1889), Vol. II, pp. 561-592.

42. P. Le Corbeiller and C. Lange, Étude sur les Lignes en T dissymetriques et Application aux Filtres de Bandes, Onde Élec. 2, 560-570 (1923).

43. R. Courant and H. Robbins, What Is Mathematics? (Oxford University Press, New York, reprint 1953).

44. G. A. Deschamps, Geometrical representation of the polarization of a plane electromagnetic wave, Proc. IRE 39, 540-544 (May 1951).

45. G. A. Deschamps, A geometrical method of analyzing the effects of site reflections on direction-finding systems (Abstract), Proc. IRE 40, 225 (Feb. 1952); paper presented at IRE National Convention, New York, March 3-6, 1952.

46. G. A. Deschamps, Geometric viewpoints in the representation of waveguides and waveguide junctions, Proc. Symposium on Modern Network Synthesis, Polytechnic Institute of Brooklyn, April 1952, pp. 277-295.

47. G. A. Deschamps, A simple graphical analysis of a two-port waveguide junction, Proc. IRE 42, 859 (May 1954).

48. G. A. Deschamps, New Chart for the solution of transmission-line and polarization problems, Trans. IRE, vol. PGMTT-1, pp. 5-13 (March 1953); Elec. Comm. 30, 247-254 (Sept. 1953); Addendum: Elec. Comm. 31, 188 (Sept. 1954).

49. G. A. Deschamps, A hyperbolic protractor for microwave impedance measurements, Federal Telecommunication Laboratories, Nutley, New Jersey, 1953.

50. G. A. Deschamps, Determination of reflection coefficients and insertion loss at a wave-guide junction, J. Appl. Phys. 24, 1046-1050 (Aug. 1953).

51. G. A. Deschamps, A variant in the measurement of two-port junctions, Trans. IRE, vol. MTT-4, no. 2, pp. 159-161 (April 1957).

52. J. M. C. Dukes, Transmission-line termination, Wireless Eng. 32, 266-271 (Oct. 1955).

53. A. Feige, Über Wellenwiderstand und Dämpfung inhomogener Gebilde, ENT 1, 73-74 (Sept. 1924).

54. R. Feldtkeller, Einführung in die Vierpoltheorie des elektrischen Nachrichtentechnik, 6 Auflage (S. Hirzel Verlag, Zürich, 1953).

55. L. R. Ford, Automorphic Functions (Chelsea Publishing Company, New York, 2d edition, 1951).

56. W. C. Graustein, Introduction to Higher Geometry (Macmillan Company, New York, 1930), pp. 259-261.

57. E. A. Guillemin, Communication Networks (John Wiley and Sons, Inc., New York, 1935), Vol. II.

58. L. O. Hesse, Ein Übertragungsprincip, J. reine u. angew. Math. 66, 15-21 (1866); L. O. Hesse's Gesammelte Werke (G. Franz Verlag, München, 1897), pp. 531-538.

59. D. Hilbert, Über Flächen von constanter Gaussscher Krümmung, Trans. Am. Math. Soc. 2, 87-99 (1901); Grundlagen der Geometrie (B. G. Teubner Verlag, Leipzig, 7th edition, 1930), Appendix V.

60. D. Hilbert and S. Cohn-Vossen, Geometry and the Imagination (Chelsea Publishing Company, New York, 1952); Anschaulische Geometrie (Springer Verlag, Berlin, 1932).

61. R. W. P. King, Transmission-line Theory (McGraw-Hill Book Company, Inc., New York, 1955).

62. F. Klein, Vergleichende Betrachtungen über neuere geometrische Forschungen. Programm zum Eintritt in die phil. Facultät und den Senat der Univ. zu Erlangen (Diechert, Erlangen, 1872); Math. Ann. 43, 63-100 (1893); F. Klein Gesammelte Mathematische Abhandlungen, Bd. I, herausgegeben von R. Fricke und A. Ostrowski (Springer Verlag, Berlin, 1921), pp. 460-497.

63. F. Klein, Über die sogenannte Nicht-Euklidische Geometrie, Math. Ann. 4, 573-625 (1871); Felix Klein Gesammelte Mathematische Abhandlungen, op. cit., Bd. I, pp. 254-305.

64. F. Klein, Vorlesungen über Höhere Geometrie, bearbeitet und herausgegeben von W. Blaschke (Springer Verlag, Berlin, 1926).

65. F. Klein, Elementary Mathematics from an Advanced Standpoint, Vol. II, Geometry (Dover Publications, Inc., New York, 1939).

66. F. Klein, Vorlesungen über Nicht-Euklidische Geometrie, für den Druck neu bearbeitet von W. Rosemann (Springer Verlag, Berlin, 1928).

67. F. Klein, Vorlesungen über die Hypergeometrische Funktion, ausgearbeitet von E. Ritter, herausgegeben von O. Haupt (Springer Verlag, Berlin, 1933).

68. F. Klein, Vorlesungen über die Theorie der elliptischen Modulfunctionen, Bd. I, Ausgearbeitet und vervollständigt von R. Fricke (B. G. Teubner Verlag, Leipzig, 1890).

69. F. Klein, Eine Uebertragung des Pascalschen Satzes auf Raumgeometrie, Math. Ann. 22, 246-248 (1883); F. Klein, Gesammelte Mathematische Abhandlungen, op. cit., Bd. I, pp. 406-408.

70. K. Knopp, Elemente der Funktionentheorie (Sammlung Göschen, Bd. 1109, Berlin, 1949).

71. H. König, Über die Abhängigkeit des Scheinwiderstandes eines symmetrischen Vierpols von der Belastung, Helv. Phys. Acta 4, 281-289 (1931).

72. R. L. Kyhl, The use of non-Euclidean geometry in measurements of periodically loaded transmission lines, Trans. IRE, vol. MTT-4, no. 3, pp. 111-115 (July 1956).

73. H. Lueg, Über die Transformationseigenschaften verlustloser Vierpole zwischen homogenen Leitungen und ein kreisgeometrischen Beweis des Weissflochschen Transformatorsatzes, AEÜ 7, 478-484 (Oct. 1953).

74. H. Lueg, Eine Verallgemeinerung des Weissflochschen Transformatorsatzes, AEÜ 8, 137-141 (March 1954).

75. S. J. Mason, A simple approach to circle diagrams, Massachusetts Institute of Technology, Cambridge, Mass., 1954 (unpublished).

76. H. F. Mathis, Maximum efficiency of four-terminal networks, Proc. IRE 43, 229-230 (Feb. 1955).

77. W. F. Mayer, H. Mohrmann, Encyclopädie der Matematischen Wissenschaften mit Einschluss ihrer Anwendungen, Vol. III, Geometrie (B. G. Teubner Verlag, Leipzig, 1914-1931), pp. 82-91, 1137-1172.

78. F. D. Murnaghan, The Theory of Group Representations (Johns Hopkins University Press, Baltimore, 1938).

79. H. Poincaré, Théorie des Groupes Fuchsiens, Acta Mat. 1, 1-62 (1882).

80. B. Riemann, Über die Hypothesen, welche der Geometrie zu Grunde liegen, Abh. Königl. Gesell. Wiss. Göttingen, No. 13 (1868); Bernhard Riemann's Gesammelte Matematische Werke, herausgegeben unter Mitwirkung von R. Dedekind von H. Weber (B. G. Teubner Verlag, Leipzig, 1829), pp. 272-287.

81. B. Riemann, On the hypotheses which lie at the bases of geometry, English translation by W. K. Clifford, Nature 8, No. 183, 14-17; No. 184, 36-37 (1873); Mathematical Papers by W. K. Clifford, edited by R. Tucker (Macmillan Company, London, 1883).

82. B. Riemann, Über die Hypothesen welche der Geometrie zu Grunde liegen, neu herausgegeben und erläutert von H. Weyl (Springer Verlag, Berlin, 3rd edition, 1923).

83. M. Riesz, En åskådlig bild av den icke-euklidiska geometrien. Geometriska strövtåg inom relativitetsteorien, Lunds Univ. Årsskrift, N.F. Avd 2, 38, No. 9 (1943); Kungl. Fysiograf. Sällsk. Handl. N.F. 53, No. 9 (1943). (In Swedish).

84. J. Rybner, Cirkeldiagrammer i Firpolteorien (J. Gjellerup, Copenhagen, 1947).

85. J. Rybner, Circle diagrams of impedance or admittance for four-terminal networks, J. Inst. Elec. Engrs. (London) Part III, 95, 243-252 (July 1948).

86. A. A. W. Ruhrmann, Die Energieausbreitung auf Leitungen mit exponentiell veränderlichem Wellenwiderstand, Hochfr. u. Elak. 58, 61-69 (Sept. 1941).

87. A. A. W. Ruhrmann, Die Exponentialleitung bei der Grenzwellenlänge und im Sperrbereich, AEÜ 4, 401-412 (March 1950).

88. F. Schilling, Über die geometrische Bedeutung der Formeln der sphärischen Trigonometrie im Falle complexer Argumente, Math. Ann. 39, 598-600 (1891).

89. F. Schilling, Beiträge zur geometrischen Theorie der Schwarz'schen S-Funktion, Math. Ann. 44, 161-260 (1894).

90. F. Schilling, Über die Abbildung der projektiven Ebene auf eine geschlossene singularitätenfreie Fläche im erreichbaren Gebiet des Raumes, Math. Ann. 92, 69-79 (1924).

91. F. Schilling, Projektive und Nichteuklidische Geometrie (B. G. Teubner Verlag, Leipzig u. Berlin, 1931), Bd. II.

92. F. Schilling, Die Pseudosphäre und die Nichteuklidische Geometrie (B. G. Teubner Verlag, Leipzig u. Berlin, 1935).

93. F. Schilling, Pseudosphärische, hyperbolisch-sphärische und elliptisch-sphärische Geometrie (B. G. Teubner Verlag, Leipzig u. Berlin, 1937).

94. F. Schilling, Die Extremaleigenschaften der ausserhalb des absoluten Kegelschnittes gelegenen Strecken in der projektiven Ebene mit hyperbolischer Geometrie, Deutsche Mat., Jahrg. 6, 33-49 (1941).

95. F. Schilling, Die Bewegungstheorie im nichteuklidischen elliptischen Raum (Danzig, 1943).

96. F. Schilling, Die Bewegungstheorie im nichteuklidischen hyperbolischen Raum (Leibniz-Verlag, München, 1948), Vols. I, II.

97. H. Schulz, Über Abbildungen linearer komplexer Funktionen unter Benutzung ihrer Fixpunkte, TFT 32, 218-222 (Oct. 1943); 231-234 (Nov. 1943).

98. J. Van Slooten, De transformatoreigenschappen van een vierpool, Tijds Ned. Radiogen. 9, 217-234 (1941).

99. J. Van Slooten, Meetkundige Beschouwingen in Verband met de Theorie der Electrische Vierpolen (W. D. Meinema, Delft, 1946).

100. F. Steiner, Die Anwendung der Riemannschen Zahlenkugel und ihrer Projektionen in der Wechselstromtechnik, Radiowelt 1, 23-26 (Oct. 1946).

101. J. E. Storer, L. S. Sheingold, and S. Stein, A simple graphical analysis of a two-port waveguide junction, Proc. IRE 41, 1004-1013 (Aug. 1953).

102. E. Study, Beiträge zur Nicht-Euklidischen Geometrie, Am. J. Math. 29, 101-167 (1907).

103. L. Wedekind, Beiträge zur geometrischen Interpretation binärer Formen, Math. Ann. 9, 209-217 (1876).

104. H. A. Wheeler, Geometric relations in circle diagrams of transmission-line impedance, Wheeler Monographs No. 4, 1948. (With 26 references).

105. H. A. Wheeler and D. Dettinger, Measuring the efficiency of a superheterodyne converter by the input impedance circle diagram, Wheeler Monographs No. 9, March 1949.

106. A. Weissfloch, Die Wirkleistungsabgabe eines Generators mit konstanten Innenwiderstand und konstantem EMK an beliebige komplexe Aussenimpedenzen, Hochfr. u. Elak. 60, 10-11 (July 1942).

107. A. Weissfloch, Ein Transformationssatz über verlustlose Vierpole und seine Anwendung auf die experimentelle Untersuchungen von Dezimeter- und Zentimeterwellen-Schaltungen, Hochfr. u. Elak. 60, 67-73 (Sept. 1942); Bemerkungen, ibid., 61, 57 (Feb. 1943).

108. A. Weissfloch, Die Wirkleistungsverluste in linearen Vierpolen in Abhängigkeit vom Wert des transformierten Scheinwiderstandes, ENT 19, 259-265 (Dec. 1942).

109. A. Weissfloch, Kreisgeometrische Vierpoltheorie und ihre Bedeutung für Messtechnik und Schaltungstheorie des Dezimeter- und Zentimeterwellengebietes, Hochfr. u. Elak. 61, 100-123 (April 1943).

110. A. Weissfloch, Schaltungstheorie und Messtechnik des Dezimeter- und Zentimeter-Wellengebietes (Birkhäuser Verlag, Basel, 1954).